PATENT
Attorney Docket No. 33846/US/2/TAL
Attorney File No.: 454892-00018

IN THE UNITED STATES PATENT AND TRADEMARK OFFICE
BEFORE THE BOARD OF PATENT APPEALS AND INTERFERENCES

In re application of: Semple *et al.*	Examiner: Dave T. Nguyen
Serial No. 10/086,477	Art Unit: 1632
Filed: March 1, 2002	"EXPRESS MAIL" LABEL NO.: EV 792966312 US
For: *COMPOSITIONS FOR STIMULATING CYTOKINE SECRETION AND INDUCING AN IMMUNE RESPONSE*	

APPELLANT'S BRIEF

Mail Stop Appeal Brief - Patents
Commissioner for Patents
P.O. Box 1450
Alexandria, VA 22313-1450

Sir:

This appeal brief, filed in triplicate in connection with the above-captioned patent application, is in response to the final Office Action mailed May 6, 2005. This appeal is taken pursuant to Rule 1.192, following the Notice of Appeal filed August 8, 2005 and received in the U.S. Patent and Trademark office on August 14, 2005. This brief is being filed on or before February 14, 2006, along with a request for a four-month extension of time and the requisite fee. Although Appellants do not believe any additional fees are required, the Commissioner is authorized to charge any additional fees, including extension fees or other relief, which may be required, or credit any overpayment to Deposit Account No. 50-2319 (Our Order No. 454892-00018; Our Docket No.: 33846/US/2).

I. REAL PARTY IN INTEREST

The real party in interest is the University of British Columbia, Canada, the owner by assignment of the above-identified patent application.

II. RELATED APPEALS AND INTERFERENCES

Appellants are not aware of any related appeals or interferences which will directly affect, be directly affected by or have a bearing on the Board's decision in the pending appeal.

III. STATUS OF CLAIMS

The present application was originally filed with Claims 1-21. In response to a Restriction Requirement, Claims 2, 13 and 20-21 were cancelled without prejudice or disclaimer. In addition, Claims 4 and 15 were withdrawn without prejudice or disclaimer. Appellants amended Claims 1 and 3 by the amendment filed February 3, 2005. The claims on appeal, Claims 1, 3, 5-12, 14, and 16-19, as currently pending are set forth in Appendix A.

IV. STATUS OF AMENDMENTS

No amendments to the claims have been made subsequent to the final rejection of those claims herein.

V. SUMMARY OF INVENTION

Lipid–based vehicles have been disclosed previously in the art for the delivery of a wide variety of small and large molecule therapeutics, including chemotherapy agents, proteins, peptides and sequence-specific nucleic acids such as, *e.g.*, plasmids and antisense. Depending on the nature of the lipid composition selected, one can preferentially target particular cell types such as tumor cells or immune cells. Likewise, by varying the lipid composition one may also selectively deliver a desired therapeutic agent extracellularly (*e.g.*, to interstitial spaces) as well as intracellularly. In the case of intracellular delivery this can be, for example, either endosomal

delivery or cytoplasmic delivery with subsequent access to sites such as the nucleus.

The selection of an appropriate lipid formulation depends to a great extent upon the nature of the therapeutic agent, its underlying biological mechanism of action and the particular indication to be treated. In the case of small molecule anticancer drugs, for example, suitable lipid formulations are employed that extravasate through leaky blood vessels within tumors resulting in preferential carrier accumulation in the interstitial space. Encapsulated drugs are released into the extracellular medium and are then rapidly taken up by the surrounding tumor cells. For sequence-specific nucleic acids such as plasmid DNA or antisense, which are unable to permeate across the plasma membrane, the lipid formulation may be selected to deliver the nucleic acid into the cytoplasm, allowing subsequent access to the nucleus via passive diffusion. Thus, the selection of an appropriate lipid formulation typically depends upon and requires detailed knowledge of the pharmacokinetics and pharmacodynamics of the therapeutic agent to be delivered, as well as consideration of the site of action of the therapeutic agent.

Immune stimulatory sequences ("ISS") such as CpG oligonucleotides represent a newer class of therapeutic DNA molecules having, it turns out, a very distinct mechanism and site of action in comparison with sequence-specific nucleic acids. *See* Latz *et al., Nature Immunol.* 5:190-198 (2004) (reporting a previously unknown mechanism of cellular activation whereby TLR9 is recruited from the endoplasmic reticulum to sites of CpG uptake) (attached as Exhibit A hereto). Significantly, however, the correlation between TLR9 and CpG signaling was not discovered until well after the priority date of the instant case, and even then was the subject of active academic debate. *Compare* Hemmi *et al. Nature* 408:740-745 (2000) (proposing involvement of a newly-discovered Toll-like receptor, TLR9, in CpG signaling) (attached as Exhibit B hereto) with Chu *et al. Cell* 103:909-18 (2000) (suggesting that a DNA-dependent

protein kinase, DNA-PK, is required for CpG signaling) (attached as Exhibit C hereto). As noted by Hemmi *et al.*, the nature and localization of the putative CpG receptor was still controversial in December of 2000, and there was evidence for both cell-surface activation by CpG as well as internalization of CpG. *Id.* at 743, 1st column. This lack of an adequate understanding of the mechanism or site of action of ISS such as CpG as of the priority date created significant uncertainty in the art as to how such molecules should be formulated for therapeutic delivery.

The present invention stems from the discovery that lipid-based delivery of immunostimulatory nucleic acid sequences ("ISS"), such as CpG dinucleotides, can lead to truly synergistic improvements in immune stimulatory activity depending on the nature of the lipid vehicle employed. As demonstrated in the specification and in the Declaration submitted by Appellants during prosecution, all lipid-based vehicles are not the same and do not provide uniformly beneficial results for this particular class of therapeutics. In comparison with conventional lipid delivery vehicles such as lipid complexes, Appellants' fully-encapsulated liposomal particles provide dramatic increases in immune stimulatory activity, including the generation of immune stimulatory activity even from non-ISS. Further, the immune response to specific target antigens can be induced by administration of an antigenic molecule in association with lipid particles containing such non-sequence specific oligodeoxynucleotides.

VI. ISSUES

The final Office Action mailed May 6, 2005, presents two issues for which Appellants request review:

1) An issue of patentability under 35 U.S.C. §103 of Claims 1, 3, 5-8, 11, 14, and 16-19 as being obvious over Krieg (U.S. Patent No. 6,207,646 ('646)) or Krieg (U.S. Patent No. 6,429,199 ('199)), taken with any of Wheeler *et al.* (U.S. Patent No. 5,981,501 ('501)), MacLachlan (WO 99/39741 ('741)) or Semple (WO 98/51278 ('278));

2) An issue of patentability under 35 U.S.C. §103(a) of Claims 1, 3, 5-12, 14, and 16-19 as being obvious over Krieg ('646) or Krieg ('199), taken with any of Wheeler *et al.* ('501), MacLachlan ('741) or Semple ('278), and further in view of Meers (U.S. Patent No. 6,143,716 ('716)).

VII. GROUPING OF CLAIMS

The Examiner has rejected Claims 1, 3, 5-12, 14, and 16-19. For purposes of appeal, Claims 1, 3, 5-12, 14, and 16-19 are grouped together and stand or fall together.

VIII. ARGUMENT

REJECTION UNDER 35 U.S.C. §103 OVER KRIEG ('646) OR KRIEG ('199), TAKEN WITH ANY OF WHEELER *ET AL.* ('501), MACLACHLAN ('741) OR SEMPLE ('278) SHOULD BE WITHDRAWN

A. The Examiner Has Not Established a *Prima Facie* Case of Obviousness

In order to establish a *prima facie* case of obviousness, three criteria must be met. First, there must be some suggestion or motivation, either in the references themselves or in the knowledge generally available to one of ordinary skill in the art, to modify the references or to combine their teachings. Second, there must be a reasonable expectation of success. Finally, the prior art reference (or references when combined) must teach or suggest all of the claimed limitations. The teaching or suggestion to make the claimed combination and the reasonable expectation of success must be found in the prior art, and not based on the applicant's disclosure. *In re Vaeck*, 947 F.2d 488 (Fed. Cir. 1991). Appellants respectfully submit that the Examiner has failed to establish at least two of these criteria, and thus a *prima facie* case of obviousness has not been set forth in the instant case.

1. A Motivation or Suggestion to Combine is Lacking

The initial burden is on the Examiner to provide some suggestion of the desirability of doing what the inventor has done. To support the conclusion that the claimed invention is directed to obvious subject matter, the references must expressly or impliedly suggest the claimed invention, or the Examiner must present a convincing line of reasoning as to why the skilled artisan would have found the claimed invention to be obvious in light of the teachings of the references. *Ex parte Clapp*, 227 USPQ 972, 973 (Bd. Pat. App. & Inter. 1985). Neither basis for combining the cited references has been properly established in the present case.

a. No Motivation Can be Drawn from the References Themselves

With respect to the first basis for combining, there is no motivation or suggestion in the references themselves to combine their teachings as proposed. The Krieg references very generally describe a wide variety of potential delivery options for their immunostimulatory nucleic acids, including a non-specific suggestion of "nucleic acids associated with: . . . a lipid (e.g. a cationic lipid, virosome or liposome)." ['646 Patent, Col. 12, ll. 30-33]. As the Examiner admits, however, neither of the Krieg patents include any teaching, suggestion or motivation to fully encapsulate their immunostimulatory nucleic acids within a lipid particle as presently claimed. [Office Action mailed 10/7/04, p. 11]. Indeed, lipid-based delivery is proposed only in passing, embedded among a number of other possibilities, none of which are exemplified.

Clearly, neither Krieg reference would motivate the skilled artisan to select any particular lipid delivery vehicle from the genus of "nucleic acids associated with a lipid," any more than one of the myriad other vehicles disclosed therein, including sterols ('199 patent, col. 14), target cell specific binding agents ('199 patent, col. 15), coupling or crosslinking agents such as protein

A, carbodiimide, and N-succinimidyl-3-(2-pyridyldithio) propionate (SPDP) ('199 patent, col. 22) or virosomes ('199 patent, col. 22). Instead, the preferred embodiments actually disclosed in the examples utilize phosphorothioate-modified oligodeoxynucleotides in simple intraveneous solutions, which is clearly set forth as the preferred embodiment. Accordingly, neither of the Krieg patents even impliedly suggest the claimed invention, let alone expressly do so. *See In re Baird*, 16 F.3d 380, 29 USPQ2d 1550 (Fed. Cir. 1990) (finding no motivation to combine where the prior art reference disclosed a vast number of possibilities and gave as a preferred embodiment different compositions).

Conversely, there is also no mention or suggestion in the cited lipid patents that they could or should be employed for the delivery of immune stimulatory nucleic acids. To the contrary, the references relied on by the Examiner are more generally directed to the disparate therapeutic field of gene and antisense therapy, where the clear stated objective is to reduce if not substantially eliminate any immune response. There is certainly no motivation to be drawn from any of these disclosures to support their combination with the immunostimulatory nucleic acids of Krieg. To the contrary, the divergent therapeutic objectives of these sequence-specific therapeutic applications actually undercut any such motivation to combine.

Specifically, the Wheeler and MacLachlan references are both directed to gene therapy (*i.e.*, sequence-specific) applications, which explicitly teach to reduce immunogencity and consequent elimination by the host immune system. [*See, e.g.*, MacLachlan at p. 18, lines 11-22; Wheeler at p. 35]. As the Examiner has previously admitted, the stated objective of Semple in reducing the immune clearance of their disclosed antisense therapeutics also conflicts with the immune stimulatory objective of the present case:

> **On the contrary, the parent application, when read as a whole**, clearly envisions **the advantages in utilization of** encapsulated cationic amphiphile/**antisense** complexes **mainly by their lesser clearance response**. The intended application of an encapsulated cationic lipid/antisense DNA . . . neither supports in any way a broader genus of any encapsulated cationic lipid/nucleic acid polymer complexes for use as an immunostimulatory composition, let alone other specific claimed limitations which recites CpG motifs and secretion of a cytokine ...

[Office Action mailed 3/27/03, U.S. Appln. S/N 09/649,527, p. 3 (emphasis in original)]. The Examiner has taken a similar position in the instant application, (Office Action mailed 12/22/03, p. 5). This same disparity in the basic biological objectives of immune stimulation versus gene and antisense therapy also undercuts any alleged motivation to combine the cited lipid encapsulation references with the immune stimulatory nucleic acids taught by Krieg.

Accordingly, Appellants respectfully submit that the requisite motivation or suggestion to combine the immune stimulatory nucleic acids of Krieg with the gene therapy lipid vehicles of Wheeler, MacLachlan and/or Semple cannot be properly drawn from their disparate disclosures, and thus a *prima facie* case of obviousness cannot be established on this basis.

b. The "Totality" of the Prior Art is Also Not Supportive of the Examiner's Obviousness Rejection

With respect to the second basis, the Examiner also failed to present a convincing line of reasoning as to why the skilled artisan would have found the claimed invention obvious in light of the teachings of the references. The Examiner's general assertions that "the art of making lipid particle comprising a cationic lipid as a carrier in encapsulating a bioactive agent such as DNA is well known in the prior art," (Office Action mailed 5/6/05, p. 3), are an inadequate and inappropriate basis for rejecting the presently claimed invention, as well as being inaccurate. *See In re Dembizak*, 175 F.3d 994, 1000, 50 USPQ2d 1614, 1617 (Fed. Cir. 1999) ("Broad conclusory statements regarding the teaching of multiple references, standing alone, are not

evidence.") Reliance on a high skill level in the art as a justification for a proposed combination is equally improper. *See In re Rouffet*, 149 F.3d 1350, 47 USPQ2d 1453 (Fed. Cir. 1998) (PTO erred in finding suggestion or motivation to combine prior art references based solely on the high level of skill in the art). Moreover, and contrary to the Examiner's assertion, Appellants are not ignoring the "totality"of the prior art in arguing against the Examiner's rejection. Rather, Appellants maintain that the totality of the prior art is not supportive of the Examiner's obviousness rejection of the presently-claimed invention, including prior art that the Examiner thus far refuses to consider.

Implicit in the Examiner's position is the erroneous assumption that all lipid-based delivery vehicles will work the same for every therapeutic molecule and for any desired indication, an assumption clearly disproven by the data provided by Appellants in the specification and again by way of declaration. As the Examiner can appreciate, there are myriad types of liposomal delivery vehicles, having a wide variety of components, and capable of delivering a range of therapeutic molecules to different locations and cells in the body. Necessarily, changing the lipid vehicle changes the pharmacodynamics and pharmacokinetics of the associated therapeutic molecule, and by altering the lipid composition the therapeutic agent can be targeted to particular cell types and can further be released extracellularly or intracellularly, depending on the properties and site of action of the particular therapeutic.

Accordingly, Appellants respectfully submit that the Examiner's stated reliance on the "totality of the art" and broad characterizations of the liposome field is overly simplistic and ignores important differences in the structure and composition of the presently-claimed compositions that lead to significantly improved results. The issue presented for decision herein is not whether lipid vehicles were known for DNA delivery in general, but rather whether

Appellants' selection of the particular lipid vehicle claimed herein and the resulting discovery of the synergistic enhancement of immunostimulatory activity of fully encapsulated ISS ODN are nonobvious and unexpected in view of the totality of the art. Appellants maintain that they are. The Examiner's rejection overlooks the complexity of lipids as a class of delivery vehicles and erroneously assumes that one size liposome fits all therapeutic agents, including agents having a completely uncharacterized mechanism of action.

At best, the simple statement in Krieg that their CpG oligonucleotides could be associated with "a sterol," "a lipid" or "a target cell specific binding reagent," Krieg, column 12, lines 31-35, is merely an invitation to the skilled artisan to engage in hit-or-miss experimentation on an almost limitless number of possible delivery options, with little or no guidance or direction, and without any understanding of the underlying mechanism or site of action of the particular therapeutic agent at issue. This suggests a classic obvious-to-try situation, where "what would have been 'obvious to try' would have been to vary all parameters or try each of numerous possible choices until one possibly arrived at a successful result, where the prior art gave either no indication of which parameters were critical or no direction as to which of many possible choices is likely to be explored." *See In re O'Farrell*, 853 F.2d 894, 7 USPQ2d 1673 (Fed. Cir. 1988). Thus, to the extent that the Examiner is asserting based on Krieg it would have been obvious to try delivering immunostimulatory oligonucleotides in lipid delivery vehicles such as the particular lipid vehicles described and claimed by Appellants, this argument is improper and also does not support the Examiner's obviousness rejection based on the cited references.

c. Conventional Wisdom as of the Priority Date was to Employ Cationic Lipid / DNA Complexes for Immunostimulatory Purposes

If anything, the totality of the prior art suggests an entirely different solution than that pursued by Appellants. In this regard, the Examiner is directed again to the teachings by Dow *et al.*, who published contemporaneous academic articles in addition to the patent disclosures previously submitted by Appellants. Dow *et al.*, *J. Immunol.* 163:1552-61 (1999) (attached as Exhibit D). These references provide a clear teaching to the skilled artisan that immune stimulatory oligonucleotides complexed with cationic lipids provided potent immune activation. The Dow group's complexation approach is further consistent with the previous teachings by Zelphati and others, who taught that lipid complexes were sufficient to protect against serum nucleases. Zelphati and Szoka, *J. Lip. Res.* 7:31-49 (1997) (attached hereto as Exhibit E). Indeed, Zelphati *et al.*. further suggested to the skilled artisan in 1997 that "in contrast to all other types of liposomes, cationic liposomes do not require any encapsulation step that limits the application of these carriers." *Id.*

Appellants respectfully submit that these clear teachings with respect to lipid-based delivery of immune stimulatory DNA coupled with the absence of any other more relevant disclosures plainly demonstrate that the conventional wisdom in the liposome field as of the priority date of the instant case was systemic delivery of immunostimulatory oligonucleotides using cationic lipid complexes. In this regard, the Examiner is reminded that a person of ordinary skill in the art is "one who thinks along the line of conventional wisdom in the art and is not one who undertakes to innovate . . . ." *Standard Oil Co. v. American Cyanamid Co.*, 774 F.2d 448, 227 USPQ 293 (Fed. Cir. 1985).

As the Federal Circuit recently noted, a critical step in analyzing the patentability of claims under §103 is casting the mind back to the time of the invention, to consider the thinking of one of ordinary skill in the art, guided only by the prior art references and the then-accepted wisdom in the field. *In re Kotzab* , 208 F.3d 1352, 54 UPSQ2d 1308 (Fed. Cir. 2000). Close adherence to this methodology is particularly important in cases where the very ease with which the invention can be understood may prompt one to fall victim to hindsight wherein only that which the invention taught is used against is teacher. *Id.* Appellants' invention as presently claimed went against the conventional wisdom of lipid-nucleic acid complexation, a fact which is strongly indicative of nonobviousness.

2. There Was No Reasonable Expectation of Success with Respect to the Effectiveness of the Lipid / Nucleic Acid Composition as Presently Claimed

As noted above, in rejecting the presently-claimed invention the Examiner selectively relies on Appellants' own art describing encapsulation of therapeutic genes and antisense molecules in lipid formulations, which all have in common the objective of delivering these sequence-specific nucleic acids to the nucleus of a target cell.[1] Certainly, the requisite site of action for these types of therapeutic molecules was known and thus researchers were better able to develop lipid formulations to get them to their destination. Nevertheless, although there was general consensus at the time regarding the desired target site there was still active investigation and debate regarding the mechanism by which lipid vehicles released oligonucleotides into cells, and there were a number of obstacles still to overcome. *See, e.g.* Zelphati, *supra* ("Cationic liposomes are a useful in vitro but as yet unproven in vivo delivery mechanism."); Hope *et al.*, *Mol. Membrane Biol.* 15:1-14 (1998) ("The ill-defined nature and unpredictable behavior of the

[1] In this regard, Appellants have reconsidered and concur with the Examiner's position that Wheeler *et al.* discloses liposome encapsulation as opposed to complexation.

resulting [cationic lipid/DNA] particles are major hurdles to overcome in generating non-viral, genetic pharmaceuticals."). These contemporaneous statements from skilled artisans in the field of liposomal delivery vehicles are directly contrary to the Examiner's position that such compositions are "routine and conventional" in the art. Indeed, even where the site and mechanism of action of the therapeutic DNA was known, there was still significant debate among scientists as to the most efficacious way to deliver these therapeutics and considerable variability in such formulations.

In marked contrast to the antisense and therapeutic genes contemplated in the Examiner's selected art references, the underlying mechanism of action and requisite delivery profile for ISS such as CpG oligonucleotides was by no means certain at the priority date of the instant case. In fact, the search for the elusive ISS receptor was still ongoing at the time and there was evidence of both cell-surface and intracellular signaling. Hemmi *et al.* at p. 743. In formulating the pending rejection the Examiner is also erroneously assuming that the delivery of ISS should necessarily follow the same path as the delivery of sequence-specific nucleic acids, an assumption we now know to be incorrect. More to the point, however, as of the priority date of the instant case no one knew the site of action of the ISS and thus the skilled artisan was left to speculate on the most appropriate formulation, lipid or otherwise.

Given the uncertainties and challenges with respect to *in vivo* lipid delivery noted by skilled artisans in the contemporaneous art references above, and the complete absence of knowledge of the mechanism and/or site of action of immune stimulatory olignonucleotides as of the priority date of the instant case, Appellants respectfully submit that there is an inadequate factual basis to support a reasonable expectation of success with the presently-claimed compositions. Quite simply, without trying it, one would not know whether it works. If

anything, the successes claimed by researchers such as Dow *et al.* with cationic lipid/DNA complexes pointed to complexation, rather than encapsulation, as the better approach.

B. Appellants' Evidence of Superior and Unexpected Results Rebuts Any *Prima Facie* Case of Obviousness

Assuming, *arguendo*, that the Examiner has established a *prima facie* case of obviousness, Appellants have nevertheless rebutted any such case with their evidence of unexpectedly superior results. *In re Chupp*, 816 F.2d 643, 646 (Fed. Cir. 1987) (evidence of unobvious or unexpected advantageous properties, such as superiority in a property the claimed invention shares with the prior art, can rebut *prima facie* obviousness). Thus far, the Examiner has largely ignored Appellants' data and arguments in this regard. The Federal Circuit has emphatically and repeatedly held that objective evidence of nonobviousness must always be taken into account and not just when the decision maker is in doubt: "objective evidence such as commercial success, failure of others, long-felt need, and unexpected results must be considered before a conclusion on obviousness is reached." (*Hybridtech Inc. v. Monoclonal Antibodies, Inc.*, 231 USPQ 81 (Fed. Cir. 1986). *See also Bausch & Lomb, Inc. v. Barnes Hindes, Inc.*, 230 USPQ 416 (Fed. Cir. 1986); *Jones v. Hardy*, 220 USPQ 1021 (Fed. Cir. 1984)).

As noted previously above, the most recent and pertinent teachings in the art directed specifically to the present field of invention, that is, the combination of lipids and nucleic acids for immune stimulatory purposes, teach that complexation rather than encapsulation provides a synergistic benefit. *See* Dow *et al.*, *supra*. Dow *et al.* teach that nucleic acid:lipid complexes are significantly more immunostimulatory than DNA administered alone (*i.e.* naked DNA as exemplified by Krieg), and that DNA from any source when complexed with lipids at low doses can synergize to provide a strong immunostimulatory effect. *Id.* Indeed, in their corresponding

patent disclosures Dow *et al.* assert that their lipid complexes provide synergistic benefits. *See, e.g.,* U.S. Patent No. 6,693,086, submitted previously. Despite these alleged successes, however, the compositions described and claimed by Appellants were still shown to be at least four- to ten-fold more active in stimulating immune responses compared to the nucleic acid:lipid complexes taught by Dow and others. *See* Declaration of Michael J. Hope submitted June 23, 2004 (attached hereto as Exhibit F). In addition, the lipid encapsulated nucleic acid particles were shown to be much more effective in rendering the test animals tumor-free than the nucleic acid:lipid complexes. *Id.* These profound differences in immunostimulatory activity and tumor efficacy are proof of the superior and truly synergistic immune stimulatory properties resulting from the claimed lipid encapsulation approach, which compels a finding of nonobviousness.

For the foregoing reasons, Appellants respectfully request withdrawal of the Examiner's rejection of Claims 1, 3, 5-8, 11, 14, and 16-19 under 35 U.S.C. §103 based on the combination proposed above.

REJECTION UNDER 35 U.S.C. §103 OVER KRIEG ('646) OR KRIEG ('199), TAKEN WITH ANY OF WHEELER *ET AL.* ('501), MACLACHLAN ('741) OR SEMPLE ('278), AND FURTHER IN VIEW OF MEERS ('716) SHOULD BE WITHDRAWN

The claims are non-obvious over Krieg ('646) or Krieg ('199), taken with any of Wheeler *et al.* ('501), MacLachlan ('741) or Semple ('278), for the same reasons set forth in the preceding paragraphs.

The Examiner further cites the Meers patent as prior art. Appellants maintain that the Meers patent is directed principally to peptide-lipid conjugates and their use in liposomes. It has very little relevance to the claimed invention since it does not describe with any specificity the making of a lipid-nucleic acid composition, let alone the lipid-encapsulated nucleic acid

compositions as claimed. In addition, it does not cure the deficiencies of the other references as discussed above. Accordingly, Appellants respectfully request withdrawal of this ground of rejection as well.

IX. CONCLUSION

In conclusion, Appellants respectfully submit that the Examiner did not establish a *prima facie* case of obviousness. Moreover, even if a *prima facie* case of obviousness was established, Appellants have submitted ample evidence of the unexpected superiority of the claimed invention in an inducing immune response, which rebuts any such *prima facie* case and compels a finding of nonobviousness.

As such, Appellants respectfully request that the rejections be withdrawn.

Respectfully submitted,

DORSEY & WHITNEY LLP

Date 12/14/05

Todd A. Lorenz
Registration No. 39,754

DORSEY & WHITNEY LLP
555 California Street, Suite 1000
San Francisco, CA 94104-1513
(415) 781-1989 (telephone)
(415) 398-3249 (fax)

APPENDIX A

1. (Currently amended) An immunostimulatory composition comprising an oligodeoxynucleotide fully encapsulated in a lipid particle comprising a cationic lipid, wherein said oligodeoxynucleotide is a non-sequence specific immunostimulatory sequence including at least one CpG motif or palindromic sequence.

2. (Canceled)

3. (Currently amended) The composition according to claim 1, wherein ~~the nucleic acid polymer~~said oligodeoxynucleotide includes at least one CpG motif.

4. (Withdrawn) The composition according to claim 1, wherein the nucleic acid polymer has no detectable immunostimulatory activity in the mammal in the absence of the lipid particle.

5. (Previously presented) The composition according to claim 1, wherein said oligodeoxynucleotide consists of deoxynucleotide residues joined by phosphodiester linkages.

6. (Original) The composition according to claim 1, wherein the cationic lipid is selected from among DODAP, DODMA, DMDMA, DOTAP, DC-Chol, DDAB, DODAC, DMRIE, DOSPA and DOGS.

7. (Original) The composition according to claim 1, wherein the lipid particle further comprises an exchangeable steric barrier lipid.

8. (Original) The composition according to claim 7, wherein the exchangeable steric barrier lipid is a PEG-lipid, a PAO-lipid or a ganglioside.

9. (Original) The composition according to claim 1, further comprising a drug or cytotoxic agent.

10. (Original) The composition of claim 9, wherein the drug or cytotoxic agent is associated with the lipid particle.

11. (Original) The composition according to claim 1, further comprising an antigenic molecule selected from among polypeptides, glycolipids and glycopeptides comprising at least one epitope of the target antigen and nucleic acids encoding at least one epitope of the target antigen.

12. (Original) The composition according to claim 11, wherein the antigenic molecule is associated with the lipid particle.

13. (Canceled)

14. (Previously presented) The composition according to claim 11, wherein said oligodeoxynucleotide includes at least one CpG motif.

15. (Withdrawn) The composition according to claim 11, wherein the nucleic acid polymer has no detectable immunostimulatory activity in the mammal in the absence of the lipid particle.

16. (Original) The composition according to claim 11, wherein the oligodeoxynucleotide consists of deoxynucleotide residues joined by phosphodiester linkages.

17. (Original) The composition according to claim 11, wherein the cationic lipid is selected from the among DODAP, DODMA, DMDMA, DOTAP, DC-Chol, DDAB, DODAC, DMRIE, DOSPA and DOGS.

18. (Original) The composition according to claim 11, wherein the lipid particle further comprises an exchangeable steric barrier lipid.

19. (Original) The composition according to claim 17, wherein the exchangeable steric barrier lipid is a PEG-lipid, a PAO-lipid or a ganglioside.

20. (Canceled)

21. (Canceled)

nature immunology

TLR9 signals after translocating from the ER to CpG DNA in the lysosome

Eicke Latz[1], Annett Schoenemeyer[1], Alberto Visintin[1], Katherine A Fitzgerald[1], Brian G Monks[1], Cathrine F Knetter[1,2], Egil Lien[1], Nadra J Nilsen[2], Terje Espevik[2,3] & Douglas T Golenbock[1,3]

Microbial DNA sequences containing unmethylated CpG dinucleotides activate Toll-like receptor 9 (TLR9). We have found that TLR9 is localized to the endoplasmic reticulum (ER) of dendritic cells (DCs) and macrophages. Because there is no precedent for immune receptor signaling in the ER, we investigated how TLR9 is activated. We show that CpG DNA binds directly to TLR9 in ligand-binding studies. CpG DNA moves into early endosomes and is subsequently transported to a tubular lysosomal compartment. Concurrent with the movement of CpG DNA in cells, TLR9 redistributes from the ER to CpG DNA–containing structures, which also accumulate MyD88. Our data indicate a previously unknown mechanism of cellular activation involving the recruitment of TLR9 from the ER to sites of CpG DNA uptake, where signal transduction is initiated.

Among the microbial products continuously sampled by the mammalian immune system is DNA. The first microbial DNA found to have immunostimulatory activity was genomic DNA from the vaccine strain of *Mycobacterium bovis* (bacille Calmette-Guérin)[1,2]. The ability to reproduce the immunostimulatory activity present in microbial DNA led to the elucidation of optimal stimulatory motifs and the identification of functional groups in nucleotides that influence inflammatory activity. Nonmethylated CpG motifs in a particular base context determine stimulatory and species-specific activity[3–5].

Toll-like receptors are germline-encoded receptors that recognize various conserved molecular structures[6]. The stimulatory capacity of DNA is lost in TLR9-null mice[7]. These studies, together with the finding that optimal stimulatory CpG DNA sequences show species specificity[8], suggest that TLR9 interacts with CpG DNA. Direct binding of CpG DNA to TLR9 has not been shown, however, raising the possibility that CpG DNA activates TLR9 indirectly by binding to an intermediate molecule, which in turn undergoes a species-specific conformational change to function as a TLR9 ligand. This latter explanation is analogous to the observation that *Drosophila melanogaster* Toll is activated by invasive microorganisms through the pathogen-induced proteolytic processing of Prospätzle to Spätzle[9], the actual Toll-binding ligand[10].

Much evidence suggests that CpG DNA actively signals in intracellular compartments; for example, immobilized CpG DNA is inactive[3,11], lipofection enhances the stimulatory activity of CpG DNA[12,13] and endosomal maturation is required for stimulation[14,15]. Although TLR9 is known to be expressed intracellularly[16,17], the subcellular compartment in which TLR9 is expressed and where signaling by CpG DNA is initiated remain unknown.

Here we have investigated where TLR9 is located, whether it interacts directly with CpG DNA, and where it is activated by using genetically engineered human cell lines, primary DCs and primary macrophages. In all cell types tested, we found that TLR9 is initially located in the ER. CpG DNA is internalized via a clathrin-dependent endocytic pathway and rapidly moves into a tubular lysosomal compartment. We also show that CpG DNA directly binds to TLR9. On stimulation of DCs and macrophages with CpG DNA, both TLR9 and MyD88 are rapidly redistributed toward sites of CpG DNA accumulation. Thus, TLR9 is expressed in the ER and translocates to a CpG DNA–containing lysosomal compartment for ligand binding and signal transduction.

RESULTS

Fluorescent TLR9 is active and localized in the ER

We engineered a chimera of TLR9 and fluorescent protein by fusing the carboxy terminus of the full-length complementary DNA of TLR9 to a gene encoding a fluorescent protein (cyan fluorescent protein, CFP; green fluorescent protein, GFP; or yellow fluorescent protein, YFP). All versions of fluorescently tagged TLR9 were fully functional signaling molecules that specifically recognized CpG DNA when heterologously expressed in HEK cells (see **Supplementary Fig. 1** online).

To determine the subcellular localization of TLR9, HEK cells expressing GFP-tagged TLR9 were stained with a cell-surface fluorescent membrane marker and living cells were immediately examined by confocal microscopy. TLR9 was expressed exclusively on a large pool of intracellular interconnected membranes. These intracellular membranes showed contact with the plasma membrane in some areas (**Fig. 1a**, white arrow) but were not observed to extend

[1]University of Massachusetts Medical School, Division of Infectious Diseases and Immunology, 364 Plantation Street, Lazare Research Building 308, Worcester, Massachusetts 01605, USA. [2]Norwegian University of Science and Technology, Institute of Cancer Research and Molecular Medicine, Olav Kyrres gt. 3, N-7489 Trondheim, Norway. [3]These authors contributed equally to this work. Correspondence should be addressed to D.T.G. (douglas.golenbock@umassmed.edu).

Published online 11 January 2004; doi:10.1038/ni1028

EXHIBIT A

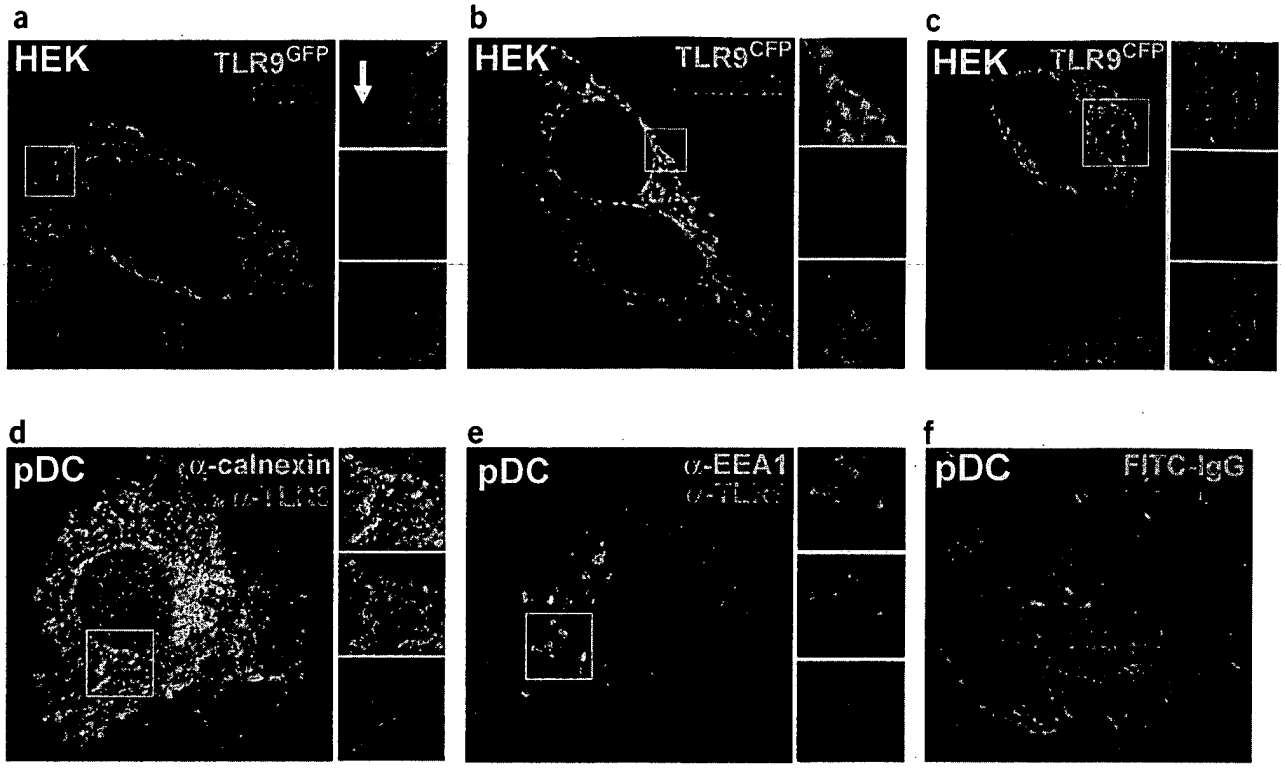

Figure 1 Fluorescently labeled TLR9 is expressed in the ER. (**a**) Confocal images of HEK cells expressing GFP-tagged TLR9 (green) stained with choleratoxin subunit B (CTXB, red). Arrow indicates contact between internal membranes (TLR9) and the plasma membrane. (**b**) Confocal images of HEK cells expressing CFP-tagged TLR9 (green) stained intracellularly for the ER protein calnexin (red). (**c**) Confocal images of HEK cells expressing YFP-tagged TLR4 (red) transiently transfected with CFP-tagged TLR9 (green). YFP-tagged TLR4 is expressed in the Golgi and on the plasma membrane[18]. (**d**) Confocal images of pDCs stained intracellularly with anti-TLR9 (red, Alexa647) and anti-calnexin (green, FITC). (**e**) Confocal images of pDCs stained with anti-TLR9 (red, Alexa647) and anti-EEA1, an early endosome marker (green, FITC). (**f**) pDCs stained with directly conjugated control antibodies.

into the plasma membrane. The expression pattern of fluorescently labeled TLR9 was similar in several different clones and different cell lines (data not shown), indicating that this pattern of protein expression is not specific to HEK cells. On the basis of the pattern of fluorescence, we considered that TLR9 might be expressed on ER membranes.

HEK cells expressing GFP-tagged TLR9 were permeabilized and counterstained with a monoclonal antibody (mAb) to calnexin, an ER-resident protein. Although the architecture of stained cells was not as crisply preserved as in living cells, TLR9 and calnexin were expressed in the same intracellular pool of ER membranes (**Fig. 1b**). We also cotransfected a construct expressing the calreticulin ER-targeting sequence fused to YFP with a construct encoding CFP-tagged TLR9. Living cells were examined by confocal microscopy and complete colocalization was observed (data not shown).

TLR4 is expressed on the plasma membrane and in the Golgi apparatus of transfected HEK cells and wild-type human monocytes[18]. We expressed CFP-tagged TLR9 in a cell line that stably expressed YFP-tagged TLR4. Overlaid confocal microscopic images of the CFP-tagged TLR9 and the YFP-tagged TLR4 chimeric proteins did not define a common area of expression (**Fig. 1c**, upper cell). Thus, using colocalization of TLR4 as a criterion of subcellular localization, we found that TLR9 is not expressed in either the plasma membrane or the Golgi apparatus. We conclude that the TLR9–fluorescent protein chimeras are expressed in the ER of quiescent HEK cells.

Expression of endogenous TLR9 in human DCs

It was possible that the subcellular localization of fluorescently tagged TLR9 might be due to overexpression or misfolding of the genetically modified protein, despite the normal function of YFP-tagged TLR9 as a CpG DNA receptor. We therefore confirmed the expression pattern of TLR9 in wild-type cells by immunofluorescence analysis of the endogenous protein. We investigated the subcellular localization of TLR9 in human plasmacytoid DCs (pDCs), because these cells express high levels of *TLR9* messenger RNA and are activated by CpG DNA[19,20]. We used an anti–human TLR9 mAb that specifically recognized heterologously expressed fluorescently tagged TLR9 in HEK cells (see **Supplementary Fig. 2** online) to stain endogenous TLR9 in pDCs.

We purified pDCs from blood mononuclear cells and allowed them to mature in culture. Confocal microscopic images showed intracellular staining of TLR9. The cells were counterstained for the ER-resident protein calnexin. The observed colocalization of the fluorescent signals showed that endogenous TLR9 is expressed in the ER of wild-type pDCs (**Fig. 1d**). A marker protein for early endosomes (EEA1) did not colocalize with TLR9 in resting cells (**Fig. 1e**), and isotype-matched control mAbs did not stain pDCs (**Fig. 1f**). Thus, endogenous and fluorescently tagged TLR9 are expressed in the ER of resting cells.

CpG DNA traffics into tubular lysosomes

We investigated the uptake pathway and trafficking of CpG DNA in cells to determine whether CpG DNA moves to the same

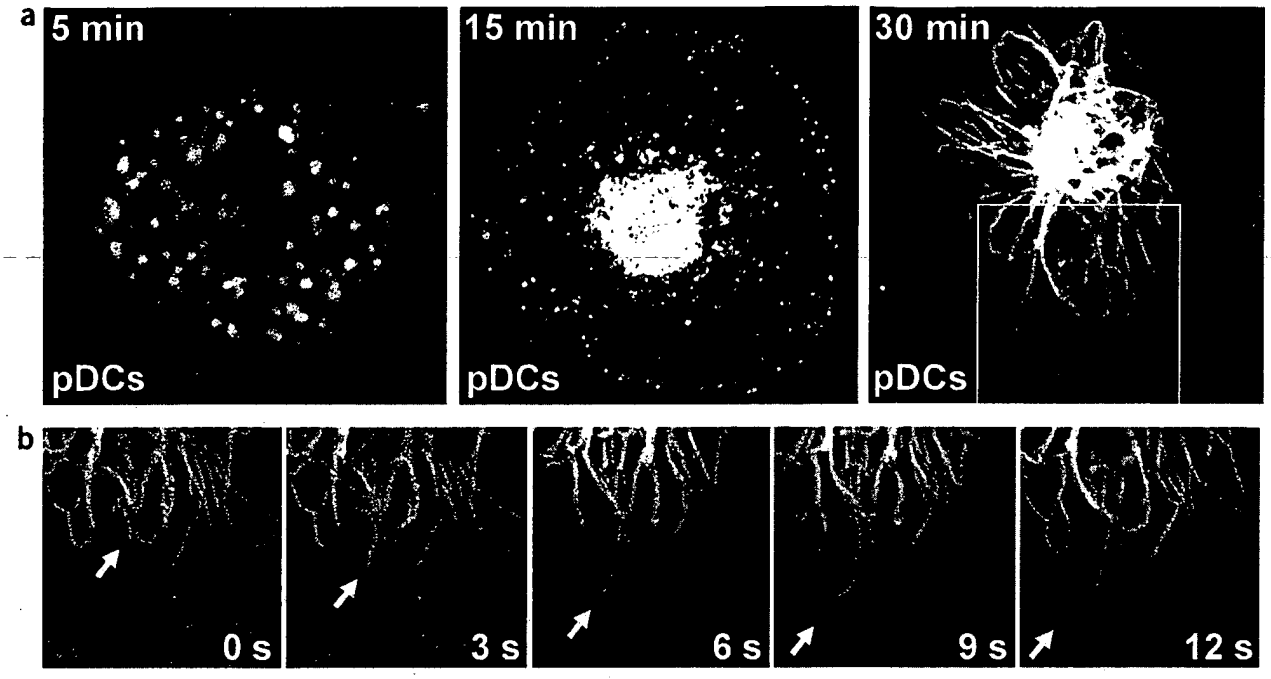

Figure 2 Fluorescent CpG DNA enters pDCs in vesicular structures and moves into a tubular compartment. (**a**) Confocal images of pDCs incubated with fluorescently labeled CpG DNA for the indicated durations. (**b**) Individual frames obtained by time-lapse confocal microscopy of a cell incubated for 30 min with CpG DNA (box in **a**).

compartment in which TLR9 is expressed. Adherent pDCs were incubated with fluorescently labeled CpG DNA for various durations and, after being washed, were observed by confocal microscopy at 37 °C.

When cells were incubated with labeled CpG DNA for a short duration (**Fig. 2a**, 5 min), small vesicular structures were observed in the cell periphery. These structures moved towards the center of the cells. Colocalization studies of cells coincubated with CpG DNA and fluorescently labeled transferrin indicated that these structures were early endosomes (**Fig. 3a**). These structures were also labeled with the phosphatidylinositol-3-phosphate (PI3P)-binding construct FYVE-GFP[21], which is used as a marker for early endosomes (**Fig. 3b**). CpG DNA–positive vesicles did not contain caveolin-1 and did not colocalize with human albumin, indicating that the uptake pathway was caveolin independent (**Fig. 3c,d**).

After 10–15 min of incubation, many of the DNA-positive vesicles were concentrated in juxtanuclear areas (**Fig. 2a**, 15 min). Tubular structures filled with CpG DNA began to appear as early as 15 min after exposure. By 30 min of incubation, almost all of the CpG DNA was localized in large tubular structures (**Fig. 2a**, 30 min). The tubules were highly motile and could be observed extending towards the cell periphery and plasma membrane and then retracting back again towards the cell center every 10–15 s. A short sequence extracted from a confocal time-lapse series is shown for a cell that was exposed to labeled CpG DNA for 30 min (**Fig. 2b**). This sequence highlights the motility of the observed tubular structures containing CpG DNA (**Fig. 2b**, white arrows). Colocalization studies of CpG DNA and fluorescently labeled dextran or ovalbumin identified these structures as the tubular lysosomal compartment (see **Supplementary Fig. 3** online).

CpG DNA binds to TLR9

To address whether the movement of CpG DNA in cells is related to TLR9 signal transduction, we exposed HEK cells expressing CFP-tagged TLR9 to CpG DNA and examined them by confocal microscopy. We found that TLR9 is actively recruited to CpG DNA–containing cellular structures from the ER (shown in detail below for primary cells). We therefore considered that these intense contact areas might be areas of ligand-receptor interaction.

We did ligand-binding studies on stably transfected HEK cell lines. HEK cells expressing YFP-tagged TLR9 or TLR4 were incubated with biotin-labeled CpG DNA 2006, which stimulates human TLR9 (ref. 8), or with the a biotin-labeled nonstimulatory GpC DNA, oligonucleotide 2006GC (see also **Supplementary Fig. 1** online). After 8 h, the cells were lysed and the biotinylated DNA was precipitated using streptavidin-coated beads. Immunoblotting showed that both the stimulatory and nonstimulatory DNA bound and captured TLR9 (**Fig. 4a**, left). In contrast, neither CpG DNA 2006 nor GpC DNA 2006GC bound or precipitated YFP-tagged TLR4 (**Fig. 4a**, right).

To eliminate the process of DNA uptake from the binding assay, we prepared cellular lysates of HEK cells expressing YFP-tagged TLR9 or TLR4 and added both stimulatory and nonstimulatory CpG DNA at 4 °C. As above, streptavidin precipitation and immunoblotting showed that both types of oligonucleotide bound to TLR9 but not to TLR4 (data not shown). We also tested whether TLR9 bound to a labeled oligonucleotide that was optimized for mouse TLR9 and its counterpart nonstimulatory GpC DNA sequence (1668 and 1668GC)[8]. All versions of the biotinylated CpG DNA and GpC DNA bound and precipitated human TLR9 (**Fig. 4b**). Thus, CpG DNA directly binds TLR9 in a CG sequence–independent manner. When the cellular lysates of YFP-tagged TLR9 expressing HEK cells were simultaneously incubated with biotinylated CpG DNA and a tenfold excess of unlabeled oligonucleotides, competitive inhibition was observed (**Fig. 4b**), indicating that the binding observed was saturable.

The ability of the various oligonucleotides to bind TLR9 suggested that each construct might be able to modulate inflammatory responses. To test this, HEK cells expressing TLR9 were incubated with CpG DNA either alone or together with increasing

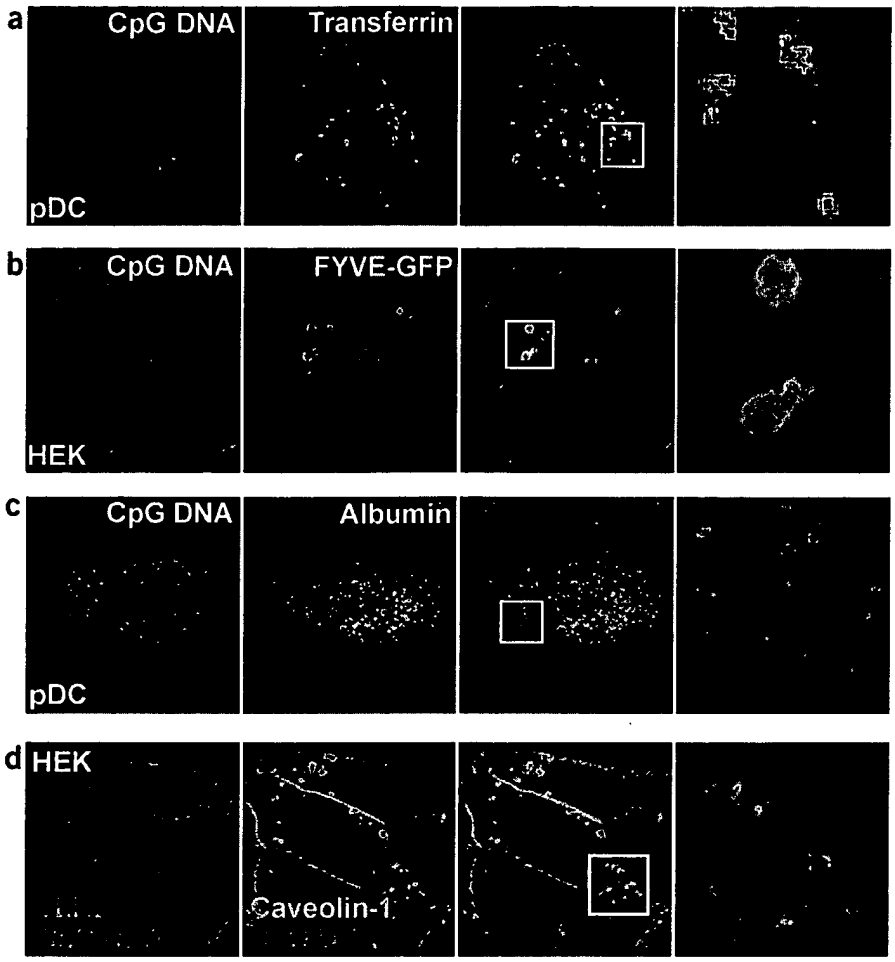

Figure 3 CpG DNA enters cells via a clathrin-dependent, caveolin-independent pathway. (**a**) Confocal images of pDCs incubated with CpG DNA (red) and transferrin (green) for 5 min. (**b**) Confocal images of HEK cells expressing FYVE-GFP, which binds to PI3P on early endosomes, incubated with CpG DNA for 5 min. (**c**) Confocal images of pDCs incubated with albumin (green), a marker for caveolae-mediated internalization, and CpG (red) for 5 min. (**d**) Confocal images of HEK cells expressing YFP-tagged TLR9 (red) and CFP-tagged caveolin-1 (green) incubated with CpG DNA (blue) for 5 min.

concentrations of nonstimulatory GpC DNA (2006GC) or the mouse optimized CpG DNA (1668), and NF-κB activation was assessed. Both GpC DNA 2006GC (**Fig. 4c**, left) and CpG DNA 1668 (**Fig. 4c**, right) potently inhibited TLR9 signaling, whereas neither oligonucleotide inhibited interleukin 1 (IL-1) signaling. Taken together, these data suggest that nonstimulatory oligonucleotides can block CpG-induced TLR9 stimulation by competing for binding to TLR9.

TLR9 and MyD88 are recruited to endocytosed CpG DNA

To investigate the spatial behavior of TLR9 and the adaptor protein MyD88 on treatment with CpG DNA, we transduced mouse bone marrow–derived DCs and macrophages with a retrovirus carrying a gene for fluorescently labeled TLR9 (**Fig. 5** and **Supplementary Fig. 4** online). In resting wild-type immune cells, YFP-tagged TLR9 was expressed in the ER (**Fig. 5a** and **Supplementary Fig. 4** online), similar to the expression of human fluorescently labeled TLR9 in HEK cells and human pDCs. In contrast, YFP-tagged TLR2 and TLR4 were both expressed on the surface of mouse DCs, and a fluorescent variant of MyD88 was ubiquitously expressed in the cytoplasm of resting cells (**Fig. 5a**). Note that TLR2 and TLR4 both recycle from the cell surface to the Golgi apparatus in resting cells[18], which accounts for the intracytoplasmic accumulations of fluorescence that are visible on close inspection (data not shown).

When mouse DCs expressing YFP-tagged TLR9 were incubated with fluorescently labeled CpG DNA, the movement of CpG DNA was identical to that observed in human pDCs (**Supplementary Fig. 4** online). We also observed a rapid reorganization of TLR9 towards the cell entry sites of CpG DNA. Extensive colocalization of fluorescently labeled TLR9 was observed in these areas as early as 5 min after the

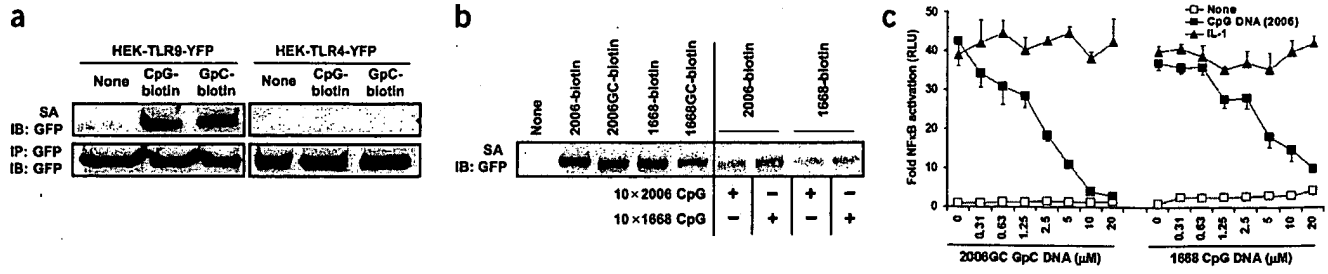

Figure 4 CpG DNA binds to TLR9. (**a**) YFP-tagged TLR9 or TLR4 expressing HEK cells were incubated with biotin–CpG DNA (2006) or biotin–GpC DNA (2006GC) for 8 h at 37 °C. Biotin-DNA was precipitated from lysates and the associated proteins were analyzed by immunoblotting for TLRs with anti-GFP. (**b**) Lysates of HEK cells expressing YFP-tagged TLR9 were incubated with different biotinylated CpG oligonucleotides. Sequence 2006 is stimulatory for human TLR9 (2006GC control) and 1668 optimally stimulates mouse TLR9 (1668GC control). After 1 h, biotinylated CpG DNA was precipitated and the associated proteins were analyzed by immunoblotting with anti-GFP. A tenfold excess of unlabeled CpG DNA was added to identically treated samples (right). (**c**) HEK cells expressing TLR9 were treated with 1 μM CpG DNA or 100 ng/ml of IL-1 in the presence of increasing doses of nonstimulatory GpC DNA or mouse TLR9–optimized CpG DNA. Cellular activation was assessed by luciferase measurements.

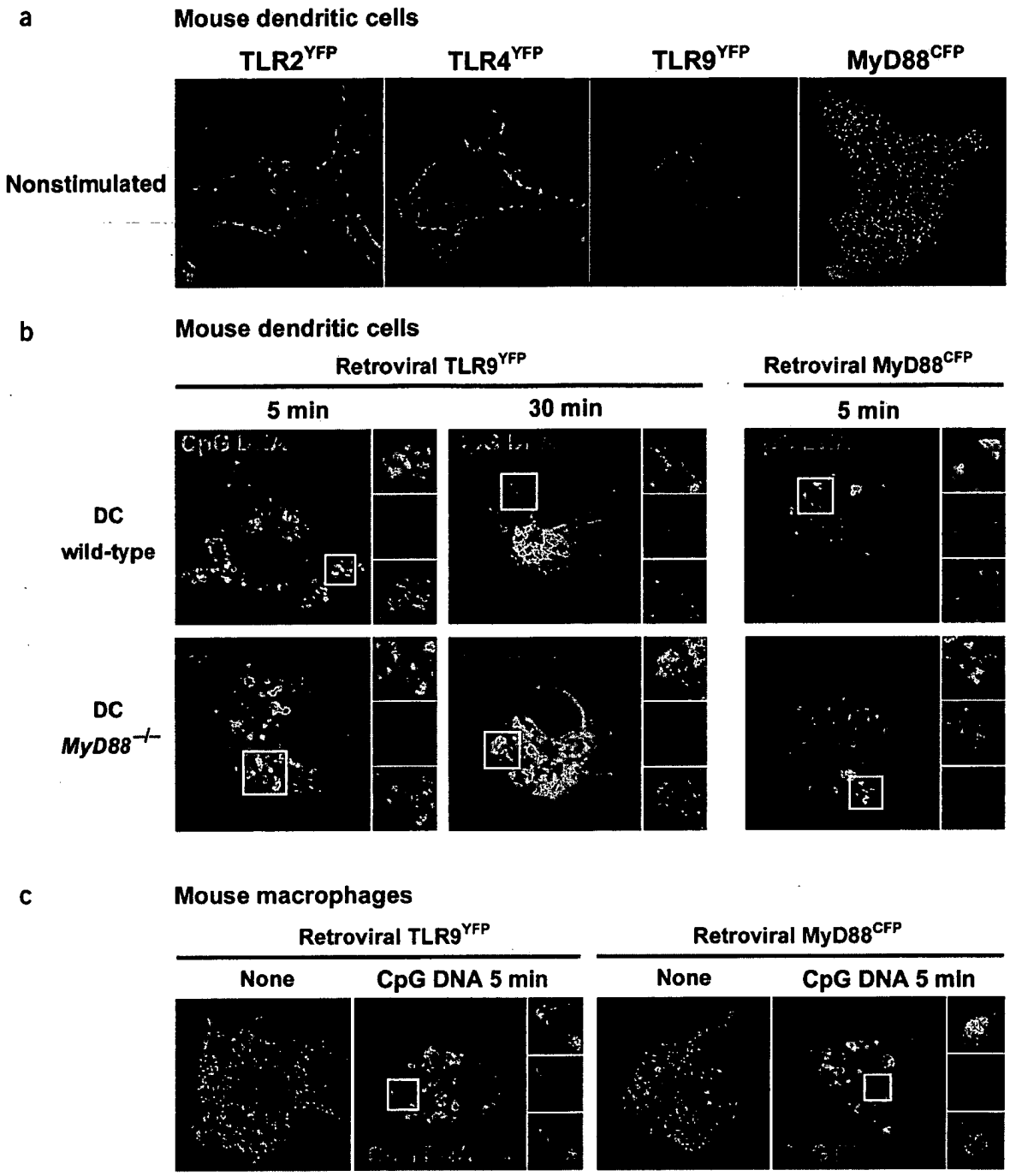

Figure 5 TLR9 and MyD88 translocate to sites of CpG DNA in a MyD88-independent manner. (**a**,**b**) Mouse DCs expressing YFP-tagged TLR2, TLR4 or TLR9, or CFP-tagged MyD88 were left untreated (**a**) or incubated with fluorescently labeled CpG DNA (**b**) for the indicated durations. DCs isolated from wild-type (**b**, top) or *Myd88*$^{-/-}$ mice (**b**, bottom) were transduced with retroviruses containing YFP-tagged TLR9 or CFP-tagged MyD88. Cells were incubated with fluorescently labeled CpG DNA for the indicated durations and living cells were analyzed by confocal microscopy. (**c**) Mouse macrophages expressing YFP-tagged TLR9 or CFP-tagged MyD88 were incubated with CpG DNA for 5 min or left untreated (none).

addition of CpG DNA (**Fig. 5b**). In addition, MyD88 was recruited to the entry site of CpG DNA in a similarly rapid time frame. After longer incubations, CpG DNA moved into tubular lysosomal structures that also contained TLR9. The observed movement of TLR9 and MyD88 to CpG DNA–containing structures was retained in DCs derived from *Myd88*-null mice (**Fig. 5b**, bottom). We observed similar redistributions of fluorescently tagged TLR9 and MyD88 in mouse macrophages (**Fig. 5c**). These results suggest that TLR9 is localized in the ER in resting cells and is rapidly recruited to the sites of CpG DNA accumulation in a MyD88-independent manner.

To investigate whether endogenous TLR9 is redistributed in a pattern similar to that of heterologously expressed fluorescently labeled TLR9, we incubated human pDCs with fluorescently labeled CpG DNA and visualized TLR9 by direct immunofluorescence. TLR9 was

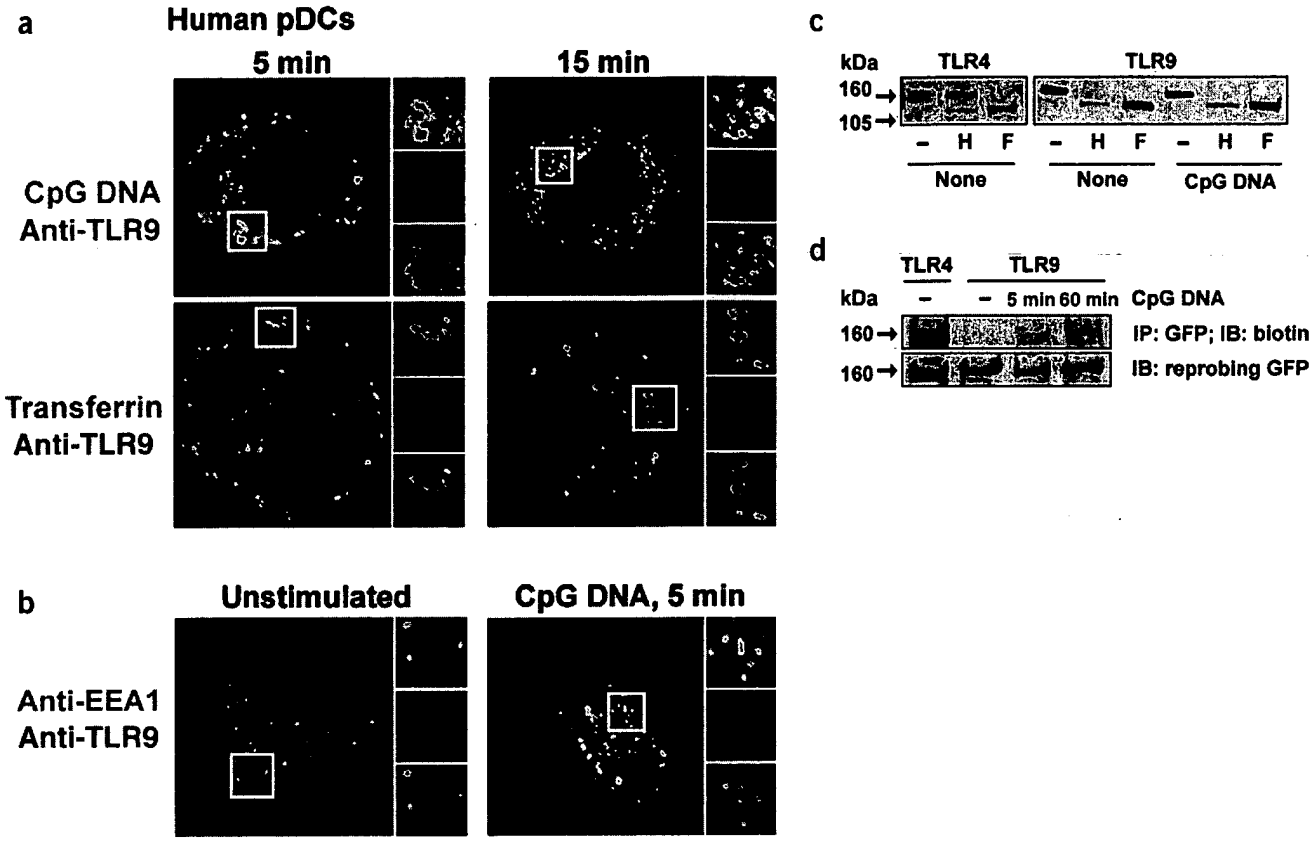

Figure 6 Endogenous TLR9 redistributes to CpG-containing compartments. (**a**) Human pDCs were incubated with Texas Red–conjugated CpG DNA or Alexa546-conjugated transferrin for the indicated durations. After fixation, TLR9 was stained intracellularly by direct immunofluorescence with anti-TLR9. (**b**) Nonstimulated pDCs or pDCs stimulated with CpG DNA for 5 min were stained with anti-TLR9 and the early endosome marker protein EEA1 (FITC) and imaged by confocal microscopy. (**c**) Stably tranfected HEK cells were grown in monolayers and left untreated or stimulated as indicated. Cells were lysed, and immunoprecipitated TLRs were left untreated (–) or were treated with endoglycosidase H (H) or peptide-*N*-glycosidase F (F). Deglycosylated or untreated TLRs were subjected to SDS-PAGE and immunoblotting for GFP. (**d**) HEK cells expressing YFP-tagged TLR4 or TLR9 were left untreated (–) or stimulated with CpG DNA (2006, 1 μM) for the indicated durations. The surfaces of cooled cells were labeled with biotin and total TLRs were immunoprecipitated and subjected to SDS-PAGE. Membranes were probed for biotin and reprobed for TLRs via anti-GFP.

recruited—like its fluorescent counterpart—to CpG DNA as early as 5 min after incubation, and followed CpG to intracellular compartments. In contrast, when pDCs were incubated with fluorescently labeled transferrin, which also results in the formation of early endosomes, no colocalization of TLR9 with transferrin was observed (**Fig. 6a**). When resting pDCs were stained for both TLR9 and the early endosome marker protein EEA1, TLR9 was excluded from the early endosome compartment. As early as 5 min after CpG DNA stimulation, however, a portion of TLR9 was detected in an EEA1-positive compartment (**Fig. 6b**). These observations indicate the specificity of this translocation event.

We investigated the mechanism by which TLR9 reaches the endosomal compartment from the ER after stimulation. One possibility was that TLR9 might be released from the ER and reach the endosomal pathway through the Golgi apparatus. Proteins that are targeted to the plasma membrane are normally released from the ER and travel through the Golgi apparatus via the secretory pathway. To test whether TLR9 enters the secretory pathway, we used the glycosidases endoglycosidase H (Endo H) and peptide-*N*-glycosidase F (PGNase F). Whereas PGNase F cleaves all ER- and Golgi-derived carbohydrate modifications, Endo H loses its ability to cleave carbohydrate species once they have been modified by Golgi-localized enzymes[22].

Fluorescently tagged TLR4 and TLR9 were immunoprecipitated and incubated in the presence or absence of Endo H or PGNase F. The molecular masses of the treated proteins were then examined by SDS-PAGE and immunoblotting. PGNase F treatment resulted in complete cleavage of the carbohydrate modifications of both YFP-tagged TLR4 and TLR9 (**Fig. 6c**, 'F'). In contrast, only a few of the TLR4 molecules were cleaved by Endo H treatment, indicating that TLR4 enters the secretory pathway. Conversely, all of the carbohydrate modifications of TLR9 were cleaved by Endo H (**Fig. 6c**, 'H'). Thus, TLR9 does not enter the secretory pathway. The lack of TLR9 expression in the Golgi, observed by confocal microscopy (**Fig. 1c**), correlates with the complete sensitivity of TLR9 to Endo H. TLR9 moved out of the ER in CpG DNA–stimulated cells but did not acquire Endo H resistance, providing evidence against a role of the secretory pathway in TLR9 redistribution to CpG DNA–containing compartments.

An alternative possibility for the mechanism by which TLR9 translocates to CpG DNA–containing compartments was that the ER might fuse with the plasma membrane and contribute its membranes to the developing endosomes. A similar mechanism has been proposed for phagocytic uptake pathways[23,24]. During these fusion events, ER proteins can leak into the plasma membrane in small

quantities, as has been observed for the ER-resident protein calnexin. To test this possibility, we labeled the surface of HEK cells expressing YFP-tagged TLR9 with biotin and either left them untreated or stimulated them with CpG DNA. After CpG stimulation, a small portion of the total TLR9 (**Fig. 6d**) expressed in these cells became surface accessible, as judged by the acquisition of biotin. Thus, TLR9 is likely to access the developing endosome by fusing with the plasma membrane.

DISCUSSION

TLR9 is widely referred to as a receptor for bacterial DNA[5,7], although it also has been implicated in the recognition of viral DNA[25]. Owing to the nature of their hosts, both bacterial DNA and viral DNA are not immediately accessible for recognition. DNA must be released from microbes before it can interact with its mammalian receptors. Although there is consensus that TLR9 signaling takes place in intracellular compartments, the subcellular expression and signaling mechanism of TLR9 have not been elucidated in detail.

Our data show that TLR9 is located in the ER of resting cells, including transfected cell lines, primary DCs and macrophages. The expression of TLR9 in the ER contrasts sharply with the expression pattern of other TLRs such as TLR2 and TLR4, which both enter the secretory pathway and travel to the plasma membrane[18,26], where they recognize their ligands and initiate cellular activation[18,26,27].

We have provided evidence that CpG DNA is internalized into a subcellular compartment and this is followed by the apparent translocation of its binding receptor to the same compartment. As CpG DNA is internalized, the distribution of TLR9 changes, with a portion of the total protein moving first into early endosomes and later into the tubular lysosomal compartment. The importance of TLR9 movement to the CpG-rich compartments seems to be to enable CpG-TLR9 binding to occur and signal transduction to be initiated. Our binding assays of CpG DNA–TLR9 interactions successfully predicted the pharmacological responses of cells to various CpG oligonucleotides, including the ability of nonstimulatory GpC DNA to interfere with signal transduction induced by CpG DNA. Further evidence that signal transduction begins in these CpG-rich compartments is the rapid appearance of MyD88 in the same area. Although this mechanism of cellular activation seems to be unique, TLR9 shares many properties with TLR7 and TLR8 (ref. 28), raising the possibility that other receptors may share a similar mechanism of activation.

There are several possible ways that proteins can reach lysosomal compartments from the ER. For example, lysosomes can be accessed via the secretory pathway[29], whereby proteins travel via the Golgi to the plasma membrane, where they are internalized and shuttled to their destination by means of sequence-inherent lysosomal sorting motifs. Our biochemical studies with endoglycosidases suggest that TLR9 does not enter the secretory pathway, because TLR9—in both resting and CpG DNA–stimulated cells—does not acquire Endo H resistance.

It has been shown in a proteomics approach that, unexpectedly, phagosomes contain several ER-resident proteins[30]. These results have been followed by electron microscopic studies showing that the ER is recruited to the phagosome and that ER membranes are a chief source of phagocytic membranes in macrophages and cell lines[23,24]. These ER-phagosome fusion events have been implicated as having profound physiological importance for the process of cross-presentation in DCs[31,32]. During ER-phagosome fusion, ER-resident proteins and MHC class I molecules become part of the membrane of the phagosome. Thus, the phagosome can become an antigen-presenting organelle that acquires proteins for cross-presentation by fusion with the ER.

In an analogous scheme, TLR9 (and potentially other ER-resident TLRs) might become accessible to endosomal and lysosomal compartments after the ER fuses with sites of microbial cell entry. Thus, we propose that ER-phagosome fusion contributes not only to antigen presentation but also to microbial recognition by Toll receptors. We observed that TLR9 is absent from the plasma membrane; however, our surface biotinylation studies in stimulated TLR9-expressing cells showed that a small portion of TLR9 becomes surface accessible after exposure to CpG DNA, similar to previous observations that small amounts of ER-resident proteins can be detected on the plasma membrane[33,34]. This suggests that, on exposure to CpG DNA, fusion events occur between the ER and the plasma membrane, as well as between the ER and the lysosomal compartment.

Our studies resolve the issue of whether TLR9 and CpG DNA actually bind one another. The observation that the binding of CpG DNA to TLR9 is sequence independent raises the possibility that more potent inhibitors of signal transduction might be found by using this or a related assay as the basis of a pharmacological screen. Clearly, candidate molecules do not need to have CpG-related motifs, which greatly expands the possible types of structures that might be therapeutic for DNA-related chronic inflammatory diseases such as systemic lupus erythematosis[35]. The tools available to translate our knowledge of CpG DNA into the therapeutic arena are now substantial. We are optimistic that, as we proceed forward, the development of new clinical agents will lead to a better understanding of the biology of CpG DNA. Such therapeutic agents are likely to shed light on the true role of TLR9 in health and disease, a fundamental issue to which there is still no obvious resolution.

METHODS

Reagents. Phosphothioate CpG DNA was from MWG Biotech. We labeled DNA at the 3′-prime end with either fluorescent tags or biotin. The sequences of stimulatory CpG DNA have been published[8]. Rhodamine-labeled choleratoxin subunit B was from List Biological Laboratories. Fluorescently labeled transferrin and dextran, DQ-ovalbumin, ER-Tracker Blue White DPX, Mitotracker Red, polyclonal antibodies to GFP and ethidium monoazide were from Molecular Probes. We purchased IL-3 and granulocyte-macrophage colony-stimulating factor from Peprotech. Polyclonal antibodies to calnexin were from Stressgen. Fluorescein isothiocyanate (FITC)-conjugated calnexin mAb (clone 37), FITC-conjugated anti-EEA1 (clone 14) and anti-GFP (clone JL-8) were from Transduction Labs. Anti–human TLR9 (eB72-1665) was from eBiosciences. We obtained Sulfo-NHS-Biotin from Pierce. Endoglycosidase H and peptide–*N*-glycosidase F were from New England Biolabs.

Fluorescent DNA constructs. The fluorescently tagged TLR2 and TLR4 constructs have been described[18]. We used PCR to construct chimeric fluorescently labeled cDNAs of TLR9. The primers for TLR9 were 5′-GAAGCCCCTGCCCG GATCCATGGGTTTCTGC-3′ and 5′-TCCGGCTCACTCGAGTTCGGCCGTG GGTCCCTG-3′. PCR fragments were cloned into the *Bam*HI and *Xho*I sites of pcDNA3-CFP, pcDNA3-YFP and pcDNA3-GFP[18]. Retroviral constructs containing CFP-tagged TLR9 and CFP-tagged MyD88 were constructed similarly, and PCR products were cloned into peak12mmp.

Cellular activation assays. Cellular activation was assessed by an NF-κB–luciferase reporter assay as described[18].

Isolation and culture of pDCs. We purified pDCs from human peripheral blood mononuclear cells with anti-BDCA4–coated microbeads (Miltenyi

Biotech). Cells were consistently 95–98% pure, as assessed by flow cytometry. The pDCs were cultured in RPMI 1640 supplemented with 10% fetal bovine serum, 2 mM L-glutamine, 110 μg/ml of sodium pyruvate, 10 μg/ml of ciprofloxacin and 10 ng/ml of IL-3 at a cell density of 5×10^5 cells/ml at 37 °C and 5% CO_2 for 7 d.

Viral transduction of mouse DCs. To produce recombinant viruses, 293 T EBNA cells were cotransfected with a peak12mmp plasmid encoding YFP-tagged TLR9 or CFP-tagged MyD88 and plasmids carrying the retroviral *gag-pol* genes and the envelope protein VSV-G. The virus-containing supernatant was diluted 1:2 in cell culture medium, and Polybrene was added to a final concentration of 8 μg/ml. Mouse DCs were derived from bone marrow[7] of C57BL/6 mice or mice homozygous null for the myeloid differentiation primary response gene 88 (*Myd88*$^{-/-}$ mice; five generations backcrossed) and transduced on day 2 of culture.

Confocal microscopy. We used an inverted Axiovert 100-M microscope equipped with a Zeiss LSM 510 META scanning unit and a 1.4 NA 63× plan apochromat objective (Zeiss), and an inverted Leica LSM TSC SP2 AOBS. Cells were cultured on glass-bottom 35-mm tissue-culture dishes (Mattek). Dual or triple color images were acquired by consecutive scanning with only one laser line active per scan to avoid cross-excitation.

CpG-DNA uptake assays. On day 7 of culture, adherent pDCs were incubated with 3 μM fluorescently labeled CpG DNA in growth medium for various durations. Washed cells were imaged immediately by confocal microscopy at 37 °C. Fluorescently labeled CpG DNA (3 μM) was coincubated with fluorescently labeled transferrin or human albumin (10 μg/ml). We labeled the lysosomal compartment in DCs by incubating cells with 250 μg/ml of fluorescently labeled dextran for 30 min (ref. 36). Alternatively, cells were incubated with DQ-ovalbumin (5 μg/ml) for 30 min before imaging.

Immunofluorescence. Cells were either fixed by incubation in PBS containing 2% freshly prepared paraformaldehyde at 20 °C for 20 min or by incubation in 100% methanol at −20 °C for 60–90 s. Cells were washed extensively and nonspecific antibody-binding sites were blocked with PBS containing 0.25% saponin, 1% bovine serum albumin and 2.5% human serum for 15–30 min at 20 °C. We stained cells by incubating them with antibody in blocking buffer at 25 °C for 45 min.

Ligand-binding studies. Monolayers of cells expressing chimeric TLRs were incubated for 8 h with 5 μM biotinylated CpG DNA before lysis[18] and subjected to microcentrifugation to remove nuclear debris. Alternatively, clarified cellular lysates were incubated with 5 μM biotinylated CpG DNA. Streptavidin-coated beads (25 μl of a 50% suspension) were added to 500 μl of lysate and rotated for 1 h at 4 °C. Alternatively, lysates were incubated with polyclonal antibody to GFP and 40 μl of packed protein A–Sepharose at 4 °C for 1 h to assess overall amounts of the chimeric TLRs. Pellets were washed four times in lysis buffer, resolved by SDS-PAGE and transferred to HyBond C nitrocellulose membranes (Amersham Biosciences). Membranes were blocked in 5% powdered milk and blotted with GFP mAb. The blots were then incubated with horseradish peroxidase (HRP)-conjugated anti-mouse and developed on Hyperfilm with the enhanced chemiluminescence HRP substrate system (Amersham Biosciences).

Surface biotinylation and deglycosylation experiments. Resting or CpG-stimulated cells grown on tissue-culture dishes were cooled on ice, washed three times with ice-cold HBSS buffer and incubated with 1 mg/ml of Sulfo-NHS-Biotin in HBSS for 30 min on ice. After cells were washed twice in ice-cold HBSS, free reactive biotin was quenched by incubation with ice-cold 1 M Tris-HCl (pH 8) for 5 min. The cells were lysed in lysis buffer and fluorescently labeled TLRs were immunoprecipitated by anti-GFP. Biotin immunoreactivity was assessed by immunoblotting with anti–biotin-HRP. The membranes were stripped and reprobed with anti-GFP to determine the total expression of the TLRs.

We assessed the glycosylation state of the TLRs by incubating immunoprecipitated and denatured TLR9 or TLR4 (via anti-GFP) with endoglycosidase H or peptide–*N*-glycosidase F for 1 h at 37 °C. The proteins were separated by SDS-PAGE and electrophoretic mobility was assessed by imunoblotting for GFP.

Note: Supplementary information is available on the Nature Immunology website.

ACKNOWLEDGMENTS

We thank K. Halmen, L. Ryan, R. Vik and K. Egeberg for technical support; S. Akira (Osaka University, Osaka, Japan) for the full-length TLR9 cDNA and the *MyD88*-deficient mice; S. Ishizaka (Eisai Research Institute, Andover, Massachusetts, USA) for the HEK–TLR9–NF-κB–luc reporter cell line; B. Seed (Harvard University and Massachusetts General Hospital, Boston, Massachusetts, USA) for the retroviral vector peak12mmp; N. Aliverdi (eBiosciences, San Diego, California, USA) for TLR9 mAbs; A. Sundan (Norwegian Institute of Science and Technology, Trondheim, Norway) for antibody labeling; and H. Stenmark (Norwegian Radium Hospital, Oslo, Norway) for the FYVE-GFP construct. This work was supported by grants from the National Institute of Health (D.T.G), the Commission of the European Communities (T.E. and D.T.G.), the Norwegian Research Council and the Norwegian Cancer Society (T.E.), and by the German Academic Exchange Program (E.L).

COMPETING INTERESTS STATEMENT

The authors declare that they have no competing financial interests.

Received 8 September; accepted 24 November 2003
Published online at http://www.nature.com/natureimmunology/

1. Tokunaga, T. *et al.* Antitumor activity of deoxyribonucleic acid fraction from *Mycobacterium bovis* BCG. I. Isolation, physicochemical characterization, and antitumor activity. *J. Natl. Cancer Inst.* **72**, 955–962 (1984).
2. Yamamoto, S., Kuramoto, E., Shimåda, S. & Tokunaga, T. In vitro augmentation of natural killer cell activity and production of interferon-α/β and -γ with deoxyribonucleic acid fraction from *Mycobacterium bovis* BCG. *Jpn. J. Cancer Res.* **79**, 866–873 (1988).
3. Krieg, A.M. *et al.* CpG motifs in bacterial DNA trigger direct B-cell activation. *Nature* **374**, 546–549 (1995).
4. Agrawal, S. & Kandimalla, E.R. Medicinal chemistry and therapeutic potential of CpG DNA. *Trends Mol. Med.* **8**, 114–121 (2002).
5. Krieg, A.M. CpG motifs in bacterial DNA and their immune effects. *Annu. Rev. Immunol.* **20**, 709–760 (2002).
6. Gordon, S. Pattern recognition receptors: doubling up for the innate immune response. *Cell* **111**, 927–930 (2002).
7. Hemmi, H. *et al.* A Toll-like receptor recognizes bacterial DNA. *Nature* **408**, 740–745 (2000).
8. Bauer, S. *et al.* Human TLR9 confers responsiveness to bacterial DNA via species-specific CpG motif recognition. *Proc. Natl. Acad. Sci. USA* **98**, 9237–9242 (2001).
9. Tauszig, S., Jouanguy, E., Hoffmann, J.A. & Imler, J.L. Toll-related receptors and the control of antimicrobial peptide expression in *Drosophila*. *Proc. Natl. Acad. Sci. USA* **97**, 10520–10525 (2000).
10. Weber, A.N. *et al.* Binding of the *Drosophila* cytokine Spatzle to Toll is direct and establishes signaling. *Nat. Immunol.* **4**, 794–800 (2003).
11. Manzel, L. & Macfarlane, D.E. Lack of immune stimulation by immobilized CpG-oligodeoxynucleotide. *Antisense Nucleic Acid Drug. Dev.* **9**, 459–464 (1999).
12. Yamamoto, T., Yamamoto, S., Kataoka, T. & Tokunaga, T. Lipofection of synthetic oligodeoxyribonucleotide having a palindromic sequence of AACGTT to murine splenocytes enhances interferon production and natural killer activity. *Microbiol. Immunol.* **38**, 831–836 (1994).
13. Gursel, I., Gursel, M., Ishii, K.J. & Klinman, D.M. Sterically stabilized cationic liposomes improve the uptake and immunostimulatory activity of CpG oligonucleotides. *J. Immunol.* **167**, 3324–3328 (2001).
14. Hacker, H. *et al.* CpG-DNA-specific activation of antigen-presenting cells requires stress kinase activity and is preceded by non-specific endocytosis and endosomal maturation. *EMBO J.* **17**, 6230–6240 (1998).
15. Yi, A.K. *et al.* CpG motifs in bacterial DNA activate leukocytes through the pH-dependent generation of reactive oxygen species. *J. Immunol.* **160**, 4755–4761 (1998).
16. Ahmad-Nejad, P. *et al.* Bacterial CpG-DNA and lipopolysaccharides activate Toll-like receptors at distinct cellular compartments. *Eur. J. Immunol.* **32**, 1958–1968 (2002).
17. Takeshita, F. *et al.* Cutting edge: Role of Toll-like receptor 9 in CpG DNA–induced activation of human cells. *J. Immunol.* **167**, 3555–3558 (2001).
18. Latz, E. *et al.* Lipopolysaccharide rapidly traffics to and from the Golgi apparatus with the Toll-like receptor 4–MD-2–CD14 complex in a process that is distinct from the initiation of signal transduction. *J. Biol. Chem.* **277**, 47834–47843 (2002).
19. Hornung, V. *et al.* Quantitative expression of Toll-like receptor 1–10 mRNA in cellular subsets of human peripheral blood mononuclear cells and sensitivity to CpG oligodeoxynucleotides. *J. Immunol.* **168**, 4531–4537 (2002).
20. Kadowaki, N. *et al.* Subsets of human dendritic cell precursors express different Toll-like receptors and respond to different microbial antigens. *J. Exp. Med.* **194**, 863–869 (2001).

21. Stenmark, H., Aasland, R. & Driscoll, P.C. The phosphatidylinositol 3-phosphate-binding FYVE finger. *FEBS Lett.* **513**, 77–84 (2002).
22. Helenius, A. & Aebi, M. Intracellular functions of *N*-linked glycans. *Science* **291**, 2364–2369 (2001).
23. Desjardins, M. ER-mediated phagocytosis: a new membrane for new functions. *Nat. Rev. Immunol.* **3**, 280–291 (2003).
24. Gagnon, E. *et al.* Endoplasmic reticulum–mediated phagocytosis is a mechanism of entry into macrophages. *Cell* **110**, 119–131 (2002).
25. Lund, J., Sato, A., Akira, S., Medzhitov, R. & Iwasaki, A. Toll-like receptor 9–mediated recognition of herpes simplex virus-2 by plasmacytoid dendritic cells. *J. Exp. Med.* **198**, 513–520 (2003).
26. Flo, T.H. *et al.* Involvement of Toll-like receptor (TLR) 2 and TLR4 in cell activation by mannuronic acid polymers. *J. Biol. Chem.* **277**, 35489–35495 (2002).
27. Underhill, D.M. *et al.* The Toll-like receptor 2 is recruited to macrophage phagosomes and discriminates between pathogens. *Nature* **401**, 811–815 (1999).
28. Lee, J. *et al.* Molecular basis for the immunostimulatory activity of guanine nucleoside analogs: activation of Toll-like receptor 7. *Proc. Natl. Acad. Sci. USA* **100**, 6646–6651 (2003).
29. Mellman, I. Endocytosis and molecular sorting. *Annu. Rev. Cell. Dev. Biol.* **12**, 575–625 (1996).
30. Garin, J. *et al.* The phagosome proteome: insight into phagosome functions. *J. Cell. Biol.* **152**, 165–180 (2001).
31. Guermonprez, P. *et al.* ER-phagosome fusion defines an MHC class I cross-presentation compartment in dendritic cells. *Nature* **425**, 397–402 (2003).
32. Houde, M. *et al.* Phagosomes are competent organelles for antigen cross-presentation. *Nature* **425**, 402–406 (2003).
33. Okazaki, Y., Ohno, H., Takase, K., Ochiai, T. & Saito, T. Cell surface expression of calnexin, a molecular chaperone in the endoplasmic reticulum. *J. Biol. Chem.* **275**, 35751–35758 (2000).
34. Johnson, S., Michalak, M., Opas, M. & Eggleton, P. The ins and outs of calreticulin: from the ER lumen to the extracellular space. *Trends Cell. Biol.* **11**, 122–129 (2001).
35. Leadbetter, E.A. *et al.* Chromatin-IgG complexes activate B cells by dual engagement of IgM and Toll-like receptors. *Nature* **416**, 603–607 (2002).
36. Chow, A., Toomre, D., Garrett, W. & Mellman, I. Dendritic cell maturation triggers retrograde MHC class II transport from lysosomes to the plasma membrane. *Nature* **418**, 988–994 (2002).

Received 19 July; accepted 20 September 2000.

1. Parekh, A. B. & Penner, R. Store depletion and calcium influx. *Physiol. Rev.* **77**, 901–930 (1997).
2. Connolly, T. M., Bansal, V. S., Bross, T. E., Irvine, R. F. & Majerus, P. W. The metabolism of tris- and tetraphosphates of inositol by 5-phosphomonoesterase and 3-kinase enzymes. *J. Biol. Chem.* **262**, 2146–2149 (1987).
3. Irvine, R. F. & Moor, R. M. Micro-injection of inositol 1,3,4,5-tetrakisphosphate activates sea urchin eggs by a mechanism dependent on external Ca^{2+}. *Biochem. J.* **240**, 917–920 (1986).
4. Morris, A. P., Gallacher, D. V., Irvine, R. F. & Petersen, O. H. Synergism of inositol trisphosphate and tetrakisphosphate in activating Ca^{2+}-dependent K^+ channels. *Nature* **330**, 653–655 (1987).
5. Bird, G. S. *et al.* Activation of Ca^{2+} entry into acinar cells by a non-phosphorylatable inositol trisphosphate. *Nature* **352**, 162–165 (1991).
6. Smith, P. M., Harmer, A. R., Letcher, A. J. & Irvine, R. F. The effect of inositol 1,3,4,5-tetrakisphosphate on inositol trisphosphate-induced Ca^{2+} mobilization in freshly isolated and cultured mouse lacrimal acinar cells. *Biochem. J.* **347**, 77–82 (2000).
7. Fukuda, M. & Mikoshiba, K. The function of inositol high polyphosphate binding proteins. *BioEssays* **19**, 593–603 (1997).
8. Cullen, P. J. Bridging the GAP in inositol 1,3,4,5-tetrakisphosphate signalling. *Biochim. Biophys. Acta* **1436**, 35–47 (1998).
9. Hoth, M. & Penner, R. Depletion of intracellular calcium stores activates a calcium current in mast cells. *Nature* **355**, 353–356 (1992).
10. Parekh, A. B., Fleig, A. & Penner, R. The store-operated calcium current I_{CRAC}: nonlinear activation by $InsP_3$ and dissociation from calcium release. *Cell* **89**, 973–980 (1997).
11. Broad, L. M., Armstrong, D. L. & Putney, J. W. Role of the inositol 1,4,5-trisphosphate receptor in Ca^{2+} feedback Inhibition of calcium release-activated calcium current I_{CRAC}. *J. Biol. Chem.* **274**, 32881–32888 (1999).
12. Glitsch, M. D. & Parekh, A. B. Ca^{2+} store dynamics determines the pattern of activation of the store-operated Ca^{2+} current I_{CRAC} in response to $InsP_3$ in rat basophilic leukaemia cells. *J. Physiol. (Lond.)* **523**, 283–290 (2000).
13. Jones, S. V., Choi, O. H. & Beaven, M. A. Carbachol induces secretion in a mast cell line (RBL-2H3) transfected with the M1 muscarinic receptor gene. *FEBS Lett.* **289**, 47–50 (1991).
14. Lewis, R. S. & Cahalan, M. D. Potassium and calcium channels in lymphocytes. *Annu. Rev. Immunol.* **13**, 623–653 (1995).
15. Hirata, M. *et al.* Inositol 1,4,5-trisphosphate receptor subtypes differentially recognize regioisomers of D-*myo*-inositol 1,4,5-trisphosphate. *Biochem. J.* **328**, 93–98 (1997).
16. Guillemette, G., Favreau, I., Lamontagne, S. & Boulay, G. 2,3-Diphosphoglycerate is a nonselective inhibitor of inositol 1,4,5-trisphosphate action and metabolism. *Eur. J. Pharmacol.* **188**, 251–260 (1990).
17. Safrany, S. T. *et al.* Design of potent and selective inhibitors of *myo*-inositol 1,4,5-trisphosphate 5-phosphatase. *Biochemistry* **33**, 10763–10769 (1994).
18. Wojcikiewicz, R. J. Type I, II, and III inositol 1,4,5-trisphosphate receptors are unequally susceptible to down-regulation and are expressed in markedly different proportions in different cell types. *J. Biol. Chem.* **270**, 11678–11683 (1995).
19. De Smedt, H. *et al.* Determination of relative amounts of inositol trisphosphate receptor mRNA isoforms by ratio polymerase chain reaction. *J. Biol. Chem.* **269**, 21691–21698 (1994).
20. Bird, G. S. & Putney, J. W. Jr. Effect of inositol 1,3,4,5-tetrakisphosphate on inositol trisphosphate-activated Ca^{2+} signaling in mouse lacrimal acinar cells. *J. Biol. Chem.* **271**, 6766–6770 (1996).
21. Communi, D., Dewaste, V. & Erneux, C. Calcium-calmodulin-dependent protein kinase II and protein kinase C- mediated phosphorylation and activation of D-*myo*-inositol 1,4,5-trisphosphate 3-kinase B in astrocytes. *J. Biol. Chem.* **274**, 14734–14742 (1999).
22. De Smedt, F. *et al.* Isoprenylated human brain type I inositol 1,4,5-trisphosphate 5- phosphatase controls Ca^{2+} oscillations induced by ATP in Chinese hamster ovary cells. *J. Biol. Chem.* **272**, 17367–17375 (1997).
23. Parekh, A. B. & Penner, R. Depletion-activated calcium current is inhibited by protein kinase in RBL-2H3 cells. *Proc. Natl Acad. Sci. USA* **92**, 7907–7911 (1995).
24. Hughes, A. R., Takemura, H. & Putney, J. W. Jr. Kinetics of inositol 1,4,5-trisphosphate and inositol cyclic 1:2,4,5-trisphosphate metabolism in intact rat parotid acinar cells. Relationship to calcium signalling. *J. Biol. Chem.* **263**, 10314–10319 (1988).
25. da Silva, C. P., Emmrich, F. & Guse, A. H. Adriamycin inhibits inositol 1,4,5-trisphosphate 3-kinase activity *in vitro* and blocks formation of inositol 1,3,4,5-tetrakisphosphate in stimulated Jurkat T-lymphocytes. Does inositol 1,3,4,5-tetrakisphosphate play a role in Ca^{2+}-entry? *J. Biol. Chem.* **269**, 12521–12526 (1994).
26. Balla, T. *et al.* Agonist-induced calcium signaling is impaired in fibroblasts overproducing inositol 1,3,4,5-tetrakisphosphate. *J. Biol. Chem.* **266**, 24719–24726 (1991).
27. Riley, A. M., Mahon, M. F. & Potter, B. V. L. Rapid synthesis of the enantiomers of *myo*-inositol 1,3,4,5-tetrakisphosphate by direct chiral desymmetrization of *myo*-inositol orthoformate. *Angew. Chem. Int. Edn. Eng.* **36**, 1472–1474 (1997).
28. Yoshimura, K., Watanabe, Y., Erneux, C. & Hirata, M. Use of phosphorofluoridate analogues of D-*myo*-inositol 1,4,5-trisphosphate to assess the involvement of ionic interactions in its recognition by the receptor and metabolising enzymes. *Cell. Signal.* **11**, 117–125 (1999).
29. Worley, P. F., Baraban, J. M., Supattapone, S., Wilson, V. S. & Snyder, S. H. Characterization of inositol trisphosphate receptor binding in brain. Regulation by pH and calcium. *J. Biol. Chem.* **262**, 12132–12136 (1987).

Acknowledgements

We would like to thank D. Tani and M. Monteilh-Zoller for technical assistance; C. Erneux for the $InsP_3$ 5-phosphatase plasmid ECH10; the Wellcome Trust for Programme Grant Support (to B.V.L.P.). We acknowledge grant support by the Ministry of Education, Science, Sports and Culture of Japan (to H.T. and M.H.), Kyushu University Interdisciplinary Programs in Education and Projects in Research Development (to M.H.) and The Naito Foundation (to M.H.).

Correspondence should be addressed to R.P. (e-mail: rpenner@hawaii.edu) and requests for materials should be addressed to B.V.L.P. (e-mail: prsbvlp@bath.ac.uk).

A Toll-like receptor recognizes bacterial DNA

Hiroaki Hemmi*†, Osamu Takeuchi*†, Taro Kawai*†, Tsuneyasu Kaisho*†, Shintaro Sato*†, Hideki Sanjo*†, Makoto Matsumoto*†, Katsuaki Hoshino*†, Hermann Wagner‡, Kiyoshi Takeda*† & Shizuo Akira*†

* *Department of Host Defense, Research Institute for Microbial Diseases, Osaka University and † Core Research for Evolutional Science and Technology, Japan Science and Technology Corporation, 3-1 Yamada-oka, Suita, Osaka 565-0871, Japan*

‡ *Institute of Medical Microbiology, Immunology and Hygiene, Technical University of Munich, Trogerstr. 9, D-81675 Munich, Germany*

DNA from bacteria has stimulatory effects on mammalian immune cells[1–3], which depend on the presence of unmethylated CpG dinucleotides in the bacterial DNA. In contrast, mammalian DNA has a low frequency of CpG dinucleotides, and these are mostly methylated; therefore, mammalian DNA does not have immuno-stimulatory activity. CpG DNA induces a strong T-helper-1-like inflammatory response[4–7]. Accumulating evidence has revealed the therapeutic potential of CpG DNA as adjuvants for vaccination strategies for cancer, allergy and infectious diseases[8–10]. Despite its promising clinical use, the molecular mechanism by which CpG DNA activates immune cells remains unclear. Here we show that cellular response to CpG DNA is mediated by a Toll-like receptor, TLR9. TLR9-deficient ($TLR9^{-/-}$) mice did not show any response to CpG DNA, including proliferation of splenocytes, inflammatory cytokine production from macrophages and maturation of dendritic cells. $TLR9^{-/-}$ mice showed resistance to the lethal effect of CpG DNA without any elevation of serum pro-inflammatory cytokine levels. The *in vivo* CpG-DNA-mediated T-helper type-1 response was also abolished in $TLR9^{-/-}$ mice. Thus, vertebrate immune systems appear to have evolved a specific Toll-like receptor that distinguishes bacterial DNA from self-DNA.

The Toll-like receptor (TLR) family is a phylogenetically conserved mediator of innate immunity that is essential for microbial recognition[11]. Mammalian TLRs comprise a large family with extracellular leucine-rich repeats (LRRs) and a cytoplasmic Toll/interleukin (IL)-1R (TIR) homology domain. So far, six members (TLR1–6) have been reported[12–14], and two additional members have been deposited in GenBank as TLR7 and TLR8 (accession numbers AF240467 and AF246971, respectively). TLR2 and TLR4 are responsible for immune responses to peptidoglycan (PGN) and lipopolysaccharide (LPS), respectively[15–22].

By using a BLAST search, we identified an expressed sequence tag (EST) clone (AA273731; mouse) that showed high similarity with the previously identified TLRs. Using this fragment as a probe, we isolated a full-length complementary DNA from the mouse macrophage cDNA library. We also isolated the human counterpart. Sequence analysis revealed the presence of regions conserved in the TLR family, such as LRR and TIR domain (Fig. 1a, b). Therefore, we designated this gene TLR9. Northern blot analysis of various tissues indicated that mouse TLR9 transcripts were most abundantly expressed in the spleen (Fig. 1c).

To assess the biological function of TLR9, we generated $TLR9^{-/-}$ mice by homologous recombination in embryonic stem (ES) cells. The targeting vector was constructed to replace a 1.0-kb fragment of the mouse *Tlr9* gene encoding a part of LRR with a neomycin resistance cassette (*neo*) (Fig. 2a). Correctly targeted ES cell clones were micro-injected into C57BL/6 blastocysts, which contributed to transmission of the mutated allele through the germ line. We intercrossed heterozygotes to produce offspring that were homozygous for the disrupted *Tlr9* allele (Fig. 2b). The mutant mice were

born at the expected mendelian ratio. We then investigated expression of TLR9 messenger RNA in the spleen by northern blot analysis. When we used the carboxy-terminal fragment as a probe, we detected *Tlr9* transcripts from the mutant mice at almost the same size but in reduced amounts compared with those from wild-type mice (Fig. 2c). We next carried out polymerase chain reaction with reverse transcription (RT–PCR) using spleen mRNA from the mutant mice. Sequence analysis of these products showed that the transcribed *Tlr9* gene contained the *neo* gene. The insertion of *neo* resulted in an appearance of a stop codon at the amino-terminal portion of TLR9, indicating that a functional TLR9 protein was not expressed in the mutant mice (Fig. 2d). $TLR9^{-/-}$ mice showed no abnormal composition of lymphocytes as determined by flow cytometry (data not shown).

MyD88 is an adaptor molecule involved in the signalling through the IL-1R and TLR families. We previously showed that MyD88 is essential for the response to IL-1, IL-18, LPS and many other bacterial cell-wall components[23]. We have also shown that the responses to CpG DNA are dependent on MyD88 and TRAF6 (ref. 24). $MyD88^{-/-}$ mice did not respond to CpG DNA, whereas both $TLR2^{-/-}$ and $TLR4^{-/-}$ mice responded normally to CpG DNA. These data indicate that CpG DNA is recognized by TLRs other than TLR2 and TLR4. Therefore, we analysed responses of $TLR9^{-/-}$ mice to CpG DNA. We first investigated the proliferation of splenocytes in response to CpG DNA (Fig. 3a). CpG DNA, but not non-CpG DNA induced proliferation of wild-type splenocytes in a dose-dependent manner. In contrast, $TLR9^{-/-}$ splenocytes did not proliferate in response to either CpG DNA or non-CpG DNA, although they showed a similar proliferative response to LPS as the wild-type cells. Wild-type B cells showed enhanced surface expression of major histocompatibility complex (MHC) class II in response to CpG DNA; however, a CpG-DNA-induced increase in MHC class II expression was not observed in $TLR9^{-/-}$ B cells (data not shown). These data indicate that $TLR9^{-/-}$ B cells are defective in

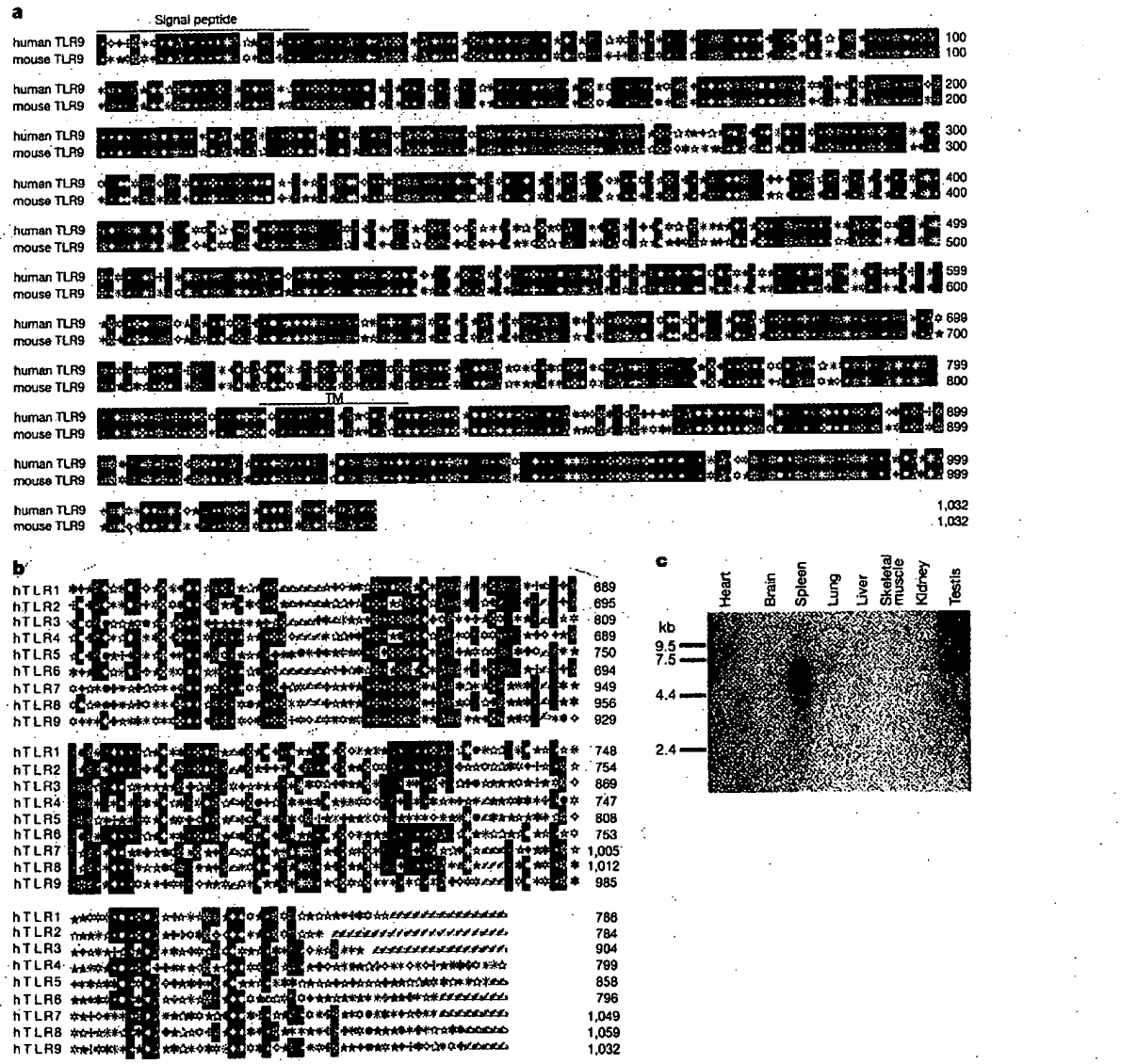

Figure 1 Amino-acid sequences and tissue distribution of TLR9. **a**, Alignment of human and mouse TLR9. Identical amino acids are indicated by a solid box. Human and mouse TLR9 share an overall amino-acid identity of 75.5%. The predicted signal peptide (human and mouse, residues 1–25) and transmembrane segments (TM; human, 819–836; mouse, 820–837) are indicated. During the preparation of this manuscript, the sequences for human TLR9 were deposited in GenBank by two other groups (accession numbers NM017442 and AF245704). **b**, Alignment of the cytoplasmic domains of human TLR family members. Amino-acid residues conserved in least four molecules are highlighted by solid boxes. **c**, A mouse multiple-tissue northern blot (Clontech) containing 2 μg of poly(A)$^+$ RNA was probed with a mouse TLR9 cDNA fragment.

their response to CpG DNA.

Next, we measured production of inflammatory cytokines from peritoneal macrophages by enzyme-linked immunoabsorbent assay (ELISA; Fig. 3b). Macrophages from wild-type mice produced tumour necrosis factor (TNF)-α, IL-6 and IL-12 in response to CpG DNA. The production was further enhanced when stimulated with a combination of interferon (IFN)-γ and CpG DNA. However, macrophages from TLR9$^{-/-}$ mice did not produce any detectable levels of inflammatory cytokines in response to CpG DNA even in the presence of IFN-γ. Macrophages from wild-type and TLR9$^{-/-}$ mice produced similar amounts of TNF-α, IL-6 and IL-12 in response to LPS, PGN, lipoprotein from *Escherichia coli*, Zymosan and whole heat-killed *Staphylococcus aureus* (Fig. 3b; and data not shown), indicating that TLR9$^{-/-}$ macrophages are specifically defective in their response to CpG DNA.

CpG-containing bacterial DNA is a potent stimulant for dendritic cells (DCs) to support T-helper type-1 (Th1) cell development[4–7]. Therefore, we examined CpG-DNA-induced cytokine production and upregulation of surface molecules in bone-marrow-derived murine DCs. Wild-type DCs produced IL-12 in response to CpG DNA; however, TLR9$^{-/-}$ DCs did not produce any detectable levels of IL-12 (Fig. 3c). Wild-type DCs showed enhanced surface expression of CD40, CD80, CD86 and MHC class II when stimulated with CpG DNA. TLR9$^{-/-}$ DCs did not show any enhanced expression of the surface molecules in response to CpG-DNA (Fig. 3d). Both wild-type and TLR9$^{-/-}$ DCs exhibited similar responses to LPS. Together, these findings indicate that TLR9 is essential for cellular responses to CpG DNA.

Signalling through TLRs occurs through the sequential recruitment of the adaptor molecule MyD88 and the serine/threonine kinase IRAK, and subsequently activates mitogen-activated protein (MAP) kinases and the nuclear factor NF-κB[23]. We next analysed activation of the intracellular signalling cascade in response to CpG DNA. In wild-type macrophages, stimulation with CpG DNA increased the DNA-binding activity of NF-κB, as determined by electrophoretic mobility shift assay (EMSA; Fig. 3e); however, NF-κB activity was not increased in response to CpG DNA in TLR9$^{-/-}$ macrophages. LPS stimulation of TLR9$^{-/-}$ macrophages led to activation of NF-κB to the same extent as that of wild-type cells, indicating that CpG-DNA-induced activation of NF-κB was impaired in TLR9$^{-/-}$ macrophages. *In vitro* kinase assay showed that CpG DNA activated c-Jun N-terminal kinase (JNK) and IRAK in wild-type macrophages. Activation of both kinases was completely abolished in TLR9$^{-/-}$ macrophages (Fig. 3f, g). Thus, CpG-DNA-mediated signal transduction is dependent on TLR9.

Finally, we addressed the *in vivo* response to CpG DNA in TLR9$^{-/-}$ mice. CpG DNA can induce lethal shock in D-galactosamine (D-GalN)-sensitized mice[25]. Wild-type mice died within 12 h after D-GalN plus CpG DNA administration with marked elevation of serum concentrations of TNF-α, IL-6 and IL-12 (Fig. 4a, b). In contrast, all TLR9$^{-/-}$ mice survived without any increase in serum concentration of these inflammatory cytokines. Thus, TLR9$^{-/-}$ mice were highly resistant to CpG-DNA-induced shock syndrome. *In vivo* administration of CpG DNA has also been shown to induce a Th1-biased response[26]. CpG DNA and ovalbumin (OVA) were injected into the footpads, and lymph node cells were isolated at the 7-day time point and stimulated with OVA. The popliteal lymph node of

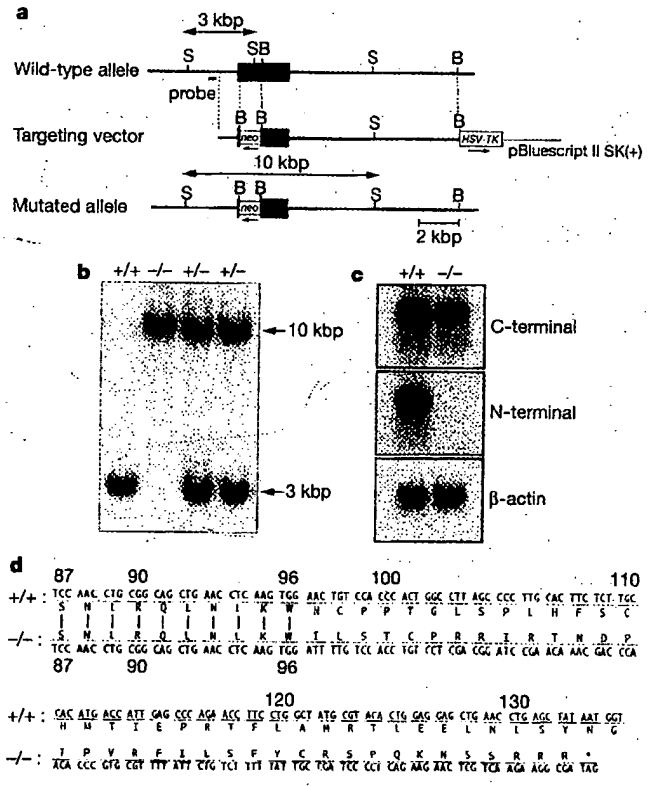

Figure 2 Targeted disruption of the mouse *Tlr9* gene. **a**, Maps of the TLR9 genome, the targeting vector and the predicted disrupted gene. Filled boxes denote the coding exon. Restriction enzymes: B, *Bam*HI; S, *Sca*I. **b**, Southern blot analysis of offspring from the heterozygote intercrosses. Genomic DNA was extracted from mouse tails, digested with *Sca*I, electrophoresed and hybridized with the radiolabelled probe indicated in **a**. Southern blotting gave a single 3.0-kb band for wild-type (+/+), a 10-kb band for homozygous (−/−) and both bands for heterozygous mice (+/−). **c**, Northern blot analysis of splenocytes. Total RNA (10 μg) extracted from splenocytes was electrophoresed, transferred to a nylon membrane, and hybridized using the TLR9 C-terminal or N-terminal fragment as a probe. The same membrane was rehybridized with a β-actin probe. **d**, Comparison of predicted amino-acid sequences between wild-type (+/+) and TLR9$^{-/-}$ (−/−) cDNA. The numbers indicate predicted amino-acid position of wild-type TLR9.

CpG DNA-treated wild-type mice showed an increase in size compared with that of PBS treated mice, whereas TLR9$^{-/-}$ mice did not show any lymphadenopathy (data not shown). Lymph node cells from CpG-DNA-treated wild-type mice produced IFN-γ in response to OVA (Fig. 4c). In contrast, production of IFN-γ from TLR9$^{-/-}$ lymph node cells was not observed. Thus, CpG-DNA-induced Th1-like response was not observed in TLR9$^{-/-}$ mice.

The nature and localization of the CpG receptor are controversial. There is evidence that CpG DNA binds to cell-surface receptors that subsequently transduce stimulatory signals, because Sepharose beads coated with active CpG DNA stimulate B cells as free CpG DNA[27]. In contrast, other reports show that internalization of the DNA is required for activity[28]. Inhibitors of endosomal maturation such as bafilomaycin A or chloroquine abolish CpG-mediated cell activation, indicating that cellular uptake by nonspecific endocytosis and subsequent endosomal maturation precede cell activation[29,30]. Acidification of endosomal CpG DNA is coupled to the rapid generation of intracellular reactive oxygen species, followed by NF-κB activation[31]. Thus, in the latter case, it has been proposed that CpG DNA works through binding to an intracellular receptor. The presence of a transmembrane segment in the TLR9 gene strongly suggests that TLR9 is inserted into the membrane, but not present in the cytoplasm. Although the localization of TLR9 awaits assessment by immunostaining, confocal data show that tagged MyD88 colocalizes with tagged CpG DNA in endosomal structures, but not at the cell membrane (H.W., unpublished data). In contrast, LPS colocalizes with MyD88 at the cell membrane. This suggests that signalling is triggered by LPS at the cell membrane, whereas CpG DNA initiates signalling after translocation to endosomes. This assumption may well correlate with the finding that CpG-DNA-induced IRAK activation is delayed as compared with that stimulated with LPS (Fig. 3g). The identification of CpG DNA signalling receptor will pave the way to understanding the mechanism by which CpG DNA is recognized as well as by which the recognition of CpG DNA is translated into a strong Th1 response. Furthermore, TLR9$^{-/-}$ mice will provide a useful model for clarifying to what extent recognition of CpG DNA contributes to host immune responses against bacterial infections. □

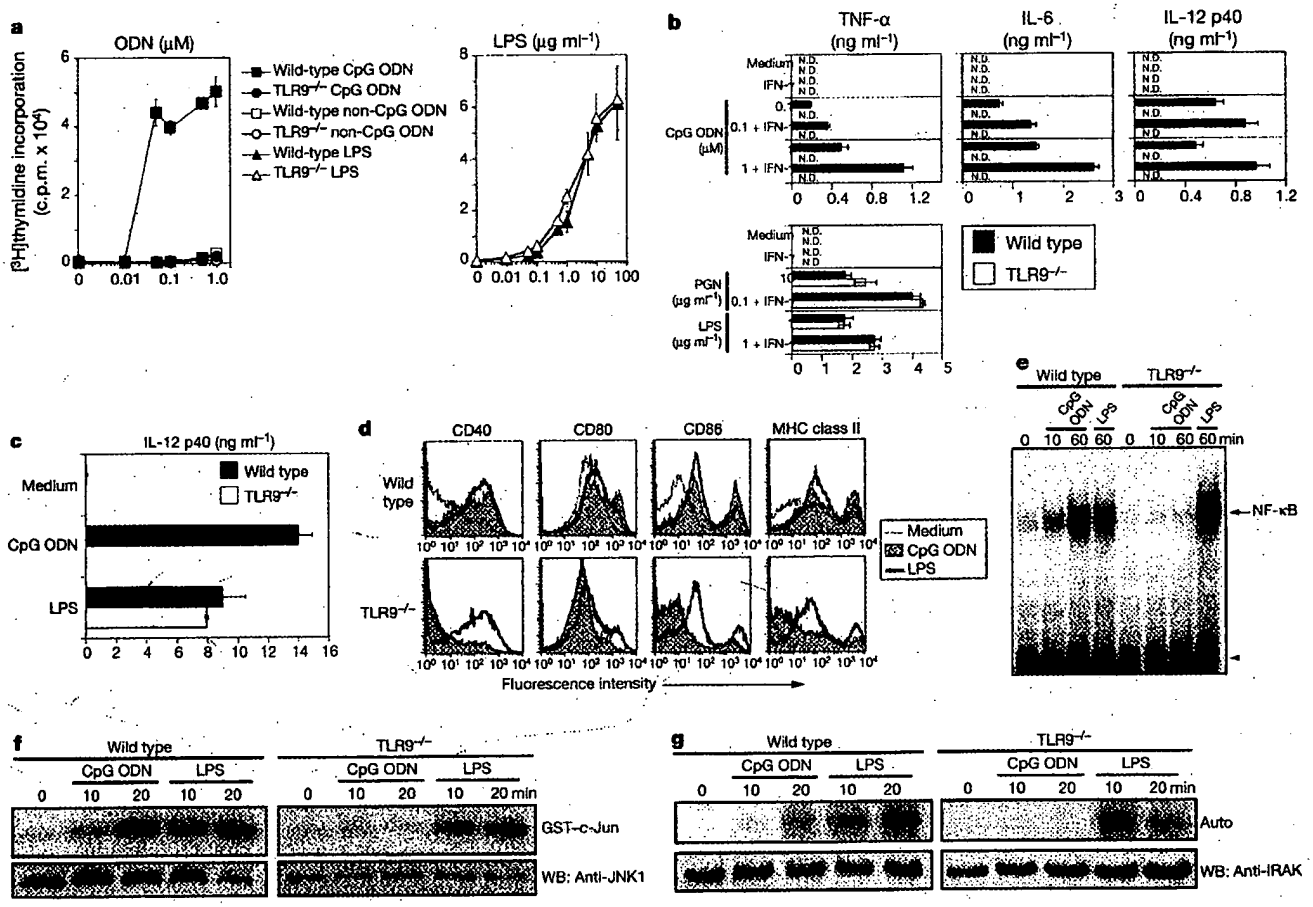

Figure 3 Impaired responses to CpG ODN in TLR9$^{-/-}$ cells. **a**, Splenocytes from wild-type or TLR9$^{-/-}$ mice were cultured with the indicated concentrations of CpG ODN, non-CpG ODN or LPS for 48 h plus pulsed [^{3}H]thymidine for the last 8 h. [^{3}H]thymidine incorporation was measured by β-scintillation counting. Data indicate mean ± s.d. of triplicate samples of one representative experiment. **b**, Peritoneal macrophages from wild-type or TLR9$^{-/-}$ mice were stimulated with CpG ODN (0.1 or 1.0 μM), PGN (10 μg ml^{-1}) or LPS (1.0 μg ml^{-1}) in the presence or absence of 30 U ml^{-1} IFN-γ for 24 h, and concentrations of TNF-α, IL-6 and IL-12 p40 in the culture supernatants were measured by ELISA. Similar results were obtained from three independent experiments. Data indicate mean ± s.d. N.D., not detected. **c**, Wild-type or TLR9$^{-/-}$ dendritic cells (DCs) derived from bone marrow were cultured with CpG ODN or LPS. Concentrations of IL-12 p40 in culture supernatants were measured by ELISA. Data indicate mean ± s.d. **d**, DCs were stimulated with CpG ODN or LPS for 48 h and analysed for cell-surface expression of the indicated molecules by flow cytometry. **e**, Peritoneal macrophages from wild-type and TLR9$^{-/-}$ mice were stimulated with 1.0 μM CpG ODN or 1.0 μg ml^{-1} LPS for the indicated durations. NF-κB activity was determined by EMSA. Arrow indicates the inducible NF-κB complex; arrowhead indicates free probe. **f**, Peritoneal macrophages from wild-type and TLR9$^{-/-}$ mice were stimulated with 1.0 μM CpG ODN or 1.0 μg ml^{-1} LPS for the indicated durations. Cell lysates were prepared and immunoprecipitated with anti-JNK antibody. JNK activity was measured by *in vitro* kinase assay using a GST–c-Jun fusion as a substrate (top). The same lysates were blotted with anti-JNK (bottom). **g**, The same cell lysates in **f** were immunoprecipitated with anti-IRAK antibody. The kinase activity of IRAK was measured by *in vitro* kinase assay (top). The same lysates were blotted with anti-IRAK antibody (bottom). Auto, autophosphorylation.

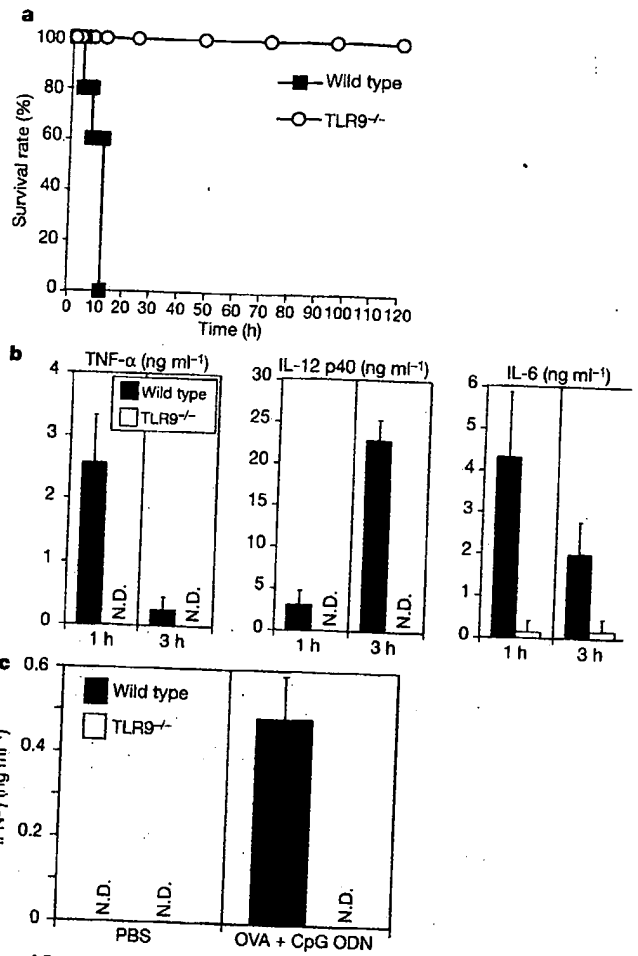

Figure 4 Resistance to CpG ODN-induced shock in TLR9$^{-/-}$ mice. **a**, Age-matched wild-type ($n = 5$) and TLR9$^{-/-}$ mice ($n = 5$) were intraperitoneally injected with CpG ODN (20 nmol) and D-GalN (20 mg). Survival was monitored for 5 d. **b**, Wild-type and TLR9$^{-/-}$ mice were intraperitoneally injected with CpG ODN and D-GalN. Sera were taken at 1 or 3 h after injection. Serum concentrations of TNF-α, IL-12 p40 and IL-6 were measured by ELISA. N.D., not detected. Results are mean of sera samples from three mice. **c**, Age-matched wild-type and TLR9$^{-/-}$ mice were injected with PBS or CpG ODN (5 nmol) plus OVA (150 μg) into the hind footpads. Popliteal lymph node cells were collected after 7 d and cultured with OVA for 24 h. Production of IFN-γ from lymph node cells was analysed by ELISA. Data indicate mean ± s.d. N.D., not detected.

Methods

Cloning of TLR9

A GenBank search resulted in identification of a mouse EST that has a significant similarity with human TLR4. Using PCR-amplified EST as a probe, a full-length cDNA clone containing the complete TLR9 open reading frame was isolated from the mouse RAW 264.7 cDNA library. Human genomic sequence that showed significant homology with the mouse TLR9 gene was found in GenBank. On the basis of this sequence, rapid amplification of cDNA ends protocol was performed to isolate full-length cDNA from U937 cDNA library.

Generation of TLR9$^{-/-}$ mice

The TLR9 genomic DNA was isolated from 129/Sv mouse genomic library and characterized by restriction enzyme mapping and sequencing analysis. The targeting vector was constructed by replacing a 1.0-kb fragment encoding a part of LRR region with a neomycin-resistance gene cassette (*neo*), and a herpes simplex virus thymidine kinase driven by MC1 promoter was inserted into the genomic fragment for negative selection (Fig. 2a). The targeting vector was transfected into embryonic stem cells (E14.1). G418 and gancyclovir doubly resistant colonies were selected and screened by PCR and southern blotting. Homologous recombinants were micro-injected into C57BL/6 blastocysts. Chimaeric mice were mated with C57BL/6 female mice, and heterozygous F_1 progenies were intercrossed in order to obtain TLR9$^{-/-}$ mice. All mice analysed here were F_1 progeny of 129/Ola × C57BL/6.

Reagents

Phosphorothioate-stabilized CpG oligodeoxynucleotide (ODN) (TCC-ATG-ACG-TTC-CTG-ATG-CT)[18] was purchased from TIB MOLBIOL or Hokkaido System Science. Phosphorothioate-stabilized non-CpG ODN (GCT-TGA-TGA-CTC-AGC-CGG-AA)[5] was purchased from Hokkaido System Science. LPS from *Salmonella minnesota* Re-595 and PGN from *Staphylococcus aureus* were purchased from Sigma and Fluka, respectively[21].

Measurement of cytokine production from macrophages

Thioglycollate-elicited peritoneal macrophages were cultured with the indicated concentrations of CpG ODN, LPS or PGN for 24 h. Concentrations of TNF-α, IL-6 and IL-12 p40 in the culture supernatants were measured by ELISA.

Preparation and analysis of dendritic cells

Bone-marrow cells from wild-type or TLR9$^{-/-}$ mice were cultured with 10 ng ml^{-1} mouse granulocyte macrophage-colony stimulating factor (Peprotech) in RPMI1640 medium supplemented with 10% fetal bovine serum. At day 6, immature DCs were collected and cultured in the absence or presence of 0.1 μM CpG ODN or 0.1 μg ml^{-1} LPS in a fresh medium for a further 2 days. The concentration of IL-12 p40 in the culture supernatants was measured by ELISA. DCs were stained with biotinylated antibodies against CD40, CD80, CD86 or MHC class II, and developed with PE-conjugated streptavidin. Flow cytometric analysis was performed using a FACSCalibur with CELLQuest software (Becton Dickinson).

EMSA and *in vitro* kinase assay

Thioglycollate-elicited peritoneal macrophages (1×10^6 cells) from wild-type and TLR9$^{-/-}$ mice were stimulated for the indicated periods and then nuclear proteins were extracted. The extracts were incubated with a specific probe containing NF-κB DNA-binding sites, electrophoresed and visualized by autoradiography.

Thioglycollate-elicited peritoneal macrophages were stimulated with 1.0 μM CpG ODN or 1.0 μg ml^{-1} LPS for the indicated periods. JNK and IRAK activities in cell lysates were measured by *in vitro* kinase assays as described[23].

Cytokine production of presensitized lymph nodes

Age-matched wild-type and TLR9$^{-/-}$ mice were injected subcutaneously with CpG ODN (5 nmol) plus soluble OVA (150 μg) into the hind footpads. Seven days later, popliteal lymph nodes were collected and cultured with 100 μg ml^{-1} OVA for 24 h. Concentrations of IFN-γ in the culture supernatants were measured by ELISA.

Received 26 June; accepted 3 October 2000.

1. Krieg, A. M. Lymphocyte activation by CpG dinucleotide motifs in prokaryotic DNA. *Trends Microbiol.* **4**, 73–76 (1996).
2. Lipford, G. B., Heeg, K. & Wagner, H. Bacterial DNA as immune cell activator. *Trends Microbiol.* **6**, 496–500 (1998).
3. Yamamoto, S., Yamamoto, T. & Tokunaga, T. The discovery of immunostimulatory DNA sequence. *Spring. Ser. Immunopathol.* **22**, 11–19 (2000).
4. Jakob, T., Walker, P. S., Krieg, A. M., Udey, M. C. & Vogel, J. C. Activation of cutaneous dendritic cells by CpG-containing oligodeoxynucleotides: a role for dendritic cells in the augmentation of Th1 responses by immunostimulatory DNA. *J. Immunol.* **161**, 3042–3049 (1998).
5. Sparwasser, T. *et al.* Bacterial DNA and immunostimulatory CpG oligonucleotides trigger maturation and activation of murine dendritic cells. *Eur. J. Immunol.* **28**, 2045–2054 (1998).
6. Hartmann, G., Weiner, G. J. & Krieg, A. M. CpG DNA: a potent signal for growth, activation, and maturation of human dendritic cells. *Proc. Natl Acad. Sci. USA* **96**, 9305–9310 (1999).
7. Häcker, H. *et al.* Cell type-specific activation of mitogen-activated protein kinases by CpG-DNA controls interleukin-12 release from antigen-presenting cells. *EMBO J.* **18**, 6973–6982 (1999).
8. Wagner, H. Bacterial CpG DNA activates immune cells to signal infectious danger. *Adv. Immunol.* **73**, 329–368 (1999).
9. Klinman, D. M., Verthelyi, D., Takeshita, F. & Ishii, K. J. Immune recognition of foreign DNA: a cure for bioterrorism? *Immunity* **11**, 123–129 (1999).
10. Krieg, A. M. The role of CpG motifs in innate immunity. *Curr. Opin. Immunol.* **12**, 35–43 (2000).
11. Medzhitov, R. & Janeway, C. A. Jr Innate immunity: the virtues of a nonclonal system of recognition. *Cell* **91**, 295–298 (1997).
12. Medzhitov, R., Preston-Hurlburt, P. & Janeway, C. A. Jr A human homologue of the *Drosophila* Toll protein signals activation of adaptive immunity. *Nature* **388**, 394–397 (1997).
13. Rock, F. L., Hardiman, G., Timans, J. C., Kastelein, R. A. & Bazan, J. F. A family of human receptors structurally related to Drosophila Toll. *Proc. Natl Acad. Sci. USA* **95**, 588–593 (1998).
14. Takeuchi, O. *et al.* TLR6: A novel member of an expanding toll-like receptor family. *Gene* **231**, 59–65 (1999).
15. Poltorak, A. *et al.* Defective LPS signaling in C3H/HeJ and C57BL/10ScCr mice: mutations in Tlr4 gene. *Science* **282**, 2085–2088 (1998).
16. Hoshino, K. *et al.* Toll-like receptor 4 (TLR4)-deficient mice are hyporesponsive to lipopolysaccharide: evidence for TLR4 as the *Lps* gene product. *J. Immunol.* **162**, 3749–3752 (1999).
17. Yoshimura, A. *et al.* Recognition of Gram-positive bacterial cell wall components by the innate immune system occurs via Toll-like receptor 2. *J. Immunol.* **163**, 1–5 (1999).
18. Brightbill, H. D. *et al.* Host defense mechanisms triggered by microbial lipoproteins through toll-like receptors. *Science* **285**, 732–736 (1999).
19. Aliprantis, A. O. *et al.* Cell activation and apoptosis by bacterial lipoproteins through Toll-like receptor-2. *Science* **285**, 736–739 (1999).
20. Underhill, D. M. *et al.* The Toll-like receptor 2 is recruited to macrophage phagosomes and discriminates between pathogens. *Nature* **401**, 811–815 (1999).

21. Takeuchi, O. *et al.* Differential roles of TLR2 and TLR4 in recognition of gram-negative and gram-positive bacterial cell wall components. *Immunity* **11**, 443–451 (1999).
22. Takeuchi, O. *et al.* Preferentially the R-stereoisomer of the mycoplasmal lipopeptide macrophage-activating lipopeptide-2 activates immune cells through a toll-like receptor 2- and MyD88-dependent signaling pathway. *J. Immunol.* **164**, 554–557 (2000).
23. Kawai, T., Adachi, O., Ogawa, T., Takeda, K. & Akira, S. Unresponsiveness of MyD88-deficient mice to endotoxin. *Immunity* **11**, 115–122 (1999).
24. Häcker, H. *et al.* Immune cell activation by bacterial CpG-DNA through myeloid differential marker 88 and tumor necrosis factor receptor-associated factor (TRAF)6. *J. Exp. Med.* **192**, 595–600 (2000).
25. Sparwasser, T. *et al.* Macrophages sense pathogens via DNA motifs: induction of tumor necrosis factor-α-mediated shock. *Eur. J. Immunol.* **27**, 1671–1679 (1997).
26. Lipford, G. B. *et al.* CpG-DNA-mediated transient lymphadenopathy is associated with a state of Th1 predisposition to antigen-driven responses. *J. Immunol.* **165**, 1228–1235 (2000).
27. Liang, H., Reich, C. F., Pisetsky, D. S., Lipsky, P. E. The role of cell surface receptors in the activation of human B cells by phosphorothioate oligonucleotides. *J. Immunol.* **165**, 1438–1445 (2000).
28. Krieg, A. M. *et al.* CpG motifs in bacterial DNA trigger direct B-cell activation. *Nature* **374**, 546–549 (1995).
29. Macfarlane, D. E. & Manzel, L. Antagonism of immunostimulatory CpG-oligodeoxynucleotides by quinacrine, chloroquine, and structurally related compounds. *J. Immunol.* **160**, 1122–1131 (1998).
30. Häcker, H. *et al.* CpG-DNA-specific activation of antigen-presenting cells requires stress kinase activity and is preceded by non-specific endocytosis and endosomal maturation. *EMBO J.* **17**, 6230–6240 (1998).
31. Yi, A. K. & Krieg, A. M. Rapid induction of mitogen-activated protein kinases by immune stimulatory CpG DNA. *J. Immunol.* **161**, 4493–4497 (1998).

Acknowledgements

We thank G. B. Lipford for helpful discussions; T. Aoki for secretarial assistance; and N. Tsuji, N. Iwami and E. Nakatani for technical assistance. We also thank Hayashibara Biochemical Laboratories, Inc. for providing anti-IRAK antibody. This work was supported in part by grants from the Ministry of Education, Science, Sports and Culture of Japan, and Research Fellowships of the Japan Society for the Promotion of Science for Young Scientists.

Correspondence and requests for materials should be addressed to S.A. (e-mail: sakira@biken.osaka-u.ac.jp). Sequences have been deposited in GenBank under accession numbers AB045180 and AB045181 for human and mouse TLR9, respectively.

Structure of the bacteriophage φ29 DNA packaging motor

Alan A. Simpson*†, Yizhi Tao*‡‡, Petr G. Leiman*, Mohammed O. Badasso§, Yongning He*, Paul J. Jardine‖, Norman H. Olson*, Marc C. Morais*, Shelley Grimes§, Dwight L. Anderson§, Timothy S. Baker* & Michael G. Rossmann*

** Department of Biological Sciences, Purdue University, West Lafayette, Indiana 47907-1392, USA*
§ Departments of Microbiology and Oral Science, 18-246 Moos Tower, University of Minnesota, Minneapolis, Minnesota 55455, USA
‖ Department of Biology, University of New Brunswick, Fredericton, New Brunswick E3B 6E1, Canada
† These authors contributed equally to this work

Motors generating mechanical force, powered by the hydrolysis of ATP, translocate double-stranded DNA into preformed capsids (proheads) of bacterial viruses[1,2] and certain animal viruses[3]. Here we describe the motor that packages the double-stranded DNA of the *Bacillus subtilis* bacteriophage φ29 into a precursor capsid. We determined the structure of the head–tail connector—the central component of the φ29 DNA packaging motor—to 3.2 Å resolution by means of X-ray crystallography. We then fitted the connector into the electron densities of the prohead and of the partially packaged prohead as determined using cryo-electron microscopy and image reconstruction analysis. Our results suggest that the prohead plus dodecameric connector, prohead RNA, viral ATPase and DNA comprise a rotary motor with the head–prohead RNA–ATPase complex acting as a stator, the DNA acting as a spindle, and the connector as a ball-race. The helical nature of the DNA converts the rotary action of the connector into translation of the DNA.

The bacteriophage φ29 (Fig. 1) is a 19-kilobase (19-kb) double-stranded DNA (dsDNA) virus with a prolate head and complex structure[4]. The prohead (Fig. 1), into which the DNA is packaged, is about 540 Å long and 450 Å wide[5]. The φ29 connector, a cone-shaped dodecamer of gene product 10 (gp10), occupies the pentagonal vertex at the base of the prohead[5] and is the portal for DNA entry during packaging and DNA ejection during infection[6]. The connector, in association with the oligomeric, φ29-encoded prohead RNA (pRNA) and a viral ATPase (gp16), is required for DNA packaging[7–9]. However, only the first 120 bases of the 174-base pRNA are essential for packaging[7]. The covalent adduct of the genomic dsDNA with gp3 (DNA–gp3) can be packaged into proheads in about three minutes *in vitro* (P.J.J., unpublished results). The connector proteins of tailed phages[6] vary in relative molecular mass (M_r) from 36,000 (36K) in φ29 to 83K in phage P22, and assemble into oligomers with a central channel. The structure of the isolated φ29 connector has been studied by atomic force microscopy[10] and cryo-electron microscopy (cryo-EM) of two-dimensional arrays[11], immuno-electron microscopy[12] and X-ray crystallography[13,14].

The connector structure, as now determined by X-ray crystallography, can be divided into three, approximately cylindrical regions: the narrow end, the central part, and the wide end, having external radii (Å) of 33, 47 and 69, respectively (Fig. 2). These regions are respectively 25, 28 and 22 Å in height, making the total connector 75 Å long. The internal channel has a diameter of about 36 Å at the narrow end, increasing to 60 Å at the wide end. Comparison with electron microscopy reconstructions[5,11] shows that the narrow end protrudes from the portal vertex of the phage head, is associated with the multimeric pRNA, and binds the lower collar in the mature virus.

The electron density of the connector was interpreted in terms of the amino-acid sequence[15] and was confirmed by the two Hg sites (see Methods section) corresponding to the only cysteine residues in the sequence. Residues 1 to 11, 229 to 246, and 287 to 309 at the carboxy terminus are not seen in the electron density. The second and third disordered regions are both located on the inside of the channel, close to the junction of the central and wide regions. The structure is dominated by three long helices (α1, α3 and α5) in each monomer that run the length of the central region, joining the two end domains of the connector (Fig. 2). These helices are arranged at an angle of about 40° with respect to the central 12-fold axis. The two end domains are composed predominantly of β-sheets and extended polypeptide chains. Immuno-electron microscopy mapping of the sequence onto the connector surface[12] is consistent with the X-ray structure only as far as localization of the external amino-terminal residues with the pRNA-binding region at the narrow end of the connector. The RNA recognition motif structure, previously predicted for the N-terminal regions of the connector monomer[16,17], is not present in the structure.

The surface of the monomer presents a net negative charge to one neighbour and a net positive charge to the other neighbour, possibly aiding the assembly of the dodecamer. The exterior of the connector has no significant regions of charge accumulation, implying that its rotation might be facilitated by its oily, smooth, external surface. However, the basic character of the disordered 11 amino-terminal residues could alter the surface properties to some extent and may facilitate interaction with the pRNA. In contrast, the inside of the channel has a preponderance of negative charge at its wide end, which may repel the DNA, permitting its smooth passage during packaging and ejection. The channel through which messenger RNA is translocated in reoviruses has similar properties[18].

We have determined the structures of four distinct types of φ29

‡ Present address: Department of Molecular and Cellular Biology, Harvard University, 7 Divinity Avenue, Cambridge, Massachusetts 02138, USA.

Cell, Vol. 103, 909–918, December 8, 2000, Copyright ©2000 by Cell Press

DNA-PKcs Is Required for Activation of Innate Immunity by Immunostimulatory DNA

Wen-Ming Chu,*‖ Xing Gong,* Zhi-Wei Li,† Kenji Takabayashi,* Hong-Hai Ouyang,‡ Yi Chen,† Augusto Lois,* David J. Chen,§ Gloria C. Li,‡ Michael Karin,† and Eyal Raz*‖
*The Sam and Rose Stein Institute for Research on Aging and
Department of Medicine 0663
†Laboratory of Signal Transduction and Gene Regulation
Department of Pharmacology
University of California, San Diego
9500 Gilman Drive
La Jolla, California 92093
‡Departments of Radiation Oncology and Medical Physics
Memorial Sloan-Kettering Cancer Center
New York, New York 10021
§Life Science Division
Lawrence Berkeley National Laboratory
Berkeley, California 94720

Summary

Bacterial DNA and related synthetic immunostimulatory oligodeoxyribonucleotides (ISS-ODN) stimulate innate immunity. However, the molecular recognition mechanism that initiates signaling in response to bacterial DNA and ISS-ODN has not been identified. Herein, we demonstrate that administration of bacterial DNA and ISS-ODN to mice lacking the catalytic subunit of DNA-PK (DNA-PKcs) and in vitro stimulation of BMDM from these mice result in defective induction of IL-6 and IL-12. Further analysis using BMDM of IKKβ$^{-/-}$ revealed that both DNA-PKcs and IKKβ are essential for normal cytokine production in response to ISS-ODN or bacterial DNA. ISS-ODN and bacterial DNA activate DNA-PK, which in turn contributes to activation of IKK and NF-κB. These results reveal a novel role of DNA-PKcs in innate immune responses and a link between DNA repair and innate immunity.

Introduction

In addition to the well-established role of bacterial cell wall components in activation of innate immunity (reviewed by Aderem and Ulevitch, 2000), it has been recognized that bacterial DNA also has profound immunostimulatory effects (Klinman et al., 1999; Van Uden and Raz, 1999; Wagner, 1999). Tokunaga and colleagues had initially demonstrated that particular sequences of oligodeoxyribonucleotides (ODN) derived from the mycobacteria genome elicit anti-tumor activity (Tokunaga et al., 1984). Subsequent analysis of shorter overlapping ODNs and insertion of active sequences into otherwise inactive ODNs suggested that palindromic hexamers, each of which contains nonmethylated CpG dinucleotides, are responsible for this immune activation (Yamamoto et al., 1992). Since this initial characterization, further studies have determined the optimal sequences for immunostimulatory activity leading Krieg and coworkers to define unmethylated 5′-Pur-Pur-CpG-Pyr-Pyr-3′ motif as the minimal active sequence that triggers IL-6 production (Krieg et al., 1995).

More recent studies have demonstrated that bacterial DNA and related ISS-ODNs activate essential cellular components of innate immunity. Upon such stimulation, macrophages, monocytes, and dendritic cells secrete proinflammatory cytokines such as IL-6 and IL-12 (Klinman et al., 1996), and overexpress costimulatory molecules such as B7 and CD40 (Bauer et al., 1999; Martin-Orozco et al., 1999). These immunomodulatory properties of ISS-ODN were proposed to mediate induction of Th1 responses to both DNA (Sato et al., 1996) and protein-based vaccines (Roman et al., 1997; reviewed by Van Uden and Raz, 1999), as well as to induce cross-presentation of exogenous, soluble antigens, and to prime cytotoxic T cell responses (Cho et al., 2000).

Curiously, methylation at the C-5 position of the cytosine in the CpG dinucleotide ($^{5\text{-methyl}}$CpG) reduces this immunostimulatory activity (Krieg et al., 1995). This phenomenon is particularly interesting because genomic DNA of vertebrates contains highly methylated cytosines (70%) of the CpG dinucleotide, whose frequency is already reduced about 5-fold from the expected frequency (CpG suppression). By contrast, bacterial genomic DNA contains the expected frequency of CpG dinucleotide, which is usually not methylated on the cytosine (Bird, 1993). These differences between bacterial/mycobacterial and mammalian DNA led to the hypothesis that the mammalian innate immune system has evolved to respond to a bacterial-specific feature of DNA structure (i.e., pattern recognition system) through unique and yet unknown pattern recognition receptors (Medzhitov and Janeway, 1997). It was speculated that a putative ISS-ODN receptor would detect the DNA of invading microbial pathogens and elicit the "immunological danger/alarm signal" necessary for protection of the mammalian host (Roman et al., 1997; Klinman et al., 1999; Wagner, 1999).

The signaling pathways that mediate the immunostimulatory properties of ISS-ODN have also been investigated. It was reported that bacterial DNA and ISS-ODNs do not induce tyrosine phosphorylation or an increase in either inositol triphosphates or intracellular Ca^{2+} in responding cells (Krieg et al., 1995). In contrast, the NF-κB and MAP kinase signaling pathways were shown to be activated (Stacey et al., 1996; Hacker et al., 1998). Inhibition of NF-κB activation prevents IL-6 production in response to ISS-ODN (Yi et al., 1998). However, the molecular link that leads from fragmented bacterial DNA or ISS-ODN to NF-κB activation remains to be elucidated.

As ISS-ODNs are taken up into cells, they are thought to signal via their interaction with certain intracellular molecules (Hacker et al., 1998), which we postulated

‖To whom correspondence should be addressed (e-mail: wmchu@ucsd.edu, eraz@ucsd.edu).

EXHIBIT C

might involve intracellular protein kinases known to be activated by DNA. One such protein kinase is the DNA-dependent protein kinase (DNA-PK). DNA-PK is a member of phosphatidlinositol 3 (PI3) kinase-like family that also includes ATM, FRAP, and FRP1 (Hartley et al., 1995; Smith and Jackson, 1999). DNA-PK can be detected in both the nucleus and cytoplasm (Carter et al., 1990; Danska et al., 1996; Koiker et al., 1999; Nilsson et al., 1999). In the nucleus, DNA-PK plays a pivotal role in repair of DNA double-stranded breaks created by environmental insults, such as ionizing radiation (Hartley et al., 1995; Kirchgessner et al., 1995; Smith and Jackson, 1999) or by intrinsic cellular processes such as programmed DNA rearrangements during lymphocyte differentiation (e.g., VDJ recombination) (Smith and Jackson, 1999). In contrast, the cytoplasmic functions of DNA-PK are unclear. At physiological salt concentrations, DNA-PK requires two components for activity: a DNA binding protein, Ku, and a catalytic subunit, DNA-PKcs (Gottlieb and Jackson, 1993). Ku is a heterodimer of 70 and 86 kDa polypeptides that binds to double-stranded DNA ends, nicks, single-stranded DNA, or transitions between double- and single-strand DNA (Mimori and Hardin, 1986; Falzon et al., 1993). DNA-PKcs has double- and single-strand DNA binding domains and is activated by both double- and single-stranded DNA ends (Leuther et al., 1999; Hammarsten et al., 2000).

We hypothesized a role for DNA-PK in the induction of innate immunity by bacterial DNA and ISS-ODNs, and obtained biochemical and genetic evidence that DNA-PKcs is indeed required for signaling events that lead to induction of innate cytokines, such as IL-6 and IL-12. We demonstrate that bacterial DNA and ISS-ODN activate DNA-PKcs, which can phosphorylate the IKKβ subunit of the IKK complex to cause NF-κB activation. Both DNA-PKcs and IKKβ are essential for induction of cytokines in response to bacterial DNA and ISS-ODN.

Results

The experiments described in this study were performed with single-stranded (ss), 22 nucleotide long, phosphothioate (ps) ODNs. These are termed as ISS-ODN where ISS stands for immunostimulatory sequence, M-ODN where M stands for mutated, and cont-ODN where cont stands for control. Single-stranded phosphodiester (po) ODNs are termed po-ISS-ODN or po-M-ODN whereas double-stranded (ds) po-ODNs are termed po-ds-ISS-ODN or po-ds-M-ODN (for more details, see Experimental Procedures).

DNA-PKcs Is Required for Innate Cytokine Induction by Bacterial DNA and ISS-ODN

Bone marrow–derived macrophages (BMDM) respond to ISS-ODN by secreting high levels of IL-6 and IL-12 (Martin-Orozco et al., 1999). Initially, BMDM from DNA-PKcs-deficient mice (Kurimasa et al., 1999) were used to explore the possible role of DNA-PKcs in induction of these innate cytokines by ISS-ODN. Very low levels of IL-6 and IL-12 were produced by DNA-PKcs-deficient BMDM upon ISS-ODN stimulation in comparison to wild-type (wt) BMDM (Figures 1A and 1B). In contrast, DNA-PKcs$^{-/-}$ BMDM exhibited normal induction of IL-6 and IL-12 in response to LPS stimulation (Figures 1A and 1B).

Since phosphothioate (ps) ODNs differ structurally from phosphodiester (po) ODNs, we compared the response of ISS-ODN to po-ISS-ODN, po-ds-ISS-ODN (unmethylated or methylated), LPS free bacterial DNA (*E. coli*), methylated *E. coli* bacterial DNA, or to LPS free calf thymus DNA. Similar activity profile was observed for po-ds-ISS-ODN and bacterial DNA in wt BMDM (Figures 1C and 1D) while po-ISS-ODN was less effective (Figures 1C and 1D). As expected, calf thymus DNA and methylated bacterial DNA induced a several-fold less IL-6 and IL-12 as compared to unmethylated bacterial DNA (data not shown). BMDM from DNA-PKcs-deficient mice were also defective in induction of IL-6 and IL-12 in response to po-ISS-ODN, po-ds-ISS-ODN, and bacterial DNA (Figures 1C and 1D), indicating that DNA-PKcs is required for induction of IL-6 and IL-12 by synthetic (ps) and natural forms (po) of ISS-enriched DNAs (i.e., bacterial DNA).

We then determined whether the lack of ISS-ODN responsiveness in DNA-PKcs-deficient BMDM was due to a defect in mRNA induction. Little induction of IL-6 and IL-12 mRNAs in response to ISS-ODN was observed in DNA-PKcs-deficient BMDM (Figure 1E). In contrast, DNA-PKcs-deficient BMDM exhibited normal cytokine mRNA induction in response to LPS stimulation.

To determine the requirement for DNA-PKcs in the induction of IL-6 and IL-12 by ISS-ODN, po-ISS-ODN, ps-ds-ISS-ODN, bacterial and calf thymus DNAs in vivo, we injected these DNAs into wt and DNA-PKcs$^{-/-}$ mice. The levels of IL-6 and IL-12 mRNAs in liver or spleen were examined by RT-PCR. IL-6 or IL-12 mRNA levels were detected in the liver or the spleen of wt controls, but were lacking in the same organs in DNA-PKcs-deficient mice (Figure 1F). Only minute amounts of mRNAs were observed in response to calf thymus DNA injection into wt mice (Figure 1F).

DNA-PKcs is a member of PI3K family and its enzymatic activity is blocked by PI3K inhibitors such as wortmannin (Wm) at high concentrations, or Ly294002 (Ly) (Hartley et al., 1995; Smith and Jackson, 1999). To further establish the role of DNA-PKcs in the induction of IL-6 and IL-12 by ISS-ODN, we examined the effects of Wm and Ly on these responses. High concentrations of Wm (>100 nM) significantly inhibited the induction of IL-6 and IL-12 by ISS-ODN (Hartley et al., 1995) (Figures 2A and 2B). Ly also blocked IL-6 and IL-12 induction by ISS-ODN (data not shown). In contrast, both Wm and Ly did not inhibit LPS-induced secretion of IL-6 and IL-12 (Figures 2A and 2B and data not shown).

The ATM gene product, which is also a member of the PI3K family, is functionally related to DNA-PKcs and its kinase activity is also Wm and Ly sensitive (Hartley et al., 1995; Xu et al., 1996). We therefore examined the induction of IL-6 and IL-12 in ATM-deficient mice. As shown in Figures 2C and 2D, normal induction of IL-6 and IL-12 by ISS-ODN was observed in ATM-deficient BMDM, excluding a role for ATM in ISS-induced activation of innate immunity.

IKKβ Is Required for BD and ISS-ODN-Induced Activation of NF-κB

Previous study had demonstrated activation of NF-κB by ISS-ODN (Stacey et al., 1996). However, the mechanism that drives this response is largely unknown. To

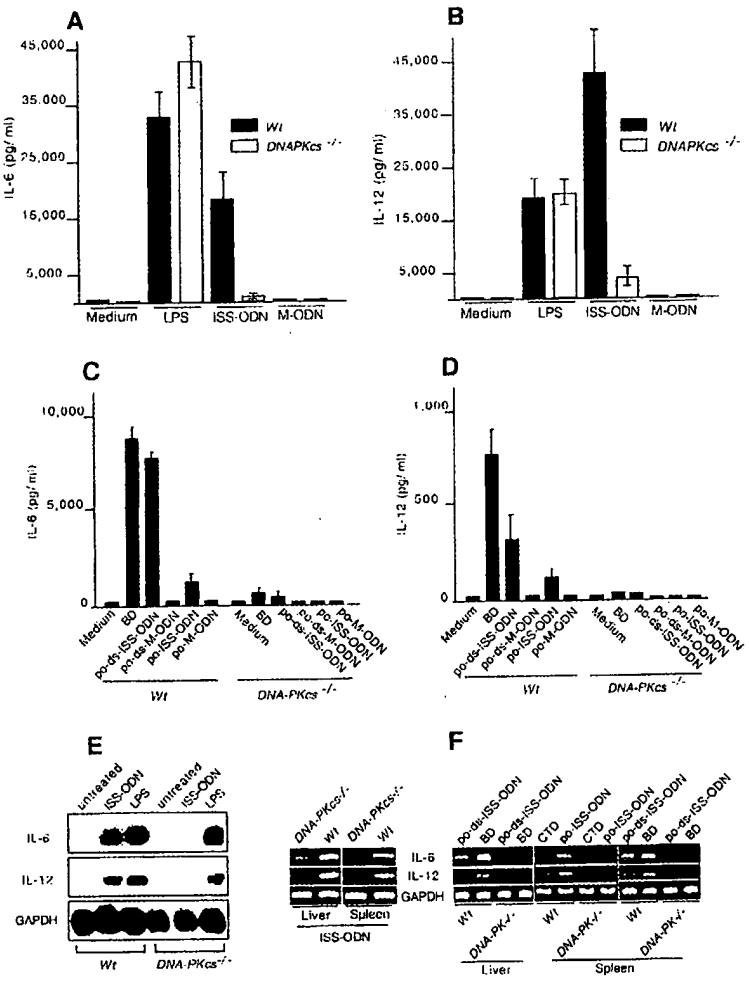

Figure 1. DNA-PKcs Is Required for Induction of IL-6 and IL-12 by ISS-ODN and Bacterial DNA

(A and B) Bone marrow-derived macrophages (BMDM) from wt or *DNA-PK*$^{-/-}$ mice were treated with ISS-ODN (5 μg/ml), M-ODN (5 μg/ml), LPS (1 μg/ml) or left untreated for 24 hr. IL-6 and IL-12 levels were determined in the supernatants by ELISA.

(C and D) BMDM from wt or *DNA-PK*$^{-/-}$ mice were treated with po-ds-ISS-ODN, po-ds-M-ODN, po-ISS-ODN, or po-M-ODN (10 μg/ml each), bacterial DNA (BD, 15 μg/ml) or calf thymus DNA (CTD, 15 μg/ml), or left untreated for 24 hr. IL-6 and IL-12 levels were determined by ELISA.

(E) Northern blot analysis. Total RNA was isolated from wt or *DNA-PKcs*$^{-/-}$ BMDM untreated or treated with ISS-ODN (5 μg/ml) or LPS (1 μg/ml) after 6.5 hr and examined for expression of IL-6, IL-12, and GAPDH mRNAs.

(F) In vivo analysis of gene expression. ISS-ODN (20 μg in PBS/mouse), po-ISS-ODN (100 μg), or po-ds-ISS-ODN (100 μg), bacterial DNA (BD, 50 μg) or calf thymus DNA (CTD, 50 μg) were i.v. injected into wt or *DNA-PKcs*$^{-/-}$ mice. After 3 hr total, RNA was extracted from the spleen or liver and subjected to RT-PCR analysis.

resolve this issue, we initially evaluated whether ISS-ODN activated IKK, which is essential for NF-κB activation by proinflammatory stimuli (reviewed by Karin and Delhase, 2000). We observed maximal IKK activation 30 min post-ISS-ODN incubation, which lasted for about 4 hr in wt BMDM (Figure 3A). While bacterial DNA and po-ISS-ODN induced IKK activation similar to ISS-ODN, little increase in IKK activity was observed with M-ODN or calf thymus DNA (Figure 3A). Optimal IKK activation was observed at an ISS-ODN concentration of 0.65 μg/ml, with little IKK activation in response M-ODN (Figure 3B).

We used BMDM isolated from *IKKβ*$^{-/-}$ *Tnfr1*$^{-/-}$ mice (Z.-W. L and M. K., unpublished data) to determine the requirement of IKK activity, which is highly reduced in these animals. The absence of IKKβ prevented IKK and NF-κB activation by ISS-ODN as well as LPS (Figure 3C) and significantly reduced the induction of IL-6 and IL-12 (Figures 3D and 3E).

DNA-PKcs Acts Upstream to IKK

The data presented above indicate that both DNA-PKcs and IKK are required for ISS-induced IL-6 and IL-12. We therefore examined the dependence of IKK activation by ISS-ODN on DNA-PKcs. While incubation of wt BMDM with ISS-ODN resulted in robust IKK activation, little increase in IKK activity was observed in similarly treated DNA-PKcs$^{-/-}$ BMDM (Figure 4A). As a result, DNA-PKcs$^{-/-}$ BMDM also exhibited impaired NF-κB activation upon treatment with ISS-ODN (Figure 4A). By contrast, DNA-PKcs-deficient BMDM were fully responsive to LPS or TNFα. Furthermore, we examined the dependence of IKK activation by bacterial DNA and po-ISS-ODN on DNA-PKcs. As expected, activation of IKK by bacterial DNA or po-ISS-ODN was largely reduced in DNA-PKcs$^{-/-}$ BMDM as compared to their wt controls (Figure 4B).

To determine whether DNA-PKcs activity is required for IKK activation, we used the PI3K inhibitor Wm. As found for IL-6 and IL-12 production (Figures 2C and 2D), only high concentrations of Wm (250 nM and above) significantly inhibited IKK activation in wt BMDM by ISS-ODN (Figure 4C). Even at 1000 nM, Wm had no effect on IKK activation by TNFα, while at lower concentrations (50–100 nM), Wm significantly inhibited IKK activation by PGDF (data not shown). We also compared ISS-ODN-induced of IKK and NF-κB activation in BMDM from wt or ATM-deficient mice (Xu et al., 1996). As shown in Figure 4D, no differences were observed for ISS-ODN-induced IKK or NF-κB activation between wt and ATM-deficient BMDM, excluding a role of ATM in this signaling.

Taken together, these results indicate that DNA-PKcs

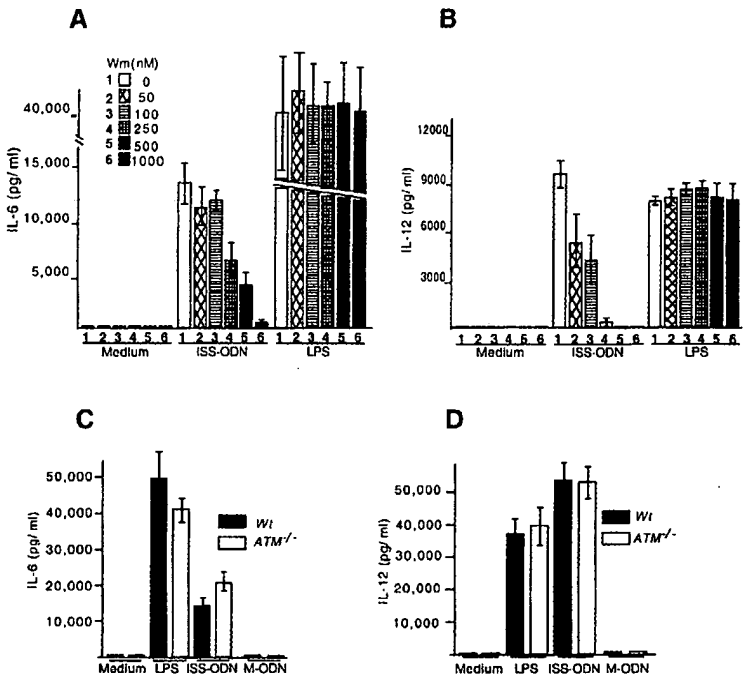

Figure 2. DNA-PK but Not ATM Activity Is Necessary for IL-6 and IL-12 by ISS-ODN

(A and B) BMDM from wt mice were treated with ISS-ODN (5 μg/ml) or LPS (1 μg/ml) in the presence of various concentrations of wortmannin (Wm). The levels of IL-6 and IL-12 in the supernatants were determined by ELISA.

(C and D) BMDM from either wt or *ATM*$^{-/-}$ mice were treated with ISS-ODN (5 μg/ml), M-ODN (5 μg/ml), LPS (1 μg/ml), or left untreated for 24 hr. IL-6 and IL-12 levels in the supernatants were determined by ELISA.

acts upstream to IKK and is specifically required for IKK activation by synthetic (ps) and natural forms (po) of ISS-enriched DNAs.

ISS-ODN Directly Activates DNA-PK

We investigated whether ISS-ODN can directly activate DNA-PK in vitro. The ability of an ISS-ODN containing the active CpG motif (5′-pur-pur-CpG-pyr-pyr-3′, i.e., 5′-AACGTT-3′) to specifically stimulate phosphorylation of the N-terminal portion of p53 (Wang and Eckhart, 1992) was compared to a battery of mutated ODNs, which include: (1) a methylated C in the CpG dinucleotide, (2) a CpC base pair instead of the CpG dinucleotide core, (3) a GpG base pair instead of the CpG dinucleotide core, (4) an ApT basepair instead of the CpG dinucleotide core, and (5) a TTCC instead of the AACG sequence of the CpG motif (see above). None of the mutant ODNs induced significant secretion of IL-6 or IL-12 upon stimulation of BMDM in vitro (data not shown). Only the ISS-ODN stimulated DNA-PK activity (Figure 5A) whereas none of the mutant ODNs, which were devoid of biological activity, led to substantial increase in DNA-PK activity.

Next, we investigated the ability of po-ISS-ODN to activate DNA-PK in vitro. Unlike ISS-ODN (Figure 4A), po-ISS-ODNs weakly activated DNA-PK only at higher concentrations (50–100 ng/reaction) (Figure 5B). By contrast, po-ds-ISS-ODN was almost as potent as ISS-ODN in activating this enzyme (Figure 5C). Methylated ISS-ODN (AA*CGTT) and methylated po-ISS-ODN (AA*CGTT) were weaker DNA-PK activators than their unmethylated counterparts (Figures 5A and 5B, respectively).

In addition, we evaluated the ability of bacterial DNA, methylated bacterial DNA, and calf thymus DNA to activate DNA-PK. To use the same equimolar amount of the various DNA preparations in the DNA-PK assays, we first measured the 5′ free ends using T4 DNA polynucleotide kinase in the DNA preparations. For bacterial DNA, this labeling yielded 6.29×10^6 cpm/0.1 μg and 4.1×10^6 cpm/1 μg of DNA, and for calf thymus DNA it yielded 8.58×10^5 cpm/0.1 μg and 4.2×10^6 cpm/1 μg of DNA. Under these conditions, calf thymus DNA was a weaker activator of DNA-PK than bacterial DNA (Figure 5D), while methylated bacterial DNA was a less potent DNA-PK activator than unmethylated bacterial DNA (Figure 5E).

To further determine whether ISS-ODN, po-ISS-ODN, or bacterial DNA activate DNA-PK in cells, we treated BMDM from either wt or DNA-PKcs-deficient mice with ISS-ODN, po-ISS-ODN, bacterial DNA, or LPS as a control. Considerable DNA-PK activity, as measured by immune-complex kinase assay, was found after a 30 min incubation with ISS-ODN, po-ISS-ODN, or bacterial DNA, which peaked after 1 hr (Figure 5F). Little or no DNA-PK activity was detected in DNA-PKcs-deficient BMDM, and LPS had no effect on DNA-PK activity even in wt cells.

DNA-PK Phosphorylates IKKβ

To explore a role of ISS-activated DNA-PK in IKK activation we tested whether affinity-purified DNA-PK can directly activate recombinant IKKα or IKKβ purified from Sf9 cells (Zandi et al., 1998). Recombinant IKKα and IKKβ display considerable basal kinase activity (Zandi et al., 1998; Chu et al., 1999), but incubation of IKKβ with DNA-PK in the presence of ISS-ODN further increased its kinase activity measured by IκB phosphorylation (Figure 6A). Furthermore, although DNA-PKcs phosphorylated IκBα, that activity was considerably lower than that achieved by IKKβ plus DNA-PK. Only a small enhancement of IκB kinase activity was found

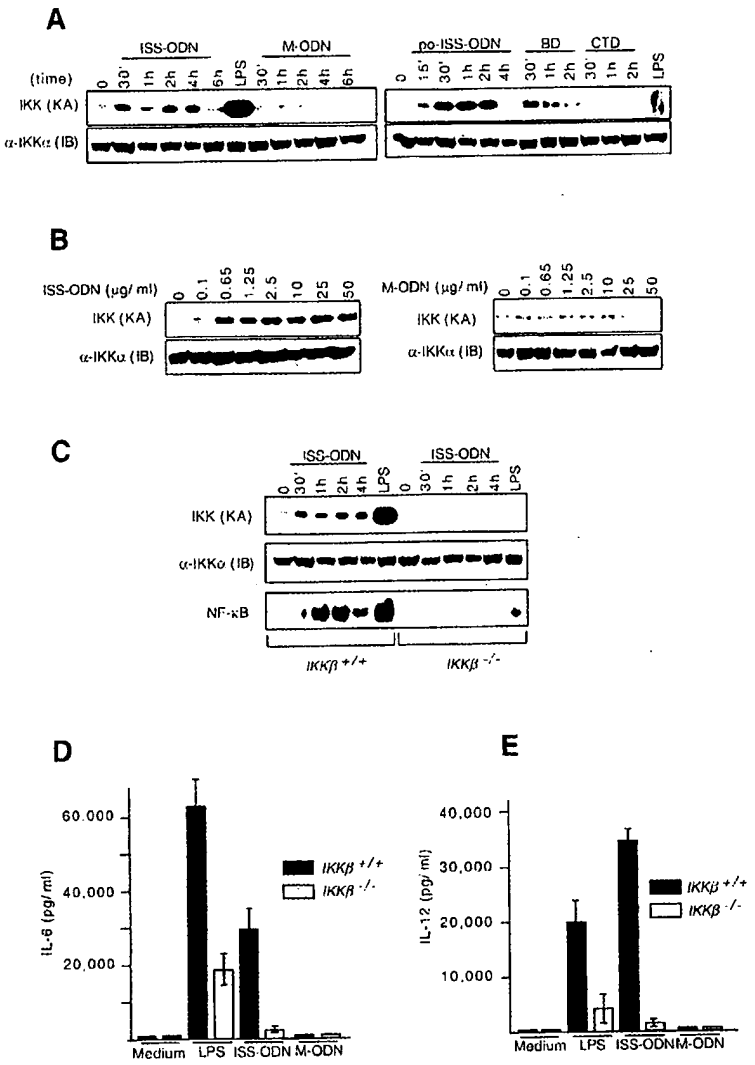

Figure 3. Involvement of IKK in NF-κB Activation by ISS-ODN and Bacterial DNA

(A) Left panel: BMDM from wt mice were treated with ISS-ODN (5 μg/ml) M-ODN (5 μg/ml) for time periods as indicated. Right panel: BMDM from wt mice were treated with po-ISS-ODN (5 μg/ml), bacterial DNA (BD, 5 μg/ml), or calf thymus DNA (CTD, 5 μg/ml) for the time periods as indicated. The cell lysates were assayed for IKK activity (KA) by an immune complex kinase assay. The recovery of IKK was determined by immunoblotting (IB) with anti-IKKα antibodies.

(B) BMDM from wt mice were treated for 2 hr with ISS-ODN (left panel) or M-ODN (right panel) at different concentrations. The cell lysates were assayed for IKK kinase activity (KA) by an immune complex kinase assay. The recovery of IKK was determined as mentioned above.

(C) BMDM from wt and *IKKβ*$^{-/-}$ *Tnfr1*$^{-/-}$ mice were treated with ISS-ODN (5 μg/ml). At the indicated time points, cells were lysed, and IKK immune complex was isolated by anti-IKKα antibodies to measure IκB kinase activity (KA). Recovery of IKK was determined by immunoblotting (IB). Cells were stimulated with LPS (10 μg/ml) for 30 min. NF-κB DNA binding activity was measured by an electrophoretic mobility shift assay (EMSA).

(D and E) IKKβ is required for induction of IL-6 and IL-12 in response to ISS-ODN. BMDM isolated from wt or *IKKβ*$^{-/-}$ *Tnfr1*$^{-/-}$ mice were treated with ISS-ODN (5 μg/ml), LPS (1 μg/ml), or left untreated for 24 hr. IL-6 and IL-12 levels were determined by ELISA.

upon incubation of IKKα with DNA-PK in the presence of ISS-ODN, but not beyond the level found with DNA-PK alone (Figure 6A, lane 6 vs. lane 5). To further confirm the activation of IKKβ by DNA-PK, we performed a coupled-kinase assay. Recombinant IKKβ was preincubated with DNA-PK in the presence or absence of ISS-ODN followed by immunoprecipitation of IKKβ and IκB kinase activity was measured. Consistent with the results described above, DNA-PK only activates IKKβ in the presence of ISS-ODN (data not shown). We next determined whether DNA-PK phosphorylates IKKβ. Recombinant catalyticly inactive IKKβ [IKKβ (KA)] purified from Sf9 cells was incubated with or without DNA-PK, in the presence or absence of ISS-ODN. As shown in Figure 6B, DNA-PK phosphorylated IKKβ (KA) when incubated with ISS-ODN.

Discussion

Infection of the mammalian host with bacterial, fungal, and viral pathogens results in rapid activation of innate immunity, which provides a rapid defense and at the same time alerts the adaptive immune system to the presence of pathogens (Medzhitov and Janeway, 1997). The innate immune response to invading pathogens involves the effective and rapid recognition of highly conserved and usually repetitive microbial structural patterns such as those found in polysaccharides, lectins, LPS, and dsRNA (Medzhitov and Janeway, 1997). This recognition usually occurs through pattern recognition receptors such as those that belong to the Toll family (Poltorak et al., 1998; Aderem and Ulevitch, 2000). It has been speculated that bacterial DNA and its synthetic analogs (i.e., ISS-ODNs), due to their relatively high content of nonmethylated CpG dinucleotides are similarly recognized as foreign structures by the innate immune system of the invaded host (Klinman et al., 1999; Wagner, 1999). The recognition mechanism, however, remained enigmatic.

The development of innate immunity appeared relatively early in evolution preceding the appearance of adaptive immunity, a protective mechanism unique to vertebrates (Hoffmann et al., 1999). Analysis of innate immune responses to bacterial and fungal pathogens in

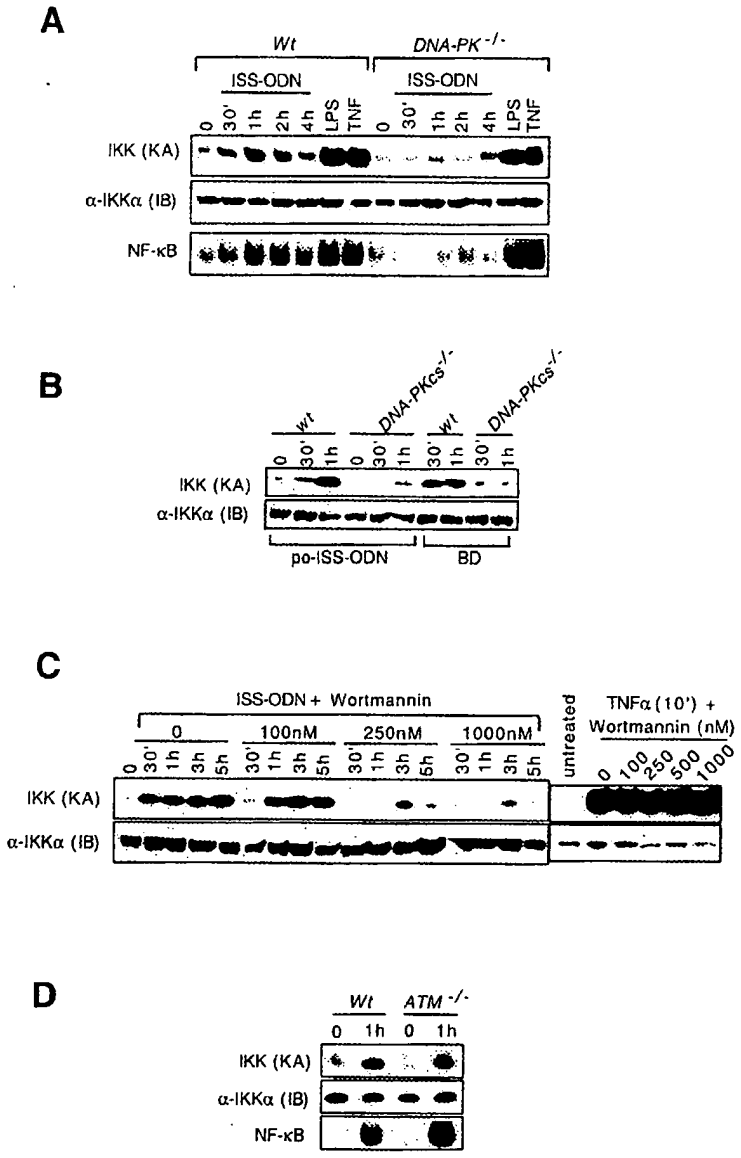

Figure 4. DNA-PKcs Activates IKK by ISS-ODN and Bacterial DNA

(A) BMDM from wt or *DNA-PKcs*$^{-/-}$ mice were treated with ISS-ODN (5 μg/ml) for various time periods, LPS (10 μg/ml for 30 min) or TNFα (10 ng/ml for 10 min). At the indicated time points, cells were lysed and IKK activity was measured by immune complex kinase assays (KA). Recovery of IKK was determined by immunoblotting (IB). NF-κB DNA binding activity was determined by EMSA.

(B) BMDM from wt or *DNA-PKcs*$^{-/-}$ mice were treated with po-ISS-ODN (5 μg/ml) or bacterial DNA (BD, 5 μg/ml). At the indicated time points, cells were lysed, IKK activity and IKK recovery were analyzed as described above.

(C) BMDM from wt mice were treated with ISS-ODN (5 μg/ml) or TNFα (10 ng/ml) as a control, in the presence of different concentrations of Wortmaninn (Wm) for the indicated time periods, after which IKK activity was measured by immune complex kinase assay (KA). Recovery of IKK was determined by immunoblotting (IB).

(D) BMDM isolated from wt or *ATM*$^{-/-}$ mice were treated with ISS-ODN for 1 hr. Cells were lysed and IKK activity, IKK recovery, and NF-κB DNA binding activity were analyzed as described above.

Drosophila has implicated the involvement of signaling pathways that are highly similar to those that activate AP-1 and NF-κB transcription factors in vertebrates (Hoffmann et al., 1999). The role of AP-1 and NF-κB in the control of the innate immune response in mammals is well recognized (Baldwin, 1996; May and Ghosh, 1998; Chu et al., 1999). It is also well established that IKK is activated by dsRNA, viral infection, or LPS, and is required for cytokine or chemokine production (Chu et al., 1999; Karin and Delhase, 2000).

The results presented here shed new light on the mechanism by which ISS-ODNs activate innate immunity by demonstrating that: (1) DNA-PKcs is required for induction of IL-6 and IL-12, (2) DNA-PKcs activates IKKβ, which is also required for IL-6 and IL-12 induction by ISS-ODN, and (3) DNA-PKcs and IKK activities are more efficiently stimulated by biologically active ISS-ODNs than by other ODNs that lack immunostimulatory activity.

Several lines of evidence indicate that DNA-PK is involved in the cellular response to DNA ds breaks (Smith and Jackson, 1999). The protein kinase activity of DNA-PK is stimulated by DNA ends (Carter et al., 1990; Gottlieb and Jackson, 1993; Leuther et al., 1999; Hammarsten et al., 2000). In addition, DNA with blunt ends, 5′ overhanging ends, or 3′ overhanging ends all activate DNA-PK with similar efficiency (Gottlieb and Jackson, 1993), whereas ds DNA with hairpin ends and supercoiled DNA are inactive (Smider et al., 1998; Hammarsten et al., 2000). Other studies revealed that DNA-PKcs binds both ds and ss DNA (Leuther et al., 1999; Smith and Jackson, 1999; Hammarsten et al., 2000). The minimal length of ds-DNA required for efficient DNA-PKcs binding is no less than 12 bp while the optimal length of ss DNA needed for efficient DNA-PKcs activation is between 5 and 10 nucleotides (Leuther et al., 1999; Hammarsten et al., 2000).

Our results here have identified a novel function for

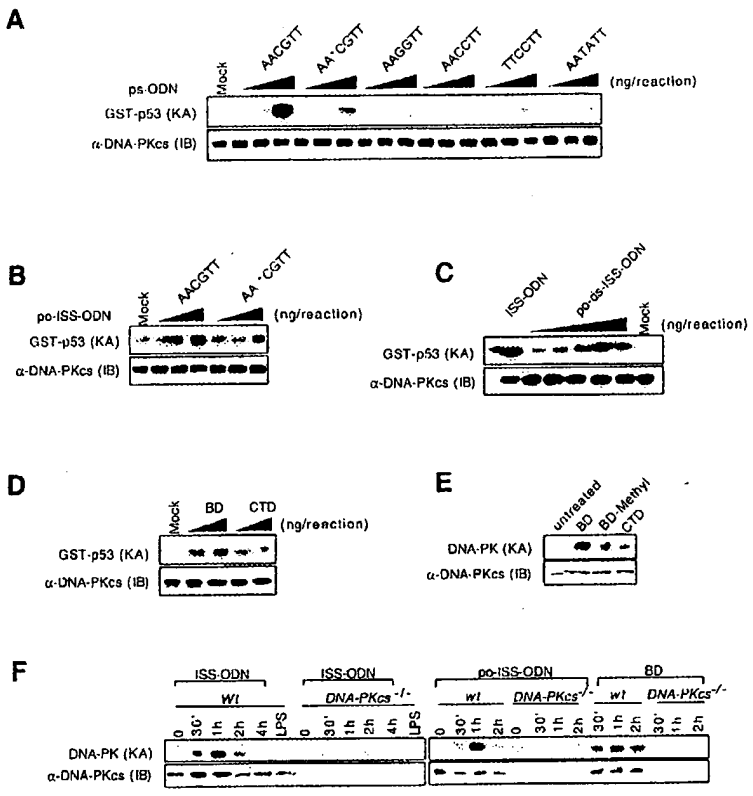

Figure 5. ISS-ODN and Bacterial DNA Activate DNA-PK In Vitro and In Vivo

(A) The ODNs; ISS-ODN (...AACGTT), methylated ISS-ODN at the ^{5}C position of the CpG dinucleotode (...AA*CGTT) or mutated ODN (M-ODNs: ...AAGGTT..., ...AACCTT... or AA TATT) at a concentration of 0, 0.1, 0.3, or 1 ng/reaction were incubated with affinity-purified DNA-PK (Promega), 0.5 μg of GST-p53 (1–70), and 3.3 μCi of γ-^{32}P-ATP at 30°C for 30 min. The reactions were stopped by addition of 4× sample buffer and the samples were boiled, separated on 9% SDS-PAGE, transferred on a PVDF membrane, and visualized by autoradiography at −80°C for 1 hr.

(B) The po-ODNs ISS-ODN (...AACGTT) and methylated po-ISS-ODN (...AA*CGTT) at a concentration of 20, 50, or 100 ng/reaction were incubated with affinity-purified DNA-PK. DNA-PK activity was determined as described above.

(C) The ISS-ODN (AACGTT) at concentrations of 0.3 and 1 ng/reaction was compared to stimulate DNA-PK activity to the po-ds-ISS-ODN (AACGTT) at concentrations of 0.2, 1, 2, 5, 10 ng/reaction. DNA-PK activity was determined as described above.

(D) Equimolar amounts of bacterial DNA (BD) or calf thymus DNA (CTD) as measured by γ-^{32}P labeling of free 5′ ends (4.1×10^5 and 4.2×10^8 cpm per 1 μg of DNA, respectively). 5 ng of each DNA, roughly equal to 2×10^4 cpm, was incubated with affinity-purified DNA-PK and 3.3 μCi of γ-^{32}P-ATP at 30°C for 30 min. The DNA-PK activity was determined as described above.

(E) BMDM isolated from wt mice were treated with bacterial DNA (BD, 2.5 μg/ml), methylated bacterial DNA (2.5 μg/ml), or calf thymus DNA (CTD, 2.5 μg/ml) for 1 hr and then lysed. DNA-PK activity was determined as described above.

(F) BMDM isolated from wt and *DNA-PKcs*$^{-/-}$ mice were treated with ISS-ODN (ps-ss) (5 μg/ml), po-ISS-ODN (ss) (5 μg/ml), bacterial DNA (BD, 2.5 μg/ml), LPS (10 μg/ml), or left untreated for the indicated time periods. Cells were then lysed and the 100 μg of lysates were assayed for DNA-PK activity by an immune complex kinase assay (KA) using anti-DNA-PKcs monoclonal antibodies (mAb) and GST-p53 (1–70) as a substrate. Recovery of DNA-PKcs was determined by immunoblotting (IB).

DNA-PK, i.e., interaction and activation by fragments of bacterial DNA and ISS-ODN (Figure 5). Optimal activation of DNA-PKcs by ISS-ODNs appears to be sequence specific since mutations within the CpG motif which impair immunostimulatory activity (Krieg et al., 1995) also reduce the ability to activate DNA-PK (Figure 5). Nevertheless, even biologically inactive ODNs retain the ability to activate DNA-PK, an effect mediated by DNA ends. Using BMDM from DNA-PKcs-deficient mice or high concentrations of Wm sufficient for DNA-PK inhibition, we obtained genetic and biochemical evidence that the activation of DNA-PK by ps and po ISS-ODNs as well as bacterial DNA is required for induction of IL-6 and IL-12 (Figure 1). Although DNA-PK was also activated by methylated ISS-ODN and methylated bacterial DNA (Figure 5), which have reduced biological activity, this activation was weaker than that observed for nonmethylated ISS-ODN or bacterial DNA (Figure 5). It is likely, however, that DNA-PKcs, although essential for activation of innate immunity by ISS-ODN is not sufficient for complete discrimination between methylated vs. nonmethylated and mammalian vs. bacterial sequences. Additional components may exist that further increase the discriminatory ability of this molecular recognition system. The MyD88 is a potential component of this auxiliary recognition system as it was recently shown to mediate signaling by ISS-ODN and to be required for ISS-induced IKK activation (Hacker et al., 2000). However, the molecular link between DNA-PK and MyD88 has yet to be established.

Our results also demonstrate that in addition to its requirements for cytokine induction, DNA-PKcs is required for NF-κB activation in response to ISS-ODN. Although DNA-PK can phosphorylate sites at the C terminus of IκBα, it is not directly involved in induction of IκBα degradation (Basu et al., 1998; Liu et al., 1998). Rather, DNA-PKcs is likely to affect NF-κB activation via IKK. The defect in NF-κB activation in DNA-PKcs-deficient cells correlates with their inability to rapidly activate the IKK complex in response to ISS-ODN. The activation of IKK by ISS-ODN is largely dependent on IKKβ phosphorylation, as was shown for other pro-inflammatory stimuli (Chu et al., 1999; Li et al., 1999; Tanaka et al., 1999). Although DNA-PKcs was first identified as a nuclear protein (Smith and Jackson, 1999), several recent reports demonstrated that DNA-PKcs is also located in the cytoplasm (Carter et al., 1990; Danska et al., 1996; Nilsson et al., 1999; Koiker et al., 1999). Thus, it is plausible that ISS-ODN activates the catalytic subunit of DNA-PK in the cytoplasm, which in turn phos-

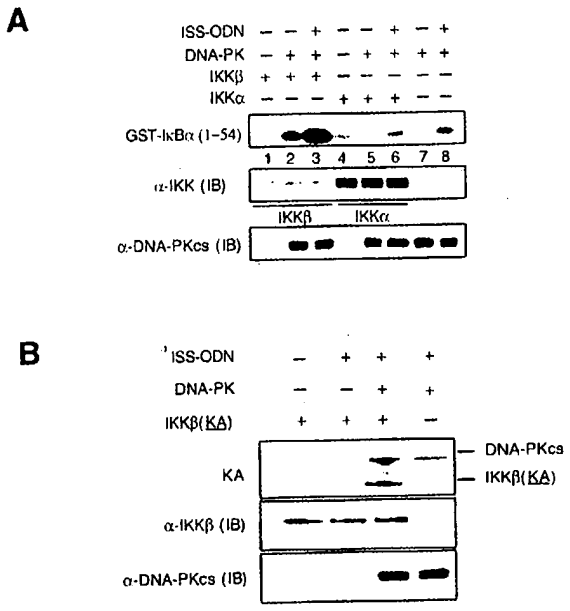

Figure 6. DNA-PK Activates IKKβ through Phosphorylation

(A) DNA-PK activates IKKβ but not IKKα. IKKβ (1 μl, 1:40 dilution) or IKKα (1 μl) purified from Sf9 cells (Zandi et al., 1998) was incubated with DNA-PK (1 μl, 1:3 dilution), 0.5 μg of GST-IκBα (1–54) and 3 μCi of γ-^{32}P-ATP in the presence or absence of ISS-ODN (2 ng) at 30°C for 30 min. The reaction was stopped by addition of 4× sample buffer. The samples were boiled, loaded on a 9% SDS-PAGE, transferred onto a PVDF membrane, and visualized by autoradiography. The presence of IKKα, IKKβ, or DNA-PK in various reactions was determined by immunoblotting (IB).

(B) DNA-PK phosphorylates catalytic inactive subunit of IKKβ [IKK (KA)]. IKKβ (KA) (3 μl) purified from Sf9 cells (Zandi et al., 1998) and 10 μCi of γ-^{32}P-ATP were incubated with DNA-PK (1 μl), or left alone in the presence or absence of ISS-ODN (2 ng) at 30°C for 45 min. The reaction was stopped by addition of 4× sample buffer. The samples were loaded, transferred onto a PVDF membrane, and visualized by autoradiography. The presence of IKKβ (KA) or DNA-PK in the reactions was determined by immunoblotting (IB).

phorylates and activates the IKKβ subunit of IKK leading to NF-kB activation. Although the absence of DNA-PKcs results in a dramatic decrease in IKK activation by ISS-ODN or bacterial DNA, some residual activity can be observed (Figure 4). This residual activity can be derived from ISS-induced TNFα production, which is not fully dependent on NF-κB, or can be due to the operation of the previously mentioned auxiliary recognition system.

DNA-PK is a member of the DNA repair machinery (so-called "caretaker") and has an essential role in the maintenance of genome stability (Smith and Jackson, 1999). DNA-PK plays a pivotal role in DNA ds breaks repair and therefore in programmed antigen receptor rearrangements during B and T cells development (Carrol and Bosma, 1991; Gottlieb and Jackson, 1993; Kirchgessner et al., 1993; Hartley et al., 1995; Danska et al., 1996; Kurimasa et al., 1999; Smith and Jackson, 1999). DNA-PKcs null mice are hypersensitive to ionizing radiation and develop severe combined immune deficiency (Kurimasa et al., 1999; Smith and Jackson, 1999). Thus, the requirement of DNA-PK in adaptive immunity is well established. Our results indicate that DNA-PKcs is also required for activation of innate immunity by ISS-ODN. This finding fits nicely with previous reports in which DNA-PKcs has been found to be degraded, apparently via a proteosomal mechanism, during herpes simplex virus (HSV) type I infection of mammalian cells (Lees-Miller et al., 1996; Parkinson et al., 1999). As a result, HSV was shown, in these studies, to replicate more efficiently in a cell line with undetectable DNA-PKcs than in a wt control cell line (Lees-Miller et al., 1996; Parkinson et al., 1999). Therefore, DNA-PKcs may also be involved in mounting innate anti-viral responses. Our results explain how a deficiency in DNA-PKcs results in defective activation of innate immunity.

In conclusion, DNA-PK plays a pivotal role in two different responses to DNA: (1) activation of DNA repair and recombination systems, and (2) activation of innate immunity. DNA-PK is involved in protecting the host genome from danger imposed by intrinsic DNA damage such as DNA ds breaks generated by ionizing radiation or produced during immunoglobulin gene rearrangement. In addition, DNA-PK is involved in protecting the host from a danger imposed by invading bacterial DNA (e.g., intracellular infection). Thus, DNA-PK provides a link between genome defense (DNA repair machinery) and host defense (innate immunity).

Experimental Procedures

Animals, Cell Culture, DNAs, ODNs, and ELISA

DNA-PKcs$^{-/-}$ and their wt control mice on the 129 genetic background were generated by Dr. G. C. Li and bred at Memorial Sloan-Kettering Cancer Center, New York, NY. *IKKβ* $^{-/-}$ *Tnfr1*$^{-/-}$ mice were generated by Drs. Z.-W. Li and M. Karin (unpublished data). *ATM*$^{-/-}$ mice on the C57BL/6 background were generated and bred by Dr. Y. Xu (UCSD) as was previously described (Xu et al., 1996) while their wt controls were purchased from Jackson Laboratories (Bar Harbor, ME). BMDMs from wt, *DNA-PKcs*$^{-/-}$ mice, *IKKβ* $^{-/-}$ *Tnfr1*$^{-/-}$, and *ATM*$^{-/-}$ mice were prepared as was previously published (Martin-Orozco et al., 1999), maintained in DMEM with 10% FBS, antibiotics, and 20% L-cell medium, and cultured for 7–10 days to allow them to mature. Prior to use, BMDM were seeded (2.5 × 10^5/well in triplicate) in 96 well plates and then treated with LPS (1 μg/ml), ISS-ODN (5 μg/ml) or M-ODN (5 μg/ml), po-ISS-ODN (10 μg/ml) or po-ds-ISS-ODN (10 μg/ml), LPS-free, ultra pure bacterial DNA (*E. coli*, Sigma) (15 μg/ml) or methylated bacterial DNA or LPS-free, ultra pure calf thymus DNA (Sigma) (15 μg/ml). Methylation of bacterial DNA was performed by SssI methylase (Biolab, Boston, MA) (15 μg/ml) following manufacturer's instruction. Where indicated, the PI3K inhibitor wortmannin (Wm), at various concentrations, was added to ISS-ODN or LPS stimulated BMDMs. After 24 hr in culture, the supernatants were collected and assayed for IL-6 and IL-12 levels by ELISA kits (PharMingen, San Diego, CA).

Most of the experiments described in this study were performed with LPS free, single-stranded (ss), 22 mer long, phosphothioate (ps) ODNs. In some experiments, ss and double-stranded (ds) 22 mer long phosphodiester (po) ODNs were used. (Trilink, San Diego, CA). The sequences of the ODNs used in this study are as follow:

- ISS-ODN (1), 5′-TGACTGTGAACGTTCGAGATGA-3′
- ISS-ODN (2), 5′-TGACTGTGAACGTTAGAGATGA-3′
- Methylated ($^{5\text{-methyl}}$C) ISS-ODN, 5′-TGACTGTGAA^{m}CGTTAGAGA TGA-3′
- Mutated (M)-ODN, 5′-TGACTGTGAAGGTTAGAGATGA-3′
- Control-ODN (1), 5′-TGACTGTGAACCTTAGAGATGA-3′
- Control-ODN (2), 5′-TGACTGTGTTCCTTAGAGATGA-3′
- Control-ODN (3), 5′-TGACTGTGAATATTAGAGATGA-3′

Kinase Assays and Immunoblotting

Kinase assays and immunoblotting were performed according to Li et al. (1999). Briefly, BMDM were treated with ISS-ODN (5 μg/ml),

M-ODN (5 μg/ml) on ps and po backbones as indicated, LPS-free bacterial DNA or methylated bacterial DNA (5 μg/ml), LPS-free calf thymus DNA (5 μg/ml), LPS (10 μg/ml), or TNFα (10 ng/ml) for the indicated time periods. Cell lysates were prepared and normalized by immunoblotting (IB) with anti-IKKα polyclonal antibodies (Santa Cruz, Santa Cruz Biotech Inc., CA), anti-IKKβ polyclonal antbodies (Santa Cruz), or anti-DNA-PKcs monoclonal antibodies (NeoMarker, CA). IκB kinase (IKK) complex or DNA-PK complex from 100 μg of the lysates were immunoprecipitated by anti-IKKα or by anti-DNA-PKcs antibodies. The kinase activities (KA) were determined by a kinase assay using the N terminus of IκBα (for IKK) or the N terminus of p53 (for DNA-PK) as a substrate as previously described (Wang and Eckhart, 1992; Li et al., 1999; Hammarsten et al., 2000).

The in vitro DNA-PK phosphorylation assay was performed according to Hammarsten et al. (2000) with modification. Briefly, affinity-purified DNA-PK (Promega, MO) was incubated with various DNA preparations (described below), 0.5 μg of GST-p53 (1–70) and 3.3 μCi of γ-^{32}P-ATP in a 20 μl reaction buffer (10 mM Tris-Cl, 5 mM $MgCl_2$, 0.3 mM EDTA, and 10 μM ATP) at 30°C for 30 min. The reaction was stopped by addition of 4× loading buffer. The samples were boiled, loaded on 9% SDS-PAGE, transferred onto a PVDF membrane and visualized by autoradiography.

The ODNs (ps-ss) used include an ISS-ODN with an active CpG motif (AACGTT), a methylated ISS-ODN at the ^{5}C of the CpG dinucleotide (AA^{5}CGTT), and various control ODNs. These ODNs were incubated at concentrations of 0, 0.1, 0.3, or 1 ng/reaction. The po-ISS-ODN was incubated at a concentration of 20, 50, or 100 ng/reaction. The po-ds-ISS-ODN was incubated at a concentration of 0, 0.5, 1, 2, 5, or 10 ng/reaction. The bacterial or calf thymus DNAs were each incubated at a concentration of 1, 2, or 5 ng/reaction. Electrophoretic gel mobility shift assay (EMSA) was performed as previously described (Chu et al., 1999; Li et al., 1999). In vitro IKK kinase assays were performed using purified IKK derived from Sf9 insect cell lysates as was previously described (Zandi et al., 1998).

RT-PCR and Northern Blots

Total cellular RNA was isolated from spleen or liver of wt or DNA-PKcs$^{-/-}$ mice injected with ISS-ODN (50 μg), po-ISS-ODN (100 μg), po-ds-ISS-ODN (100 μg), bacterial DNA (100 μg), or calf thymus DNA (100 μg), using a RNA isolation kit (Stratagene, San Diego, CA), and subjected to RT-PCR. First strand cDNA preparation and PCR amplification were performed using the SuperScript preamplification system (Gibco BRL, Gaithersburg, MD) and AdvanTaq Plus DNA polymerase (Clontech, San Francisco, CA), respectively. The primer sequences used were as follows:

- IL-6: (sense) 5′-ATGAAGTTCCTCTCTGCAAGAGACT-3′; (antisense) 5′-CACTAGGTTTGCCGAGTAGATCTC-3′
- IL-12p40: (sense) 5′-GGGACATCATCAAACCAGACC-3′; (antisense) 5′-GCCAACCAAGCAGAAGACAGC-3′
- GAPDH: (sense) 5′-ACCACAGTCCATGCCATCAC-3′; (antisense) 5′-TCCACCACCCTGTTGCTGTA-3′

PCR reactions were performed under the following conditions by appropriate cycling number (94°C: 30 s; 65°C: 30 s; 68°C: 30 s). PCR products were visualized by electrophoresis on 1.5% TAE agarose gels after being stained with ethidium bromide. BMDM isolated from either wild-type or DNA-PKcs-deficient mice were treated with ISS-ODN (10 μg/ml), LPS (10 μg/ml), or left untreated for 6.5 hr. Total RNA was isolated and 10 μg of total RNA was separated on 1% agarose gel and then transferred onto a nylon membrane. The membrane was probed with α-^{32}P-dCTP-labeled IL-6 or IL-12 or GAPDH cDNA (generated by RT-PCR as described above) followed by autoradiography.

Methylation and Labeling of Free Ends of Genomic DNAs

When indicated, 100 μg of ultra pure bacterial DNA (*E. coli*, Sigma) was incubated with or without 200 units SssI methylase (Biolab) in a 200 μl reaction buffer according to manufacturer's instruction at 37°C for 3 hr and then extracted with phenol/chloroform. The bacterial DNA was precipitated with ethanol and dissolved in TE buffer. 1 μg of mock and methylated bacterial DNA was further incubated with 10 units of BstU1 at 60°C for 4 hr, loaded on 1% agarose gel, and visualized by EB staining for the absence or presence of digest products in the methylated and in the nonmethylated bacterial DNA, respectively (data not shown).

For the DNA-PK assay, we measure the free ends in *E. coli* and calf thymus DNAs by labeling the 5′ free ends of both the DNA preparations. Thus, 0.2 μg of either bacterial or calf thymus DNAs were incubated with 15 units of T4 PNK (Stratagene, San Diego, CA) and 100 μCi of γ-^{32}P-ATP in a 20 μl of reaction at 37°C for 3 hr. To purify the labeled DNAs from the γ-^{32}P-ATP excess, the samples were loaded onto SephdexG50 column (Stratagene San Diego, CA) after the reaction was stopped. 1 μl of labeled DNA was used to measure radioactivity which yielded $4.1 \times 10^6 \pm 2 \times 10^4$ cpm/1 μg for bacterial DNA and $4.2 \times 10^6 \pm 5.2 \times 10^4$ cpm/1 μg for calf thymus DNA.

Acknowledgments

We thank Parag Bhatt, Nan Fang, Yinglin Hu, Samantha Kim, Tony Yoon, M.-D. Nguyen, Arash Ronaghy, Tomoko Hayashi, Akihiro Kurimasa, and Lucinda Beck for their excellent assistance. We also thank Dr. Yang Xu for providing us with *ATM*$^{-/-}$ mice. This work was supported in part by Dynavax Technologies Corp; by National Institutes of Health Grants to E. R. (AI 40682), M. K. (AI 43477), G. C. L. (CA-59609 and 78497), and D. J. C. (CA-505159); Cancer Research Institute postdoctoral fellowship to Z. W. L., tobacco-related disease research program to W. M. C. (9KT-00567;) and by California Cancer Research program to M. K.

Received May 31, 2000; revised October 10, 2000.

References

Aderem, A., and Ulevitch, R.J. (2000). Toll-like receptors in the induction of the innate immune response. Nature *406*, 782–787.

Baldwin, A.S. (1996). The NF-κB and IκB proteins: new discoveries and insights. Annu. Rev. Immunol. *14*, 649–668.

Basu, S., Rosenzweig, K.R., Youmell, M., and Price, B.D. (1998). The DNA-dependent protein kinase participates in the activation of NF kappa B following DNA damage. Biochem. Biophys. Res. Commun. *247*, 79–83.

Bauer, M., Heeg, K., Wagner, H.R., and Lipford, G.B. (1999). DNA activates human immune cells through a CpG sequence-dependent manner. Immunology *97*, 699–705.

Bird, A.P. (1993). Functions for DNA methylation in vertebrates. Cold Spring Harb. Symp. Quant. Biol. *58*, 281–285.

Carroll, A.M., and Bosma, M.J. (1991). T-lymphocyte development in scid mice is arrested shortly after the initiation of T-cell receptor delta gene recombination. Genes Dev. *13*, 57–66.

Carter, T., Vancurova, I., Sun, I., Lou, W., and DeLeon, S. (1990). A DNA-activated protein kinase from HeLa cell nuclei. Mol. Cell. Biol. *10*, 6460–6471.

Cho, H.J., Takabayashi, K., Cheng, P.M., Nguyen, M.-D., Corr, M., Tuck, S., and Raz, E. (2000). Immunostimulatory DNA-based vaccines induce cytotoxic lymphocyte activity by a T-helper cell-independent mechanism. Nat. Biotech. *18*, 509–514.

Chu, W.M., Ostertag, D., Li, Z.W., Chang, L., Chen, Y., Hu, Y., Williams, B., Perrault, J., and Karin, M. (1999). JNK2 and IKKbeta are required for activating the innate response to viral infection. Immunity *11*, 721–731.

Danska, J.S., Holland, D.P., Mariathasan, S., Williams, K.M., and Guidos, C.J. (1996). Biochemical and genetic defects in the DNA-dependent protein kinase in murine scid lymphocytes. Mol. Cell. Biol. *16*, 5507–5517.

Falzon, M., Fewell, J.W., and Kuff, E.L. (1993). EBP-80, a transcription factor closely resembling the human autoantigen Ku, recognizes single-to double-strand transitions in DNA. J. Biol. Chem. *268*, 10546–10552.

Gottlieb, T.M., and Jackson, S.P. (1993). The DNA-dependent protein kinase: requirement for DNA ends and association with Ku antigen. Cell *72*, 131–142.

Hacker, H., Mischak, H., Miethke, T., Liptay, S., Schmid, R., Sparwasser, T., Heeg, K., Lipford, G.B., and Wagner, H. (1998). CpG-DNA-

specific activation of antigen-presenting cells requires stress kinase activity and is preceded by non-specific endocytosis and endosomal maturation. EMBO J. *17*, 6230–6240.

Hacker, H., Vabulas, R.M., Takeuchi, O., Hoshino, K., Akira, S., and Wagner, H. (2000). Immune cell activation by bacterial CpG-DNA through myeloid differentiation marker 88 and tumor necrosis factor receptor-associated factor (TRAF) 6. J. Exp. Med. *192*, 595–600.

Hammarsten, O., DeFazio, L.G., and Chu, G. (2000). Activation of DNA-dependent protein kinase by single-stranded DNA ends. J. Biol. Chem. *275*, 1541–1545.

Hartley, K.O., Gell, D., Smith, G.C., Zhang, H., Divecha, N., Connelly, M.A., Admon, A., Lees-Miller, S.P., Anderson, C.W., and Jackson, S.P. (1995). DNA-dependent protein kinase catalytic subunit: a relative of phosphatidylinositol 3-kinase and the ataxia telangiectasia gene product. Cell *82*, 849–856.

Hoffmann, J.A., Kafatos, F.C., Janeway, C.A.J., and Ezekowiz, R.A.B. (1999). Phylogenetic perspectives in innate immunity. Science *284*, 1313–1318.

Karin, M., and Delhase, M. (2000). The I kappa B kinase (IKK) and NF-kappa B: key elements of proinflammatory signalling. Semin. Immunol. *12*, 85–89.

Kirchgessner, C.U., Patil, C.K., Evans, J.W., Cuomo, C.A., Fried, L.M., Carter, T., Oettinger, M.A., and Brown, J.M. (1995). DNA-dependent kinase (p350) as a candidate gene for the murine SCID defect. Science *267*, 1178–1183.

Klinman, D.M., Yi, A.K., Beaucage, S.L., Conover, J., and Krieg, A.M. (1996). CpG motifs present in bacteria DNA rapidly induce lymphocytes to secrete interleukin 6, interleukin 12, and interferon gamma. Proc. Natl. Acad. Sci. USA *93*, 2879–2883.

Klinman, D.M., Verthelyi, D., Takeshita, F., and Ishii, K.J. (1999). Immune recognition of foreign DNA: a cure for bioterrorism? Immunity *11*, 123–129.

Koiker, M., Awaji, T., Kataoka, M., Tsujimoto, G., Kartasova, T., Koike, A., and Shiomi, T. (1999). Differential subcellular localization of DNA-dependent protein kinase components Ku and DNA-PKcs during mitosis. J. Cell Sci. *112*, 4031–4039.

Krieg, A.M., Yi, A.K., Matson, S., Waldschmidt, T.J., Bishop, G.A., Teasdale, R., Koretzky, G.A., and Klinman, D.M. (1995). CpG motifs in bacterial DNA trigger direct B-cell activation. Nature *374*, 546–549.

Kurimasa, A., Ouyang, H., Dong, L.J., Wang, S., Li, X., Cordon-Cardo, C., Chen, D.J., and Li, G.C. (1999). Catalytic subunit of DNA-dependent protein kinase: impact on lymphocyte development and tumorigenesis. Proc. Natl. Acad. Sci. USA *96*, 1403–1408.

Lees-Miller, S.P., Long, M.C., Kilvert, M.A., Lam, V., Rice, S.A., and Spencer, C.A. (1996). Attenuation of DNA-dependent protein kinase activity and its catalytic subunit by the herpes simplex virus type 1 transactivator ICP0. J. Virol. *70*, 7471–7477.

Leuther, K.K., Hammarsten, O., Kornberg, R.D., and Chu, G. (1999). Structure of DNA-dependent protein kinase: implications for its regulation by DNA. EMBO J. *18*, 1114–1123.

Li, Z.W., Chu, W.-M., Hu, Y., Delhase, M., Deerinck, T., Ellisman, M., Johnson, R., and Karin, M. (1999). The IKKbeta subunit of IkappaB kinase (IKK) is essential for nuclear factor kappaB activation and prevention of apoptosis. J. Exp. Med. *189*, 1839–1845.

Liu, L., Kwak, Y.T., Bex, F., Garcia-Martinez, L.F., Li, X.H., Meek, K., Lane, W.S., and Gaynor, R.B. (1998). DNA-dependent protein kinase phosphorylation of IkappaB alpha and IkappaB beta regulates NF-kappaB DNA binding properties. Mol. Cell. Biol. *18*, 4221–4234.

Martin-Orozco, E., Kobayashi, H., Van Uden, J., Nguyen, M.D., Kornbluth, R.S., and Raz, E. (1999). Enhancement of antigen-presenting cell surface molecules involved in cognate interactions by immunostimulatory DNA sequences. Int. Immunol. *11*, 1111–1118.

May, M.J., and Ghosh, S. (1998). Signal transduction through NF-κB. Immunol. Today *19*, 80–88.

Medzhitov, R., and Janeway, C.A., Jr. (1997). Innate immunity: the virtues of a nonclonal system of recognition. Cell *91*, 295–298.

Mimori, T., and Hardin, J.A. (1986). Mechanism of interaction between Ku protein and DNA. J. Biol. Chem. *261*, 10375–10379.

Nilsson, A., Sirzen, F., Lewensohn, R., Wang, N., and Skog, S. (1999). Cell cycle-dependent regulation of the DNA-dependent protein kinase. Cell Prolif. *32*, 239–248.

Parkinson, J., Lees-Miller, S.P., and Everett, R.D. (1999). Herpes simplex virus type 1 immediate-early protein vmw110 induces the proteasome-dependent degradation of the catalytic subunit of DNA-dependent protein kinase. J. Virol. *73*, 650–657.

Poltorak, A., He, X., Smirnova, I., Liu, M.Y., Huffel, C.V., Du, X., Birdwell, D., Alejos, E., Silva, M., Galanos, C., et al. (1998). Defective LPS signaling in C3H/HeJ and C57BL/10ScCr mice: mutations in Tlr4 gene. Science *282*, 2085–2088.

Roman, M., Martin-Orozco, E., Goodman, J.S., Nguyen, M.D., Sato, Y., Ronaghy, A., Kornbluth, R.S., Richman, D.D., Carson, D.A., and Raz, E. (1997). Immunostimulatory DNA sequences function as T helper-1-promoting adjuvants. Nat. Med. *3*, 849–854.

Sato, Y., Roman, M., Tighe, H., Lee, D., Corr, M., Nguyen, M.D., Silverman, G.J., Lotz, M., Carson, D.A., and Raz, E. (1996). Immunostimulatory DNA sequences necessary for effective intradermal gene immunization. Science *273*, 352–354.

Smider, V., Rathmell, W.K., Brown, G., Lewis, S., and Chu, G. (1998). Failure of hairpin-ended and nicked DNA to activate DNA-dependent protein kinase: implications for V(D)J recombination. Mol. Cell. Biol. *18*, 6853–6858.

Smith, G.C., and Jackson, S.P. (1999). The DNA-dependent protein kinase. Genes Dev. *13*, 916–934.

Stacey, K. J., Sweet, M.J., and Hume, D.A. (1996). Macrophages ingest and are activated by bacterial DNA. J. Immunol. *157*, 2116–2122.

Tanaka, M., Fuentes, M.E., Yamaguchi, K., Durnin, M.H., Dalrymple, S. A., Hardy, K.L., and Goeddel, D.V. (1999). Embryonic lethality, liver degeneration, and impaired NF-kappa B activation in IKK-beta-deficient mice. Immunity *10*, 421–429.

Tokunaga, T., Yamamoto, H., Shimada, S., Abe, H., Fukuda, T., Fujisawa, Y., et al. (1984). Antitumor activity of deoxyribonucleic acid fraction from Mycobacterium bovis BCG. I. Isolation, physicochemical characterization, and antitumor activity. J. Nat. Cancer Inst. *72*, 955–962.

Van Uden, J., and Raz, E. (1999). Immunostimulatory DNA and applications to allergic disease. J. Allergy Clin. Immunol. *104*, 902–910.

Wagner, H. (1999). Bacterial CpG DNA activates immune cells to signal infectious danger. Adv. Immunol. *73*, 329–368.

Wang, Y., and Eckhart, W. (1992). Phosphorylation sites in the amino-terminal region of mouse p53. Proc. Natl. Acad. Sci. USA *89*, 4231–4235.

Xu, Y., Ashley, T., Brainerd, E.E., Bronson, R.T., Meyn, M.S., and Baltimore, D. (1996). Targeted disruption of ATM leads to growth retardation, chromosomal fragmentation during meiosis, immune defects, and thymic lymphoma. Genes Dev. *10*, 2411–2422.

Yamamoto, S., Yamamoto, T., Kataoka, T., Kuramoto, E., Yano, O., and Tokunaga, T. (1992). Unique palindromic sequences in synthetic oligonucleotides are required to induce IFN and augment IFN-mediated natural killer activity. J. Immunol. *148*, 4072–4076.

Yi, A.K, Tuetken, R., Redford, T., Waldschmidt, M., Kirsch, J., and Krieg, A.M. (1998). CpG motifs in bacterial DNA activate leukocytes through the pH-dependent generation of reactive oxygen species. J. Immunol. *160*, 4755–4761.

Zandi, E., Chen, Y., and Karin, M. (1998). Direct phosphorylation of IkappaB by IKKalpha and IKKbeta: discrimination between free and NF-kappaB-bound substrate. Science *281*, 1360–1363.

IO5123 Barb Z-016

(14)

Lipid-DNA Complexes Induce Potent Activation of Innate Immune Responses and Antitumor Activity When Administered Intravenously[1]

Steven W. Dow,[2*†] Lee G. Fradkin,[§] Denny H. Liggitt,[‡§] Andy P. Willson,[*] Timothy D. Heath,[¶] and Terry A. Potter[*‖]

Cationic lipid-DNA complexes (CLDC) are reported to be safe and effective for systemic gene delivery, particularly to the lungs. However, we observed that i.v. injection of CLDC induced immunologic effects not previously reported. We found that even very low doses of CLDC administered i.v. induced marked systemic immune activation. This response included strong up-regulation of CD69 expression on multiple cell types and systemic release of high levels of Th1 cytokines, from both lung and spleen mononuclear cells. CLDC were much more potent immune activators on a per weight basis than either LPS or poly(I:C). The remarkable potency of CLDC appeared to result from enhancement of the immune stimulatory properties of DNA, since cationic lipids alone were without immune stimulatory activity. Systemic treatment with CLDC controlled tumor growth and significantly prolonged survival times in mice with metastatic pulmonary tumors. NK cells accumulated to high levels in the lungs of CLDC-treated mice, were functionally activated, and released high levels of IFN-γ. The antitumor activity induced by CLDC injection was dependent on both NK cells and IFN-γ. Thus, DNA complexed to cationic liposomes becomes highly immunostimulatory and capable of inducing strong antitumor activity when administered systemically. *The Journal of Immunology,* **1999, 163: 1552–1561.**

Reports of efficient in vivo pulmonary gene transfer using i.v. administered cationic lipid-DNA complexes (CLDC)[3] have generated substantial interest, due in part to the apparent safety and repeated dosing capabilities of this form of gene delivery (1–5). Intravenous injection of CLDC results in preferential transfection of pulmonary vascular endothelial cells (2, 4). Adenovirus-mediated gene delivery, though extremely efficient, has been plagued by the inherent immunogenicity of adenoviral vectors, and the immune response to the adenoviral vector generally precludes repeated gene administration (6–7). Systemic gene delivery using lipid-DNA complexes has not been previously associated with systemic immunologic sequellae, though there has been mention of toxicity (3, 4). Local administration of CLDC directly into the lung via intratracheal instillation was recently reported to induce cellular infiltration and production of the cytokines IL-12 and IFN-γ in lung tissues (8, 9).

Observations made during systemic gene delivery studies using CLDC prompted us to more closely examine the immunologic effects of systemically administered CLDC. We observed that i.v. injection of CLDC, even using noncoding plasmid DNA vectors, consistently induced strong antitumor effects in mice with experimental lung tumor metastases. We also observed adverse effects in CLDC-injected mice that resembled those induced by immune activation (depression, piloerection, dehydration) in the absence of any remarkable pulmonary pathology. Thus, i.v. injection of CLDC appeared to induce systemic effects suggestive of strong, nonspecific immune stimulation.

Therefore, we investigated immunologic responses to systemic CLDC administration, in particular immune activation, cytokine release, and antitumor activity. We report here that CLDC injected i.v. triggered release of high levels of IL-12 and IFN-γ, as well as accumulation and activation of NK cells in lung and spleen tissues. Thus, CLDC administered i.v. appear to be extremely potent inducers of innate immune responses. Immune activation by CLDC is also responsible for inhibiting the growth of established tumors.

Materials and Methods

Mice

Mice used in these studies were either 8- to 12-wk-old female C57BL/6 mice, 8- to 12-wk-old female BALB/c mice, or 8- to 12-wk-old ICR mice purchased from either The Jackson Laboratory (Bar Harbor, ME) or Harlan Sprague-Dawley (Indianapolis, IN). IFN-γ gene-disrupted mice, bred on a C57BL/6 background, were obtained from The Jackson Laboratory. Mice with a disrupted and nonfunctional recombinase activating gene type 2 (RAG-2 KO) were a kind gift from Dr. Andre Augustin (National Jewish). Protocols for these experiments were approved by the Institutional Animal Care and Use Committee at the National Jewish Medical and Research Center.

Reagents

FBS, LPS, and poly(I:C) were purchased from Sigma (St. Louis, MO). Cell culture medium (modified Eagle's medium) was prepared by Life Technologies (Gaithersburg, MD).

*Division of Basic Immunology, Department of Medicine, National Jewish Medical and Research Center, Denver, CO 80206; †Department of Dermatology, University of Colorado Health Sciences Center, Denver, CO 80262; ‡Department of Comparative Medicine, University of Washington, Seattle, WA 98195; §Megabios Corporation, Burlingame, CA 94010; ¶Department of Pharmacology, University of Wisconsin, Madison, WI 53706; and ‖Department of Immunology and the Cancer Center, University of Colorado Health Sciences Center, Denver, CO 80262

Received for publication March 17, 1999. Accepted for publication May 18, 1999.

The costs of publication of this article were defrayed in part by the payment of page charges. This article must therefore be hereby marked *advertisement* in accordance with 18 U.S.C. Section 1734 solely to indicate this fact.

[1] This work was supported by the Megabios Corporation and by Grant AI-37905 from the National Institutes of Health.

[2] Address correspondence and reprint requests to Dr. Steven W. Dow, Department of Medicine, National Jewish Medical and Research Center, 1400 Jackson Street, Denver, CO 80523. E-mail address: dows@njc.org.

[3] Abbreviation used in this paper: CLDC, cationic lipid-DNA complex.

0022-1767/99/$02.00

EXHIBIT D

DNA preparation

The eukaryotic expression vector PCR3.1 (Invitrogen, San Diego, CA) without a gene insert was used as a source of plasmid DNA. The plasmid was purified from *Escherichia coli*, as described previously, using modified alkaline lysis and polyethylene glycol precipitation (2). The endotoxin content of the plasmid DNA used in these experiments was between .04 and .25 EU per μg DNA. DNA for injection was resuspended in distilled water before use. In some experiments, plasmid DNA was further purified by column chromatography to assure LPS-free conditions. In other experiments, plasmid DNA was methylated in vitro with Sss I methylase (New England Biolabs, Boston, MA) according to the manufacturer's instructions. Mock-methylated plasmid was prepared by incubation of the plasmid in the absence of the Sss I enzyme, but in the presence of the recommended enzyme reaction solution. Plasmid DNA for methylation experiments was then subsequently purified by column chromatography (Qiagen, Chatsworth, CA) before complexation with liposomes.

Cationic lipids and preparation of DNA-lipid complexes

Cationic lipids were prepared as multilamellar vesicles for in vivo use as described previously (10). Briefly, DOTAP (1, 2 dioleoyl-3-trimethylammonium-propoane; Avanti Polar Lipids, Alabaster, AL) and cholesterol (Sigma) were mixed in a 1:1 molar ratio, dried down in round-bottom tubes, then rehydrated in 5% dextrose solution by heating at 50°C for 6 h, as described previously (10). All experiments were done with DOTAP-cholesterol liposomes, unless otherwise noted. For some experiments, DOTMA ((*N*-[1-(2, 3-dioleyloxy)propyl]-*N,N,N*-triethylammonium) (Syntex, Palo Alto, CA) was substituted for DOTAP, and DOPE (diolyl phosphatidylethanolamine; Avanti Polar Lipids) was substituted for cholesterol. For in vivo injection, CLDC were prepared immediately before injection by gently mixing cationic lipids with plasmid DNA at a ratio of 32 nmol total lipid to 1.0 μg DNA, to a final concentration of 100 μg DNA per ml in a sterile solution of 5% dextrose in water.

Injection of CLDC

Lipid-DNA complexes (100 μg/ml DNA in 5% dextrose in water) were injected i.v. via the lateral tail vein. For tumor studies, injections were repeated once 7 days after the first injection.

Flow cytometric analysis of cellular activation

Early cellular activation was assessed by flow cytometric measurement of CD69 expression on T cells, B cells, monocytes, and NK cells. Single cell suspensions were prepared from spleens of mice by the NH_4Cl lysis procedure. Lung mononuclear cells were prepared from lung tissues by collagenase digestion. Briefly, lung tissues were minced, then digested in 1.0 mg/ml Type 1A collagenase in complete medium, along with 10 μg/ml DNase and 100 μg/ml soybean trypsin inhibitor, for 1 h at 37°C with occasional shaking. The lung tissues were then triturated and mononuclear cells isolated by Ficoll gradient centrifugation. For each experiment, spleen and lung cells were prepared from three to four animals per treatment group. Cells were analyzed using a Becton Dickinson (Mountain View, CA) FACScalibur flow cytometer, with analysis gates set by first gating on unstained spleen lymphocytes. Between 10,000 and 30,000 gated events were analyzed for each cell type. For analysis of cell activation, three-color flow cytometric analysis was done, using anti-CD69 PE (PharMingen, San Diego, CA) to quantitate the number of CD69-positive cells. T cells were labeled with an anti-αβTCR Ab (biotin H57.597; PharMingen) plus Abs to either CD4 (FITC RM4-5; PharMingen) or CD8 (FITC 53-6.7; PharMingen); B cells were dual-labeled with anti-B220 (biotin RA3-6B2; PharMingen) and either anti-IA^b (FITC 3F12.35; provided by Dr. John Freed, National Jewish) or anti-IA^d (FITC 14.4.4); NK cells were dual-labeled using anti-NK cell Abs (either anti-NK 1.1 (biotin PK136; PharMingen) or DX5-biotin (PharMingen)) and anti-CD3 (FITC 2C11); macrophages were evaluated using anti-CR3 (biotin Mac-1; PharMingen) and FITC anti-IA^b or anti-IA^d. The mean peak channel intensity and percentage of CD69-positive cells was determined for each cell type, and the mean percentage (±SD) of $CD69^-$ cells was plotted.

Cytotoxicity assay

A standard 4-h ^{51}Cr-release assay was used to quantitate cytotoxic activity present in freshly isolated lung and spleen mononuclear cells, using YAC-1 cells as targets. Briefly, effector cells from lung or spleen were added in decreasing concentrations to duplicate wells of a Linbro plate, to which was then added 5×10^3 target cells that had been previously labeled for 1 h with ^{51}Cr. The plates were incubated at 37°C for 4 h, then supernatants from each well were harvested and the amount of radioactive ^{51}Cr present was determined by automated gamma counter. The percentage specific lysis was calculated as: [(observed ^{51}Cr release) − (spontaneous ^{51}Cr release)]/[(maximum ^{51}Cr release) − (spontaneous release)] × 100.

NK cell depletion

Mice were depleted of NK cells in vivo by a single i.p. injection of 50 μl rabbit anti-asialoG_{M1} antiserum (Wako BioProducts, Richmond, VA). Control animals were injected with 50 μl nonimmune rabbit serum. Treatment with the asialo G_{M1} Ab eliminated detectable NK cells in spleen and lung (by flow cytometry) and also eliminated cytotoxic activity in spleen cells.

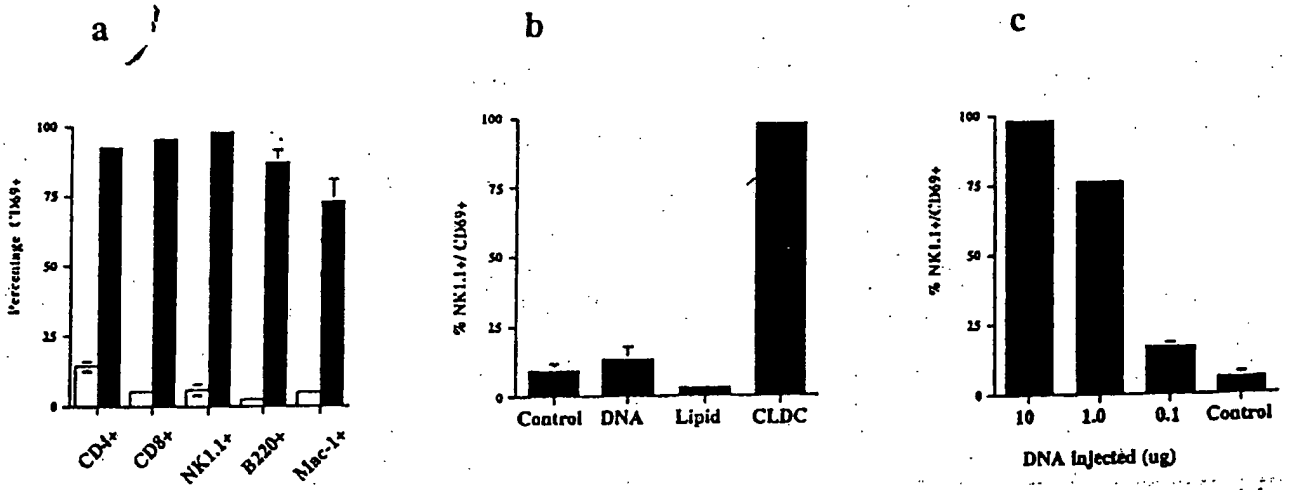

FIGURE 1. Up-regulation of CD69 expression after injection of CLDC: activation of multiple cell types, effects of DNA or lipid alone, and dose-responsiveness. *a*, CLDC-induced activation of different spleen cell populations (T cells ($CD4^+$ or $CD8^+$), NK cells ($NK1.1^+$), B cells ($B220^+$), and monocyte/macrophages ($Mac\text{-}1^+$)) was assessed by flow cytometry 24 h postinjection. The mean percentage $CD69^+$ cells (±SD) was determined for each cell type in three control mice (open bars) and three CLDC-injected mice (filled bars). *b*, C57BL/6 mice (three per group) were injected with 100 μl diluent (control), 10 μg plasmid DNA (DNA), 320 nmol cationic lipid alone (lipid), or with CLDC (10 μg DNA + 320 nmol lipid). Twenty-four hours later, the mean percentage $CD69^+$, $NK1.1^-$ spleen cells (±SD) was determined by flow cytometry and plotted for each treatment group. *c*, C57BL/6 mice (three per treatment group) were injected with either undiluted CLDC (containing 100 μg/ml DNA) or with CLDC that had been diluted 1:10 (10 μg/ml DNA) or 1:100 (1.0 μg/ml DNA) in 5% dextrose in water. CD69 expression by $NK1.1^+$ spleen cells was quantitated by flow cytometry 24 h postinjection. The mean percentage of $CD69^+/NK1.1^-$ cells (±SD) was plotted for each CLDC dosage group and compared with control animals. There was a significant increase in CD69 expression ($p < 0.0001$) for all CLDC-treated cell types, compared with control values.

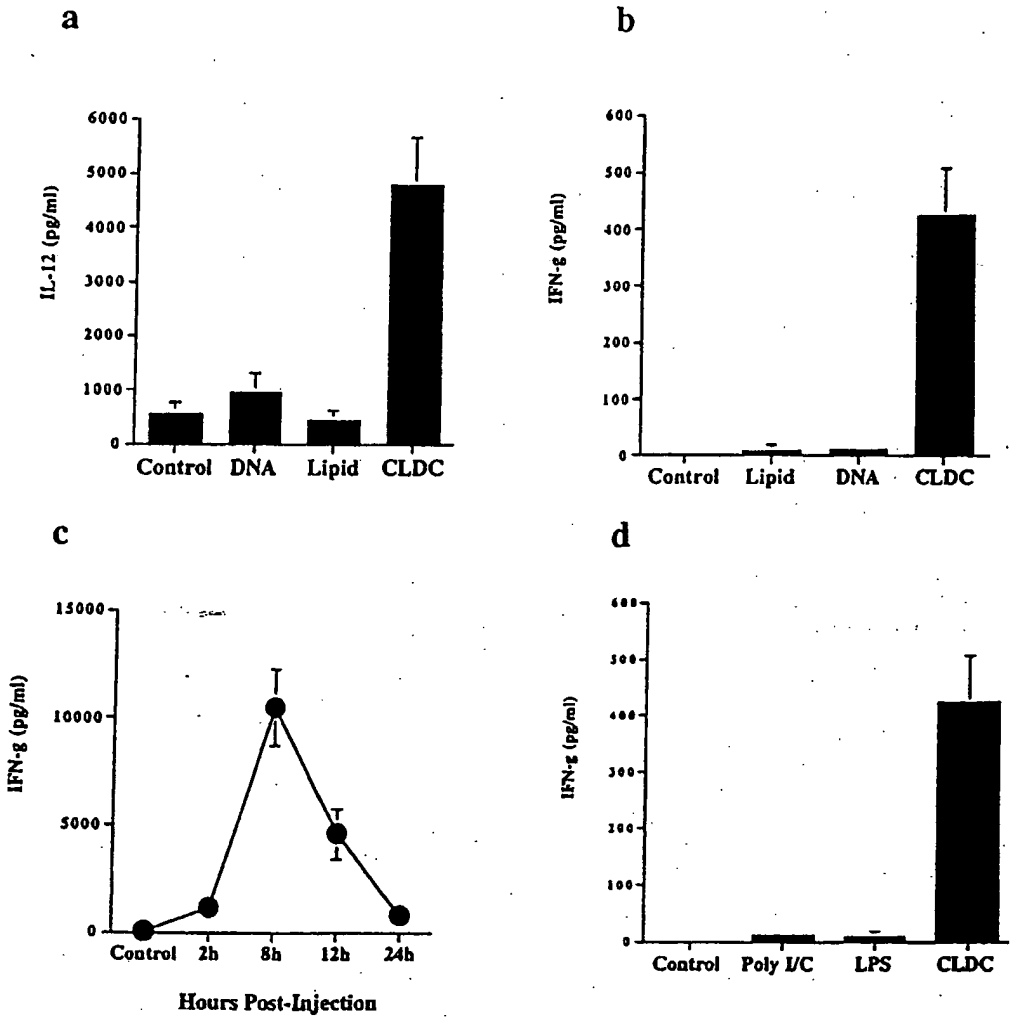

FIGURE 2. Induction of IL-12 and IFN-γ release after i.v. injection of CLDC. Spleens were harvested from C57BL/6 mice (three per treatment group) 24 h after i.v. injection of lipid alone (320 nmol/mouse), plasmid DNA alone (10 μg/mouse), or CLDC, and then cultured 18 h in vitro. Release of IL-12 (*a*) and IFN-γ (*b*) into the supernatants was quantitated by ELISA, and the mean cytokine concentration (±SE) for each treatment group was plotted. Similar results were obtained in four additional experiments, including experiments using several different strains of mice. *c*, Serum was collected from mice (five per group) at various time points before and after injection of CLDC and assayed for IFN-γ concentration. The mean (±SE) IFN-γ concentration was plotted for each time point. *d*, Mice (four per group) were injected i.v. with 10 μg poly(I:C), 10 μg LPS, or CLDC containing 10 μg DNA, and spleens were collected 24 h later and assayed for cytokine release, as in *a*. The mean concentration of IFN-γ (±SE) was plotted for each treatment group and compared with control, sham-injected mice. Similar results were also observed for lung mononuclear cells (data not shown).

Cytokine assays

Cytokine release was measured in spleen cell supernatants after either in vivo or in vitro stimulation, or in serum after in vivo injection of CLDC. For assay of cytokine release after in vivo stimulation, spleen or lung mononuclear cells were prepared from mice 6 or 24 h postinjection, then cultured at a concentration of 5×10^6 cells/ml for an additional 18 h before supernatants were harvested. For in vitro stimulation of cytokine release, spleen cells were incubated in vitro with DNA, lipid, or DNA plus lipid at a final DNA concentration of 1.0 μg/ml for 18 h, at which time the supernatants were harvested for cytokine assays. Serum was obtained by tail vein bleed at various time points postinjection. IFN-γ concentrations in serum or tissue culture supernatants were assayed using a sandwich ELISA that consisted of two mAbs (XMG1.1 and biotinylated R45G). IL-10 and IL-4 concentrations in supernatants were quantitated using specific ELISA kits (PharMingen). TNF-α, total IL-12, and IL-6 concentrations were quantitated using ELISA kits obtained from Genzyme (Boston, MA) according to the manufacturer's instructions.

Tumor lines

B16 (clone F10) cells were obtained from Dr. Isiah Fidler (M D Anderson, Houston, TX); MCA-205 cells were provided by Dr Jack Routes (National Jewish); CT-26 cells were provided by Dr. Nicholas Restifo (National Cancer Institute, Bethesda, MD). All cell lines were maintained at 37°C in MEM supplemented with essential and nonessential amino acids, penicillin and glutamine, and 5% FBS, and were treated periodically with ciprofloxacin (10 μg/ml) to maintain mycoplasma-free conditions.

Tumor challenge and quantitation of lung tumor burden

To establish experimental pulmonary metastases, mice (four per treatment group) were injected once via the lateral tail vein with 2.5×10^5 tumor cells. Treatment with CLDC was initiated 3 days after tumor injection, and was repeated once on day 10 after tumor injection. Control mice were injected with 5% dextrose in water. Mice were sacrificed on days 17–20 after tumor injection, and the number of tumor nodules per lung was determined by manual counting, as described previously (11).

Statistical analysis

Statistical analyses were done using SAS Institute (Cary, NC) software. Lung tumor counts were evaluated for statistically significant differences between treatment groups. For experiments involving two treatment groups, Student's *t* test was used for analysis, whereas the Tukey-Kramer test was used to compare differences between multiple treatment groups in

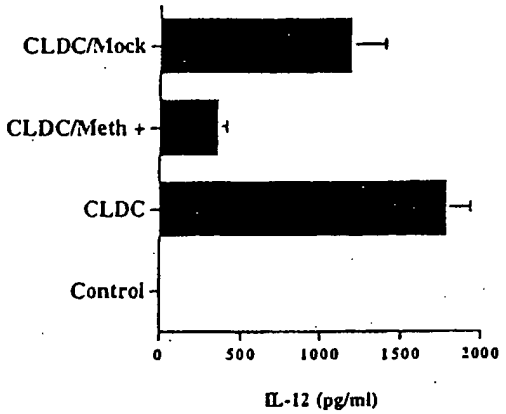

FIGURE 3. Methylation of plasmid DNA reduces immune stimulation by CLDC. The effect of plasmid DNA methylation on cytokine release by CLDC was assessed in vitro. CLDC were formed using untreated plasmid DNA (CLDC), plasmid DNA treated with methylase (Meth+), or with plasmid DNA incubated with methylation buffer solution, but with the methylase enzyme omitted (Mock). The CLDC were then added to triplicate wells of spleen cells to a final concentration of 1.0 μg DNA per ml. Other wells were incubated with an equivalent amount of unmodified DNA only or lipid only. After 18 h of incubation, the supernatants were harvested and assayed for IL-12 release by ELISA. The mean IL-12 concentration (±SE) was plotted for each treatment group.

a given experiment. Kaplan-Meier survival and Log-Rank analysis was used to compare survival times. Significance was determined for $p < 0.05$.

Results

Systemic administration of DNA-lipid complexes induces marked immune activation

The effect of CLDC injection on CD69 expression by various immunologically relevant cell types was evaluated in C57BL/6 mice (Fig. 1). Mice were injected i.v. with 100 μl of CLDC solution (which delivered 10 μg total plasmid DNA), or with 5% dextrose in water. Spleen cells were harvested 24 h postinjection, and five different cell populations ($CD4^+/TCR^+$, $CD8^+/TCR^-$, $NK1.1^+/CD3^-$, $B220^+/IA^{b\ high}$, and $Mac\text{-}1+/IA^{b\ low}$) were immunostained and evaluated by three-color flow cytometry for CD69 expression. The mean peak channel and percentage of $CD69^+$ cells (±SD) was determined for each cell population. Flow cytometric analysis demonstrated strong up-regulation of CD69 expression on $CD8^+$ and $CD4^+$ T cells, NK cells, $B220^+$ B cells, and $Mac\text{-}1^+$ cells (macrophages) following CLDC injection (Fig. 1*a*). The mean percentage of $CD69^+$ cells was significantly up-regulated ($p < 0.001$, compared with sham-treated mice) 24 h after CLDC injection in all five different cell populations evaluated, compared with control animals. Similar results were obtained in repeated experiments with C57BL/6 mice, as well as with other strains of mice, including BALB/c, 129, and ICR (data not shown). The up-regulation of CD69 expression was maximal by 6 h postinjection and declined nearly to baseline levels by 3 days postinjection. Thus, systemic administration of CLDC induced rapid and marked activation of multiple different immune effector cells.

Immune activation in vivo is mediated by the complex of DNA and lipid, not by DNA or lipid alone

Bacterial DNA has been shown previously to have immune stimulatory properties, including stimulation of IL-12 and IFN-γ release and activation of NK cells and B cells (12–15). Therefore, experiments were done to determine the relative contributions of plasmid DNA and cationic liposomes to the systemic immune activation induced by CLDC in vivo. C57BL/6 mice (three per group) were injected i.v. with either 10 μg DNA, 320 nmol of DOTAP-cholesterol liposomes, or with CLDC comprised of 10 μg DA plus 320 nmol liposomes. Twenty-four hours postinjection, CD69 up-regulation by $NK1.1^+$ spleen cells was measured flow cytometrically (Fig. 1*b*). Intravenous injection of CLDC induced marked up-regulation of CD69 expression on NK cells, whereas CD69 expression was unchanged after i.v. injection of DNA alone or lipid alone. Similar results were obtained for T cells, B cells, and macrophages (data not shown). These data, plus cytokine data (see Fig. 3, below), indicated clearly that the complex of DNA and cationic liposomes was much more immunostimulatory than either DNA or liposome alone.

Low doses of CLDC induce in vivo immune activation

The dose-responsiveness of immune activation (CD69 up-regulation) by CLDC was determined in C57BL/6 mice. Mice (three per group) were injected with 100 μl of a CLDC solution containing 100, 10, or 1.0 μg/ml plasmid DNA (Fig. 1*c*). Twenty-four hours later, the percentage of $CD69^+/NK1.1^+$ spleen cells was determined for each group of treated mice and compared with control mice. A dose-dependent increase in CD69 up-regulation was observed. Intravenous administration of as little as 100 ng DNA (in the form of CLDC) was sufficient to induce a significant increase ($p < 0.05$) in CD69 expression by NK cells. Intravenous injection of LPS and poly(I:C) also induced strong CD69 up-regulation on multiple cell types (data not shown). Injection of CLDC formulated using any of three different cationic lipid formulations (DOTAP-cholesterol, DOTAP-DOPE, or DOTMA-cholesterol, see *Materials and Methods*) all stimulated CD69 up-regulation to an equivalent degree (data not shown). Thus, the immune-activating properties of CLDC were not dependent on use of a specific liposome.

Intravenous injection of CLDC induces release of IFN-γ and IL-12

The effect of CLDC injection on cytokine release was assessed by culturing spleen or lung cells obtained from in vivo-treated mice 24 h postinjection (Fig. 2). Mice were injected with either plasmid DNA only (10 μg), liposomes only, or CLDC. Single cell suspensions of spleen and lung mononuclear cells were prepared (see *Materials and Methods*) and then cultured in vitro for an additional 18 h. Release of cytokines into the supernatants was quantitated by specific cytokine ELISA.

Spleen cells from CLDC-injected mice spontaneously released high levels of IL-12 (Fig. 2*a*) and IFN-γ (Fig. 2*b*), whereas there was minimal cytokine release from spleens of control mice or mice injected with equivalent amounts of DNA only or cationic liposomes only. Similar results were observed with cultured lung mononuclear cells (data not shown). In vitro addition of CLDC (1.0 μg DNA per ml medium) to naive spleen cells in vitro also induced release of IL-12 and IFN-γ (see Fig. 5, and data not shown). Injection of CLDC also induced release of high levels of IFN-γ into the serum, with the peak of release occurring 8 h postinjection and then declining thereafter (Fig. 2*c*). Spleens from CLDC-injected mice released high levels of IL-6, but equivalent levels of IL-2, TNF-α, IL-4, or IL-10, compared with control mice (data not shown). Thus, i.v. injection of CLDC elicited strong systemic release of Th1 cytokines in naive mice. The complex of DNA plus a cationic lipid was a much stronger stimulus for cytokine release than DNA or lipid alone.

The cytokine-releasing potency of CLDC was compared with two other classical inducers of innate immunity, LPS and poly(I:C). Twenty-four hours after i.v. injection of equivalent low doses

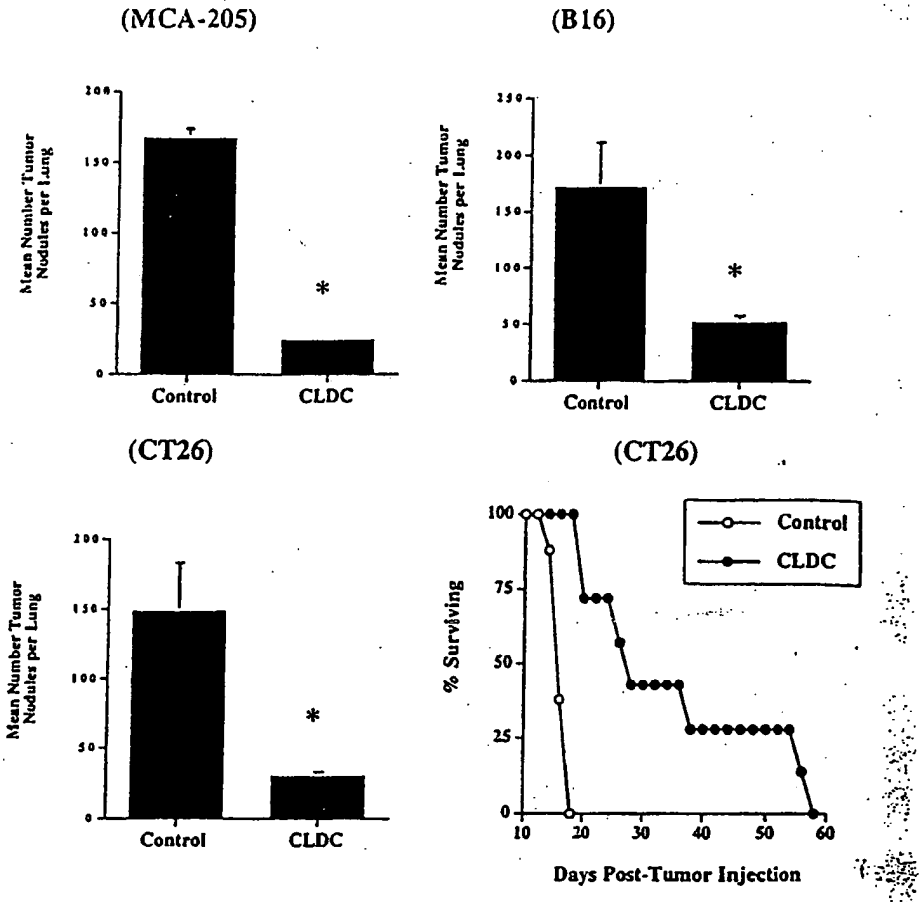

FIGURE 4. Effect of CLDC injection on tumor burden and survival times in mice with established lung tumor metastases. Lung tumors were established in mice by tail vein injection of 2.5×10^5 tumor cells per mouse. C57BL/6 mice (four per treatment group) with established MCA-205 tumors (*a*) or B16.F10 tumors (*b*) were treated 3 days posttumor injection by i.v. injection of 100 μl CLDC or by injection of diluent (control). BALB/c mice with day 3 established CT26 tumors (*c*) were treated similarly. CLDC injection was repeated once 7 days after the first injection, and the mice were sacrificed 7–10 days later (17–20 days posttumor injection) and the lung tumor burden quantitated by manual counting, as described in *Materials and Methods*. The mean number of tumor nodules per lung (±SE) was plotted for each group of mice. Each experiment was repeated at least once, with similar results. There was a significant reduction ($p < 0.0001$) in lung tumor burden for treated mice in each tumor model, compared with control mice, as determined by Student's *t* test. *d*, Mice (eight per treatment group) with day 3 established CT26 tumors were given three CLDC injections, 1 wk apart, or were sham-treated (control). The survival times for mice in each group were plotted, using a Kaplan-Meier curve. Survival times for CLDC-treated group were significantly prolonged ($p = .0001$) compared with control mice, as determined by Log-Rank survival analysis. (*, indicates a significant reduction ($p < 0.05$) in lung tumor burden, compared with sham-treated control animals).

of LPS or poly(I:C) (10 μg per mouse), cytokine release from 18-h cultured spleen cells was measured. Compared with CLDC-injected mice, spleens from LPS- or poly(I:C)-injected mice released very low levels of either IFN-γ (data not shown) or IL-12 (Fig. 2*d*). Nonetheless, these doses of LPS and poly(I:C) did induce in vivo immune activation, as revealed by pronounced CD69 up-regulation (data not shown). Thus, systemically injected CLDC were more potent activators of innate immunity on a per weight basis than LPS or poly(I:C) and induced high circulating levels of IFN-γ.

The immunogenicity of CLDC is partially dependent on the immunogenicity of bacterial DNA

Bacterial DNA is immunogenic in mammals. The immunogenicity of bacterial DNA stems in part from the high content of unmethylated CpG motifs in bacterial DNA, compared with eukaryotic DNA (12, 13, 15). Therefore, experiments were done to determine whether the marked immunogenicity of CLDC was mediated in part by increasing the immunogenicity of the plasmid DNA component of the complex. CLDC were prepared using either unmodified plasmid DNA or plasmid DNA that had been methylated in vitro (Fig. 3). Controls included plasmid DNA incubated with the appropriate buffers but without the methylase enzyme. Naive spleen cells were incubated for 18 h with modified or unmodified CLDC, and the induction of IL-12 release was quantitated.

Compared with CLDC prepared with unmodified plasmid DNA, CLDC prepared with methylated DNA elicited only 25% as much IL-12 release from spleen cells. The level of IL-12 release triggered by methylated CLDC was reduced to the levels induced by incubation with control DNA alone. Lipid alone did not induce IL-12 release (data not shown). These results suggest that formation of the CLDC greatly amplifies the inherent immunogenicity of the plasmid DNA, possibly by increasing DNA entry into cells and their nuclei. However, we have also observed immune activation by CLDC formulated with eukaryotic DNA (S.W. Dow, unpublished observations), and a recent publication suggests that any double-stranded DNA sequence is capable of inducing immune activation (16). Thus, the immune-stimulatory properties of CLDC may involve more than just immune stimulation by bacterial DNA.

Intravenous injection of CLDC controls the growth of established metastatic lung tumors

Others have reported that systemic injection of CLDC containing noncoding (empty vector) plasmid DNA can induce antitumor activity (17). Therefore, we investigated in greater detail the mechanism(s) by which systemic injection of CLDC might induce antitumor activity. Three different tumor lines (fibrosarcoma (MCA-205), melanoma (B16.F10, and colon carcinoma (CT26)) were used to assess the effect of CLDC treatment on a variety of established pulmonary metastatic tumors (Fig. 4, *a–d*). Mice (four per treatment group) were each injected i.v. with 2.5×10^5 tumor cells. C57BL/6 mice were injected with MCA-205 cells or B16.F10 cells, and BALB/c mice were injected with CT26 cells. Mice were treated by i.v. injection of CLDC solution beginning 3 days after tumor injection. The CLDC injection was repeated once 7 days later, and the mice were sacrificed 7–10 days after the second CLDC injection (day 17–20 posttumor injection). The lung

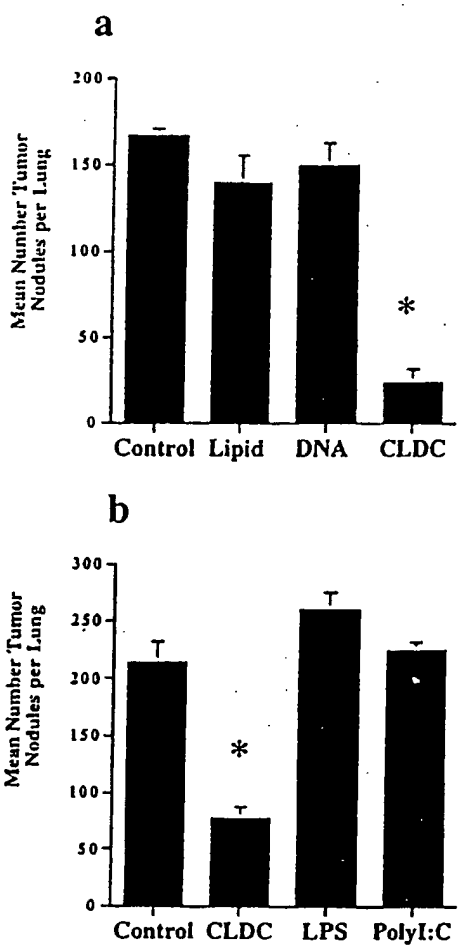

FIGURE 5. Evaluation of antitumor activity induced by injection of DNA or lipid alone, or by injection of LPS or poly(I:C), and comparison to CLDC injection. *a*, C57BL/6 mice (four per treatment group) with day 3-established MCA-205 lung metastases were injected i.v. twice (1 wk apart) with 10 μg DNA, 320 nmol liposomes, or CLDC comprised of both. The mice were sacrificed 7 days after the second injection, and the lung tumor burdens were quantitated, as described in *Materials and Methods*. The mean number of lung tumor nodules (±SE) was plotted for each treatment group. Compared with control animals, there was a significant reduction in lung tumor nodules only in CLDC-treated mice. *b*, C57BL/6 mice with day 3-established MCA-205 tumors were injected i.v. with 10 μg LPS, 10 μg poly(I:C), or with CLDC. The injections were repeated once 7 days later, and the mice were sacrificed 1 wk later, the lung tumor burdens were quantitated, and the mean number lung tumor nodules (±SE) was plotted for each treatment group. Compared with control animals, only animals injected with CLDC had a significant reduction in lung tumor nodules. (*, indicates a significant reduction ($p < 0.05$) in lung tumor burden, compared with sham-treated control animals).

tumor burden was quantitated by counting the number of lung tumor nodules, as described previously (11). In all three tumor models, injection of CLDC induced highly significant reductions ($p < 0.0001$) in the lung tumor burden, compared with control animals.

The effect of treatment with CLDC on survival times in mice with established CT26 lung tumors was also assessed (Fig. 4*d*). Mice (eight per treatment group) were treated three times with i.v. injection of CLDC on days 3, 10, and 17 posttumor injection, and then treatment was discontinued. Control mice were sham-treated with diluent. The survival time in CLDC-treated animals (mean = 35 days) was significantly increased ($p = .0001$) compared with control animals (mean survival = 15 days). Thus, injection of CLDC induced a sustained antitumor effect in animals with established lung tumor metastases.

The relative contributions of DNA and/or liposomes to the antitumor effects of systemic CLDC injection were determined in mice with established MCA-205 lung tumor metastases. Treatment with plasmid DNA alone or liposomes alone did not induce antitumor activity, whereas injection of an equivalent amount of CLDC induced significant ($p < 0.001$) antitumor activity (Fig. 5*a*). We also assessed whether the nonspecific immune stimulation induced by injection of LPS or poly(I:C) could also induce antitumor activity in these experimental models. In contrast to injection of CLDC, i.v. injection of equivalent amounts of (10 μg) of either LPS or poly(I:C) did not induce antitumor activity against established MCA-205 metastases (Fig. 5*b*). Thus, though LPS, poly(I:C), and CLDC were all capable of inducing nonspecific immune stimulation when injected systemically, only CLDC also exerted potent antitumor activity.

Accumulation of NK cells in lungs of CLDC-injected mice

Lung mononuclear cells and spleen cells were collected from mice 3 days after i.v. injection of CLDC and analyzed by flow cytometry (Fig. 6). Flow cytometric analysis revealed a pronounced, 4-fold increase in the percentage of intrapulmonary NK cells in CLDC-injected mice, compared with sham-treated control animals ($p < 0.0001$). There was also an increase in intrasplenic NK cells in CLDC-injected mice, though the increase was not as large as in the lungs. Thus, CLDC administered systemically serve as a stimulus for accumulation of NK cells in various tissues, particularly the lungs.

NK cells: the primary source of CLDC-induced IFN-γ release

The role of NK cells in IFN-γ release after CLDC injection was investigated by NK cell depletion experiments. Mice were depleted of NK cells by treatment with anti-asialo G_{M1} antiserum. Control mice were treated with nonimmune rabbit serum. Forty-eight hours after injection of anti-asialo G_{M1} antiserum, mice were injected with CLDC. Twenty-four hours after CLDC injection, spleen and lung mononuclear cells were harvested, cultured in vitro, and assayed for release of IFN-γ (Fig. 7, *a* and *b*). NK cell depletion almost completely eliminated release of IFN-γ from both spleen and lung cells, compared with mice treated with nonimmune rabbit serum or untreated control animals. Thus, NK cells were the major source of IFN-γ release triggered by CLDC injection.

High levels of NK cytotoxic activity in CLDC-injected mice

Spleen cells harvested 24 h after i.v. injection of CLDC in C57BL/6 exhibited high levels of cytotoxic activity, as assessed in a 4-h chromium release assay, using ^{51}Cr-labeled YAC-1 cells as targets (Fig. 8*a*). The cytotoxic activity was not MHC-restricted, as revealed using MHC-mismatched target cells (data not shown). The cytotoxic activity was markedly reduced in the spleens of NK cell-depleted mice. Similar results were observed using lung mononuclear cells as effector cells (data not shown). Furthermore, cytotoxic activity was not generated by injection of either DNA alone or lipid alone (data not shown). High levels of cytotoxic activity were also detected in spleen cells of RAG-2 KO mice injected with CLDC (Fig. 8*b*). Thus, i.v. administration of CLDC elicited strong functional activation of NK cells, a response that did not require T or B cells.

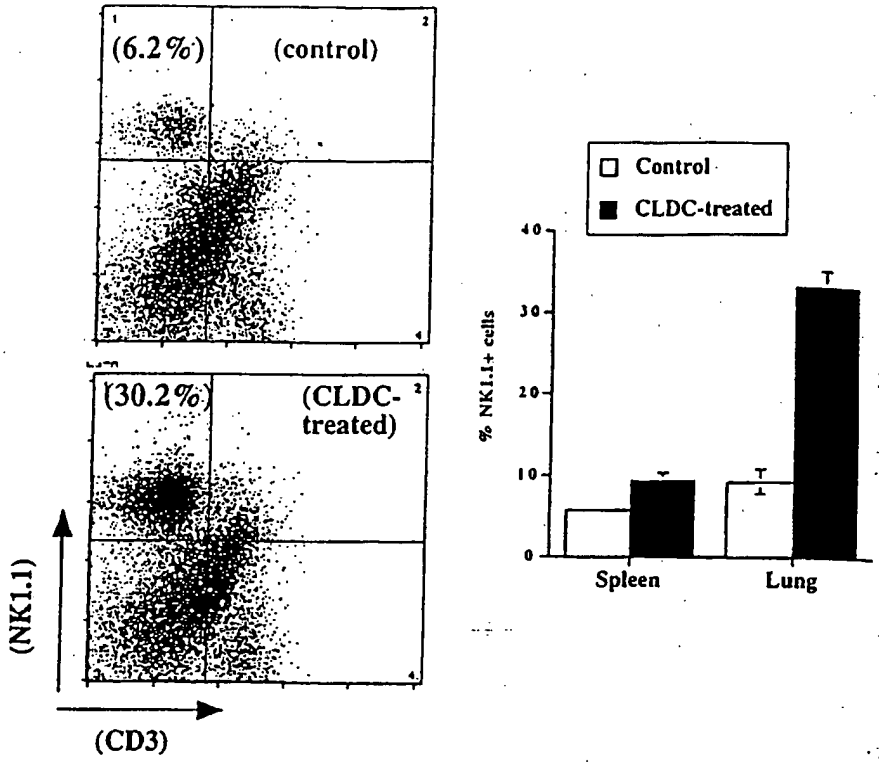

FIGURE 6. Accumulation of NK cells in lung tissues after CLDC injection. Three days after i.v. injection of CLDC in C57BL/6 mice (four per group), mononuclear cells were harvested from lung tissues of treated or control mice by enzymatic digestion, as described in *Materials and Methods*. Spleen cells were obtained from the same mice. Spleen and lung mononuclear cells were analyzed by flow cytometry for expression of NK1.1 and CD3. In a representative analysis, there was a significant increase ($p < 0.0001$) in the percentage of $NK1.1^+/CD3^-$ cells in the lungs of a mouse injected with CLDC (*b*), compared with a control mouse (*a*). The mean percentage (±SE) of NK cells in the lungs and spleens of CLDC-treated (filled bars) and control mice (open bars) was plotted in *c*. Similar results were observed in at least three additional experiments.

The antitumor activity of CLDC is mediated by NK cells and IFN-γ

The role of NK cells in mediating tumor rejection in response to CLDC injection was investigated by depleting mice of NK cells in vivo. NK cells were depleted in BALB/c mice (four per group) 1 day after i.v. injection with CT26 cells. Control mice were treated with nonimmune rabbit serum or were untreated. On day 3 posttumor injection, the mice were injected with CLDC. The Ab depletion of NK cells and CLDC treatment was repeated once 7 days later, and the mice were sacrificed on day 17 posttumor injection and the lung tumor burden was quantitated. Depletion of NK cells reduced the antitumor activity induced by systemic injection of CLDC, such that there was no significant difference in tumor burden between CLDC-treated and control mice (Fig. 9*a*). However, the tumor burden in mice treated with nonimmune rabbit serum was significantly reduced by injection of CLDC. Thus, NK cells were a key mediator of the antitumor activity induced by CLDC injection.

Since NK cells were also the primary source of IFN-γ release in response to CLDC injection, the role of IFN-γ in mediating CLDC-induced tumor rejection was investigated. CLDC-induced antitumor activity was evaluated in C57BL/6 mice with a targeted disruption of the IFN-γ gene ($IFN\text{-}\gamma^{-/-}$). Wild-type C57BL/6 mice ($IFN\text{-}\gamma^{+/+}$) or $IFN\text{-}\gamma^{-/-}$ mice with day 3 established MCA-205 tumor cells were treated with either CLDC or were sham-injected (control). The tumor burden in $IFN^{-/-}$ mice treated with CLDC was not significantly decreased, compared with control $IFN^{-/-}$ mice, whereas treatment of $IFN^{+/+}$ mice induced a significant reduction in tumor burden (Fig. 9*b*). The $IFN\text{-}\gamma^{-/-}$ mice were therefore impaired in their ability to respond to CLDC injection and control the growth of MCA-205 lung tumors. Thus, the antitumor activity induced by systemically administered CLDC was mediated to a large degree by IFN-γ released from activated NK cells.

Discussion

These studies indicate that CLDC are very immunologically active when injected systemically. Indeed, CLDC administered i.v. induced rapid, marked systemic immune activation in vivo, manifested initially by up-regulation of CD69 expression on immune effector cells (T cells, B cell, macrophages, and NK cells). Injection of CLDC also served as a potent stimulus for release of Th1 cytokines (IL-12 and IFN-γ). CLDC were particularly stimulatory for NK cells, inducing functional activation, IFN-γ release, and antitumor activity.

Bacterial DNA is immunogenic in eukaryotes. Exposure to bacterial DNA triggers innate immune responses and activation of B cell, macrophages, and NK cells (12–15). B cells and macrophages are activated directly by bacterial DNA, whereas NK cell activation is reported to be mediated indirectly by IL-12 released from DNA-stimulated macrophages (12–15, 18, 19). The immunogenicity of bacterial DNA is due in part to the increased purine content of bacterial DNA, which is enriched in CpG motifs relative to eukaryotic DNA (12–15, 20–22). The hypomethylated state of bacterial DNA is also immunogenic (12, 22). The immunogenicity of bacterial DNA has also been shown to play a role in the effectiveness of DNA vaccines, in part through induction of Th1 cytokines (23).

One surprising finding from our study was the extreme immunogenicity of lipid-DNA complexes. The cationic liposomes by themselves were without apparent immune stimulatory activity, as was the plasmid DNA alone at the low doses employed in these studies (Figs. 1 and 2). However, the complex of the two was markedly stimulatory. Complexation to liposomes was reported previously to enhance the immunogenicity of synthetic oligonucleotides (24). The enhanced immunogenicity of complexes relative to naked DNA or oligonucleotides is most likely a result of lipid-facilitated intracellular entry and nuclear translocation of

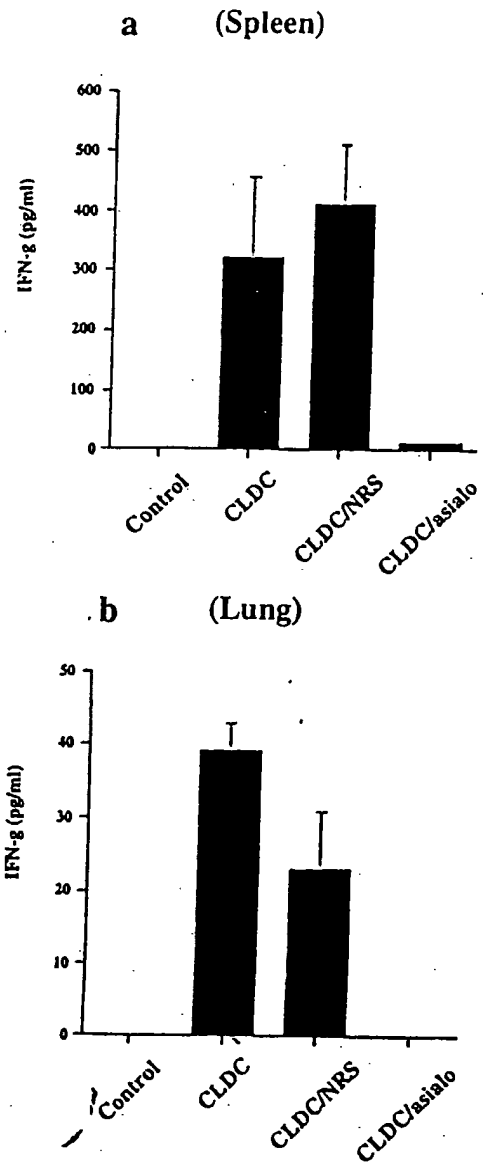

FIGURE 7. Effect of in vivo NK cell depletion on CLDC-induced IFN-γ release. Mice (three per treatment group) were pretreated 48 h before CLDC injection with rabbit anti-asialo G_{M1} antiserum (CLDC/asialo), an equivalent amount of nonimmune rabbit serum (CLDC/NRS), or were not pretreated (CLDC). Spleen and lung cells from untreated mice served as controls. Spleen (*a*) and lung (*b*) mononuclear cells were collected 24 h after injection of CLDC, then cultured for 18 additional hours, and release of IFN-γ was quantitated by ELISA. The mean IFN-γ concentration (±SE) for each treatment group was plotted.

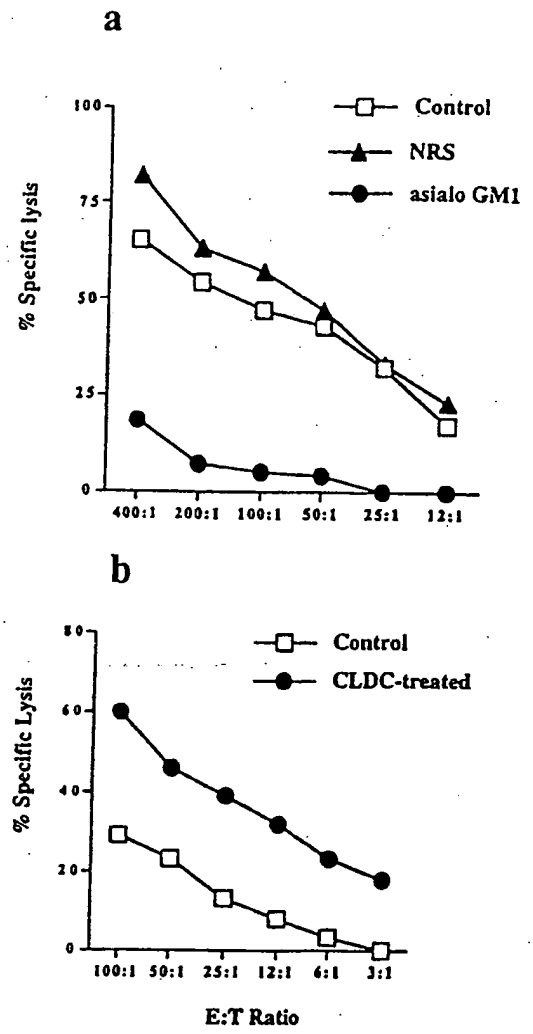

FIGURE 8. Induction of NK cell cytotoxic activity by i.v. administration of CLDC. Cytotoxic activity in spleen cells of C57BL/6 mice (three per treatment group) was quantitated 24 h after i.v. injection of CLDC (*a*). Mice were pretreated 48 h before injection of CLDC by i.p. injection of anti-asialo G_{M1} antiserum to deplete NK cells, or were pretreated with nonimmune rabbit serum (NRS). Spleen cells from CLDC-injected and control mice were assayed for cytotoxic activity against ^{51}Cr-labeled YAC-1 target cells, as described in *Materials and Methods*. The mean percentage specific lysis at each effector to target cell ratio was plotted. *b*, Cytotoxic activity was assayed in spleen cells obtained from control (□) or CLDC-injected (●) RAG-2 gene knockout mice, 24 h postinjection.

DNA, inasmuch as immune activation by bacterial DNA requires DNA entry into the cell nucleus (14, 25). In vivo, cationic liposomes protect DNA from degradation and prolong circulation time, which may in turn facilitate binding to monocytes and macrophages (26).

Previous studies have demonstrated that the formation of complexes with liposomes serves to increase the immune stimulatory properties of DNA, both in vitro and in lung tissues in vivo (8, 24). Our observation that methylation of the plasmid DNA reduced immune activation by CLDC (Fig. 3) is consistent with these prior observations. Intravenous injection of high doses (mg) of plasmid DNA has been reported to induce immune stimulation and IFN-γ release (18). However, we observed immune activation at DNA doses as low as 100 ng when the DNA was complexed to a cationic liposome (Fig. 1), indicative of the degree to which lipids increased the immunogenicity of bacterial DNA.

The immunostimulatory properties of CLDC were not due to contaminating LPS, as evidenced by the failure of DNA alone to induce immune stimulation, either in vitro or in vivo (Figs. 2 and 5). Injection of equivalent amounts of purified LPS also failed to elicit the same pattern of cytokine responses or antitumor responses as CLDC (Figs. 2 and 5). In addition, CLDC formulated with highly purified DNA (virtually free of detectable LPS) induced immune stimulatory effects indistinguishable from CLDC prepared with other sources of DNA (data not shown).

A major finding from this study was that CLDC injected i.v. could induce high levels of antitumor activity. Treatment of mice with established pulmonary metastases by CLDC injection induced significant reductions in lung tumor burden and prolonged

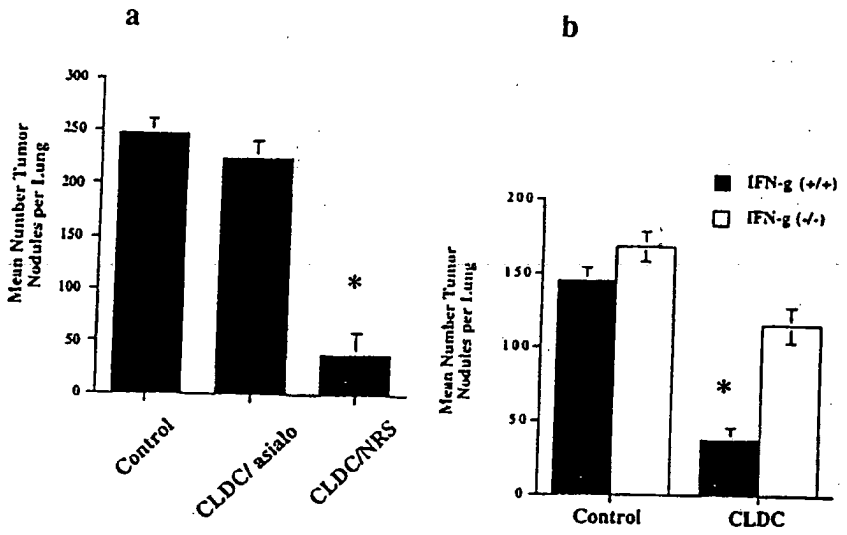

FIGURE 9. NK cells and IFN-γ mediate the antitumor effects of CLDC. The effect of NK cell depletion on the tumor response to CLDC injection was evaluated in BALB/c mice (four per treatment group) with day 3-established CT26 tumors (*a*). Tumor-bearing mice were administered an i.p. injection of anti-asialo G_{M1} antiserum (CLDC/asialo) or an equivalent amount of nonimmune rabbit serum (CLDC/NRS) 24 h before each injection of CLDC, as described in *Materials and Methods*. A third group of untreated mice served as a control. Seven days after the second CLDC injection, mice were sacrificed, the lung tumor burden was quantitated by manual counting, and the mean number of tumor nodules per lung (±SE) was plotted. There was a significant reduction ($p < 0.001$) in lung tumor burden in CLDC-treated mice pretreated with normal rabbit serum, compared with control mice. By contrast, there was no reduction in lung tumor burden in CLDC-treated mice that were also injected with anti-asialo G_{M1} antiserum. This experiment was repeated once, with similar results. *b*, MCA-205 lung tumors were established in wild-type C57BL/6 mice (IFN-$\gamma^{+/+}$) or C57BL/6 mice with a nonfunctional IFN-γ gene (IFN-$\gamma^{-/-}$). Three days later, the mice were injected with CLDC or were sham-treated (control). The treatment was repeated 7 days later, and the mice were sacrificed and lung tumors counted 7 days after that. The mean number of lung tumor nodules (±SE) per treatment group was plotted. The number of lung tumor nodules in IFN-$\gamma^{+/+}$ mice was significantly different from that of untreated IFN-$\gamma^{+/+}$ control mice ($p < 0.001$), whereas the number of lung tumor nodules in IFN-$\gamma^{-/-}$ mice treated with CLDC was not significantly different from untreated control IFN-$\gamma^{-/-}$ mice. Similar results were obtained in one additional experiment. (*, significant reduction ($p < 0.05$) in lung tumor burden, compared with sham-treated control animals).

survival times (Fig. 4). The antitumor activity induced by CLDC was unique in that it could not be reproduced by injection of equivalent low doses of other nonspecific activators of innate immunity, such as LPS or poly(I:C) (Fig. 5).

NK cells were the major mediators of the antitumor effects induced by CLDC. For example, NK cells accumulated to high levels in the lungs of CLDC-injected mice (Fig. 6) became highly cytotoxic (Fig. 8) and secreted large amounts of IFN-γ (Fig. 7). Furthermore, depletion of NK cells almost completely eliminated the antitumor activity of CLDC injection (Fig. 9). It is likely that NK cell activation occurred in response to IL-12 released following CLDC injection (Fig. 2). Bacterial DNA has been shown previously to activate NK cells by triggering release of IL-12 from macrophages (14, 19). However, we cannot exclude the possibility that CLDC injection might also induce production of IL-18, which could in turn trigger release of IFN-γ and antitumor activity. It should also be noted that the NK cells that accumulated in the lungs of CLDC-treated mice (Fig. 6) were classical NK cells ($NK1.1^+$, $CD3^-$), as opposed to the recently described natural T cells ($NK1.1^+/CD3^+$) (27).

IFN-γ also played a critical role in the antitumor effects of CLDC injection. Mice with a nonfunctional IFN-γ gene were significantly impaired in their ability to control the growth of lung tumors after treatment with CLDC (Fig. 9). Thus, NK cells activated by CLDC may have induced inhibition of tumor growth indirectly by releasing IFN-γ. Both IFN-γ and IL-12 exert multiple antitumor activities in vivo, including inhibition of tumor angiogenesis (28–30). Therefore, it is conceivable that CLDC may inhibit tumor growth in part by stimulating local release of antiangiogenic cytokines within the tumor vasculature. For example, it was demonstrated recently that CLDC preferentially bound to the neovascular endothelium of tumors following i.v. injection (31).

Our findings have important implications for systemic nonviral gene delivery using CLDC. Widespread immune activation is likely to occur when CLDC are used to deliver genes systemically to the lungs or other target organs. However, the immune response to CLDC was dose-dependent and self-limiting (Figs. 1 and 2), and could therefore be controlled by dosage adjustments. The immune response elicited by CLDC injection was not vector-specific, therefore still allowing repeated CLDC administration. The development of vector-specific immunity is, by contrast, a major drawback to repeated use of viral vectors in vivo (6, 7). Continued improvements in plasmid vectors are likely to improve the duration of gene expression following systemic gene delivery, thereby reducing the frequency of administration. Activation of innate immune responses by CLDC may also represent an unanticipated advantage for immunotherapy of cancer or allergic diseases. The Th1 cytokines elicited by CLDC may provide a strong adjuvant effect for DNA vaccines administered using CLDC. For example, the superiority of CLDC for induction of immune responses to HIV Ags using DNA vaccines was reported previously (32). The use of CLDC may prove particularly effective for systemic, therapeutic vaccination against tumor Ags, given the strong antitumor effects induced by the plasmid vector alone.

Acknowledgments

We thank Dr. David Ickle for assistance with statistical analysis.

References

1. Zhu, N., D. Liggitt, Y. Liu, and R. Debs. 1993. Systemic gene expression after i.v. delivery of DNA into adult mice. *Science 261:209.*
2. Liu, Y., D. Liggitt, G. Tu, W. Zhong K. Gaensler, and R. Debs. 1995. Cationic liposome-mediated intravenous gene delivery in mice. *J. Biol. Chem. 27:24864.*
3. Canonico, A. E., J. D. Pittman, J. T. Conary, B. O. Meyrick, and K. L. Brigham. 1994. No lung toxicity after repeated aerosol or i.v. delivery of plasmid cationic liposome complexes. *J. Appl. Physiol. 77:415.*
4. Song, Y. K., L. Feng, C. Shaoyou, and L. Dexi. 1997. Characterization of cationic liposome-mediated gene transfer in vivo by intravenous administration. *Hum. Gene Ther. 8:1585.*
5. Templeton, N., D. Lasic, P. Frederik, H. Strey, D. Roberts, and G. Pavlakis. 1997. Improved DNA:liposome complexes for increased systemic delivery and gene expression. *Nat. Biotechnol. 15:647.*
6. Yang, Y., F. A. Nunes, K. Berencsi, E. E. Furth, E. Gonczol, and J. M. Wilson. 1994. Cellular immunity to viral antigens limits E1-deleted adenoviruses for gene therapy. *Proc. Natl. Acad. Sci. USA 91:4407.*
7. Knowles, M. R., K. W. Hohneker, Z. Zhou, J. C. Olsen, T. L. Noah, P. C. Hu, M. W. Leigh, J. F. Englehardt, L. J. Edwards, K. R. Jones, and R. Boucher. 1995. A controlled study of adenovirus-vector-mediated gene transfer in the nasal epithelium of patients with cystic fibrosis. *N. Engl. J. Med. 333:823.*
8. Freimark, B. D., H. P. Blezinger, V. J. Florack, J. L. Nordstrom, S. D. Long, D. S. Deshpande, S. Nochumson, and K. L. Petrak. 1998. Cationic lipids enhance cytokine and cell influx levels in the lung following administration of plasmid: cationic lipid complexes. *J. Immunol. 160:4580.*
9. Scheule, R., J. St. George, R. Bagley, J. Marshall, J. Kaplan, G. Akita, K. Wang, E. Lee, D. Harris, C. Jiang, et al. 1997. Basis of pulmonary toxicity associated with cationic lipid-mediated gene transfer to the mammalian lung. *Hum. Gene Ther. 8:689.*
10. Liu, Y., D. Liggitt, G. Tu, W. Zhong, K. Gesler, and R. Debs. 1995. Cationic lipsome-mediated i.v. gene delivery in mice. *J. Biol. Chem. 27:24864.*
11. Wexler, H. 1966. Accurate identification of experimental pulmonary metastases. *J. Natl. Cancer Inst. 36: 641.*
12. Piseisky, D. S. 1996. Immune activation by bacterial DNA: a new genetic code. *Immunity 5:303.*
13. Krieg, A. M. 1996. Lymphocyte activation by CpG dinucleotide motifs in prokaryotic DNA. *Trends Microbiol. 4:73.*
14. Stacey, K. J., M. J. Sweet, and D. A. Hume. 1996. Macrophages ingest and are activated by bacterial DNA. *J. Immunol. 157:2116.*
15. Klinman, D. M., A. Yi, S. J. Beaucage, J. Conover, and A. M. Krieg. 1996. CpG motifs present in bacterial DNA rapidly induce lymphocytes to secrete interleukin-6, interleukin-12, and interferon-γ. *Proc. Natl. Acad. Sci. USA 93:2879.*
16. Suzuki, K., A. Mori, K. J. Ishii, J. Saito, D. S. Singer, D. M. Klinman, P. R. Krause, and D. K. Leonard. 1999. Activation of target-tissue immune recognition molecules by double-stranded polynucleotides. *Proc. Natl. Acad. Sci. USA 96:2285.*
17. Lesoon-Wood, L. A., W. H. Kim, H. K. Kleinman, B. D. Weintraub, and A. J. Mixson. 1995. Systemic gene therapy with p53 reduces growth and metastases of a malignant human breast cancer in nude mice. *Hum. Gene Ther. 6:395.*
18. Cowdery, J. S., J. H. Chace, A. Yi, and A. M. Krieg. 1996. Bacterial DNA induces NK cells to produce IFN-γ in vivo and increases the toxicity of lipopolysaccharides. *J. Immunol. 156:4570.*
19. Chace, J. H., N. A. Hooker, K. L. Mildenstein, A. M. Krieg, and J. S. Cowdery. 1997. Bacterial DNA-induced NK cell IFN-γ production is dependent on macrophage secretion of IL-12. *Clin. Immunol. Immunopathol. 84:185.*
20. Yi, A., D. M. Klinman, T. L. Martin, S. Matson, and A. M. Krieg. 1996. Rapid immune activation by CpG motifs in bacterial DNA. *J. Immunol. 157:5394.*
21. Ballas, Z. K., W. L. Rasmussen, and A. M. Krieg. 1996. Induction of NK activity in murine and human cells by CpG motifs in oligodeoxynucleotides and bacterial DNA. *J. Immunol. 157:1840.*
22. Karlen, S., W. Doerfler, and L. R. Cardon. 1994. Why is CpG suppressed in the genomes of virtually all small eukaryotic viruses but not in those of large eukaryotic viruses? *J. Virol. 68:2889.*
23. Sato, Y., M. Roman, H. Tighe, D. Lee, M. Corr, M. D. Nguyen, G. J. Silverama, M. Lotz, D. A. Carlson, and E. Raz. 1996. Immunostimulatory DNA sequences necessary for effective intradermal gene immunization. *Science 273:352.*
24. Yamamato, T., S. Yamamato, T. Katoaka, and T. Tokunaga. 1994. Lipofection of synthetic oliodeoxynulceotide have a palindromic sequence of AACGTT to murine splenocytes enhances interferon production and natural killer activity. *Microbiol. Immunol. 38:831.*
25. Friend, D. S., D. Papahadjopoulos, and R. J. Debs. 1996. Endocytosis and intracellular processing accompanying transfection mediated by cationic liposomes. *Biochem. Biophys. Acta 1278:41.*
26. McLean, J. W., E. A. Fox, P. Baluk, P. B. Bolton, A. Haskell, R. Pearlman, G. Thurston, E. Y. Umemoto, and D. M. McDonald. 1997. Organ-specific endothelial cell uptake of cationic liposome-DNA complexes. *Am. J. Physiol. 273: H387.*
27. Cui, J., T. Shin, T. Kawano, H. Sato, E. Kondo, I. Toura, Y. Kaneko, H. Koseki, M. Kanno, and M. Taniguchi. 1997. Requirement for Va14 NKT cells in IL-12 mediated rejection of tumors. *Science 278:1623.*
28. Ruegg, C., A. Yilmaz, G. Bieler, J. Bamat, P. Chaubert, and F. J. Lejeune. 1998. Evidence for the involvement of endothelial cell integrin αVβ3 in the disruption of the tumor vasculature induced by TNF and IFN-γ. *Nat. Med. 4:408.*
29. Coughlin, C. M., K. E. Salhany, M. Wysocak, E. Aruga, H. Kurzawa, A. E. Chang, C. A. Hunter, J. C. Fox, G. Trinchieri, and W. M. F. Lee. 1998. Interleukin-12 and interleukin-18 synergistically induce murine tumor regression which involves inhibition of angiogenesis. *J. Clin. Invest. 101:1441.*
30. Coughlin, C. M., K. E. Salhany, M. S. Gee, D. C. LaTemple, S. Kotenko, X. Ma, G. Gri, M. Wysocka, J. E. Kim, L. Liu, et al. 1998. Tumor cell responses to IFN-γ affect tumorigenicity and response to IL-12 therapy and antiangiogenesis. *Immunity 9:25.*
31. Thurston, G., J. W. McClean, M. Rizen, P. Baluk, A. Haskell, T. J. Murphy, D. Hanahan, and D. McDonald. 1998. Cationic liposomes that target angiogenic endothelial cells in tumors and chronic inflammation in mice. *J. Clin. Invest. 101:1401.*
32. Ishii, N., J. Fukushima, T. Kaneko, E. Okada, K. Tani, S. I. Tanaka, K. Hamajima, K. Q. Xin, S. Kawamoto, W. Koff, et al. 1997. Cationic liposomes are a strong adjuvant for a DNA vaccine of human immunodeficiency virus type 1. *AIDS Res. Hum. Retroviruses 13:1421.*

JOURNAL OF LIPOSOME RESEARCH, 7(1), 31–49 (1997)

CATIONIC LIPOSOMES AS AN OLIGONUCLEOTIDE CARRIER: MECHANISM OF ACTION

Olivier Zelphati and Francis C. Szoka, Jr.*

University of California, School of Pharmacy, Department of Pharmacy and Pharmaceutical Chemistry, San Francisco, CA 94143-0446, USA.

ABSTRACT

Cationic liposomes are a useful in vitro but as yet unproven in vivo delivery system for oligonucleotides. An understanding of the mechanism of delivery mediated by cationic lipid/oligonucleotide complexes has been lacking. In this review, we describe recent results concerning several steps of the delivery process, including the formation of complexes, the intracellular distribution of the oligonucleotide and the lipid, as well as the uptake pathway and site of intracellular release. Cationic liposomes form a polyelectrolyte complex with the oligonucleotides, protect them from nuclease degradation, enhance their cellular uptake and improve the oligonucleotide potency. In the majority of cell types studied, cationic lipids deliver oligonucleotides into the cell predominately via an endocytotic pathway rather then by fusion with the plasma membrane. We propose that the oligonucleotide is released from the complex when anionic lipids from the cytoplasmic facing lipid monolayer of the cell flip into contact with the complex, the anionic lipids then laterally diffuse into the complex and form a charged neutralized ion-pair with the cationic lipids. This leads to displacement of the oligonucleotide from the cationic lipid and its release into the cytoplasm. In most cell types this occurs after endocytosis of the complex rather than after fusion of the complex directly with the plasma membrane. These new concepts of oligonucleotide release in cells provide a useful starting point for the rationale improvement of this nucleic acid delivery system.

EXHIBIT E

INTRODUCTION

Antisense oligonucleotides (ODN) represent a promising tool in fighting viral, malignant and inflammatory diseases (1-3). Indeed, These single strands of DNA or RNA can hybridize to their complementary targets and can specifically inhibit, in principle, protein synthesis. However, before they reach their intracellular target, ODN must overcome several obstacles including their sensitivity to nucleases, their poor cellular uptake and their capacity to hybridize to their DNA or RNA target present in the cytoplasm and/or in the nucleus of cells (1-3). One of these problems, the resistance to nucleases, has essentially been solved by chemical modifications of natural phosphodiester oligonucleotides (2, 4). However, backbone-modifications have not resolved the problem of low cell membrane permeability.

An alternative strategy to bypass stability and permeability problems is to use liposomes as carriers for ODN. Indeed, liposomes (anionic, cationic, fusogenic, pH-sensitive and immunoliposomes) have been successfully used to deliver and increase the cellular uptake of ODN into cells (5). Liposomes can protect ODN from the external medium and can deliver molecules directly into cells (5). Moreover, it is also possible to specifically target liposomes by coupling proteins or antibodies on their surface (6)

Among these carriers, cationic lipids represent one of the more successful in vitro oligonucleotide carriers. ODN complexed to cationic liposomes have been successfully used in various biological models that demonstrate the potential of cationic lipids to deliver ODN to multiple cell types (5). The potency of an antisense oligonucleotide was increased between at least 100-1000 fold by cationic liposomes (7-10) and represent the most efficient oligonucleotide carrier system reported to date. However, the cellular, molecular and biophysical mechanisms of complex formation and action were unknown. The steps involved in the ODN delivery mediated by cationic liposomes *in vitro* include the formation of

the ODN/cationic lipid complexes, their delivery into the cell, their intracellular distribution and the cytoplasmic release of the ODN from the cationic lipids. These processes are nevertheless critical for the optimal utilization of antisense oligonucleotides for cell biology experiments as well as for therapeutic applications. Moreover, the understanding of the delivery process should have implications for improvements of oligonucleotide and polynucleotide cationic carriers. The purpose of this review is to describe the recent results obtained on the cellular delivery mechanisms of ODN/cationic lipid complexes (from the formation to the dissociation of the complexes).

PHYSICOCHEMICAL CHARACTERISTICS OF ODN/CATIONIC LIPID COMPLEXES

The transport of oligonucleotides by cationic lipids is based on the electrostatic interaction between negative charges of oligonucleotides and positive charges of lipids. Thus, in contrast to all other type of liposomes, cationic liposomes do not require any encapsulation step that limits the application of these carriers. In this case, oligonucleotides are directly mixed with preformed liposomes. Despite the common use of cationic lipids for oligonucleotides transport, the physicochemical properties of oligonucleotide-cationic liposome interactions have been studied only recently (11). Aggregation, lipid fusion, and interactions of the complex with different lipid bilayers were studied. Phosphorothioate oligonucleotides were associated with cationic liposomes composed of dimethyldioctadecylammonium bromide (DDAB) and dioleylphosphatidylethanolamine (DOPE) or of 1,2-dioleoyl-3-trimethylammonium-propane (DOTAP). Oligonucleotides induced aggregation and fusion of cationic liposomes as a function of charge ratio (11). Lipid fusion and interactions with different lipid bilayers indicated that either phosphatidylethanolamine or negative charges are required for fusion of cationic liposome-oligonucleotide complexes (11).

NUCLEASE PROTECTION AND CELLULAR UPTAKE

Because oligonucleotides are complexed to cationic liposomes and thus unencapsulated, one would not necessarily expect protection against nucleases when using these carriers. However, degradation of phosphodiester oligonucleotides by nucleases was markedly prevented by DOTAP both in cell culture medium and in human serum (12, 13). This can be explained by a collapse or a "coating" of the oligonucleotides after aggregation of the complexes, leading to structures where the oligonucleotides are completely covered by lipid bilayers. Nevertheless, antisense phosphodiester oligonucleotides associated with cationic lipids have not been active in cell culture *in vitro* (7-9). Only one study has reported the activity of phosphodiester antisense oligonucleotides complexed to cationic lipids (14). This points out the critical role of intracellular nucleases for oligonucleotide activity. Indeed the intracellular high-life of a phoshodiester has been estimated at about 15 minutes (16,22) which necessitates the use backbone-modified oligonucleotides that are relatively resistant to both intracellular and extracellular nucleases even if a carrier is used to deliver the oligonucleotide into the target cell.

Concerning the cellular uptake of oligonucleotides, many studies have shown that cationic lipids as DOTAP, N-[1-(2,3-dioleoyloxy)propyl]-N,N,N-trimethylammonium chloride (DOTMA, Lipofectin®), dioctadecylamidoglycyl spermine (DOGS) and DDAB associated with DOPE markedly enhance the rate of oligonucleotide uptake in several different cell types (8-10, 12). Augmentation of cellular uptake was generally reported to be 15-25 fold relative to the uptake of oligonucleotides alone. In general, cationic lipids have enhanced oligonucleotide cell association in a time- and concentration-dependent manner (8-10, 12). Moreover, the enhancement of cellular uptake requires that the complex has an excess positive charge (10) indicating that complexes bind to the cell membrane through electrostatic interactions. However, in HL-60 and RBL-1 cells the oligonucleotide cellular uptake was unaffected by the presence of the cationic lipid DOTMA (8).

INTRACELLULAR DISTRIBUTION OF ODN / CATIONIC LIPID COMPLEXES

Interestingly, it has to be noted that the enhancement of oligonucleotide cellular uptake (between 15 and 25-fold) is not sufficient to explain the increase of oligonucleotide activity; at least 1000-fold with DOTMA (8) and at least 100-fold with DOTAP (10). These observations have led to examine the question whether cationic lipids also modify the intracellular distribution of oligonucleotides. Moreover, the localization of ODN in the cells after their release by the carrier is a critical point since released free ODN have to reach their target in order to achieve a real antisense effect.

Therefore, we and others have assessed the intracellular localization of fluorescently-labeled oligonucleotides (F-ODN) delivered with or without cationic lipids (4, 8, 10). The results obtained on the intracellular localization of ODN alone, without microinjection, are rather divergent. We and several other groups were unable to detect any "naked" fluorescently-labeled oligonucleotides in the nucleus. They were localized only in punctate cytoplasmic region consistent with endocytic vesicles (2, 4, 8, 10, 15, 16), while others have shown a preferential accumulation in the nucleus (17-19). This divergence may be explained by the different cell types used, chemical nature of oligonucleotides, and the experimental methods. Contrary, all microinjection experiments demonstrated rapid diffusion and accumulation of oligonucleotides in the nucleus in a temperature- and energy-independent manner (16, 20-22). Once inside cells, phosphodiester oligonucleotides are rapidly degraded (22), but phosphorothioates and α-anomeric oligonucleotides persist at least 24 hours (20, 21).

Cationic lipids have markedly increased the cellular fluorescence and modified the intracellular distribution of ODN. Indeed, F-ODN intracellularly delivered by cationic lipids (DOTMA or DOTAP) are redistributed from punctate cytoplasmic regions into the nucleus (4, 8, 10). Some diffuse fluorescence can also be seen in the cytoplasm. The nuclear

uptake of F-ODN depends on: charge ratio (+/-), time of incubation, temperature and presence of serum (8, 10). The percentage of adherent cells (HUVEC, CV-1) exhibiting nuclear fluorescence fluctuated between 65 to 80% with DOTMA and DOTAP. F-ODN were never visualized in the nucleoli and they seem to be preferentially concentrated in specific regions of the nucleus that could be particular domains of small nuclear proteins known to interact with oligonucleotides (16, 17, 20, 23). The real significance of such interactions on the activity of oligonucleotides is not known, but too strong affinity towards some cellular components may limit their availability to hybridize to their target.

The inclusion of certain neutral lipids, especially DOPE or cholesterol, with cationic lipids has been demonstrated to increase the DNA delivery efficiency (24). We have demonstrated that the association of these molecules with DOTAP lipids did not effect the capacity of oligonucleotide delivery in contrast to gene delivery reports (10). However, the optimum charge ratio for nuclear uptake was reduced as the DOTAP was diluted with the neutral lipid (10).

Another important parameter governs the efficiency of antisense oligonucleotides is their ability to hybridize to their target RNA. In this context, if the cationic lipids are still complexed with oligonucleotides in the cells, they can limit the availability of oligonucleotides to hybridize to their target or inversely they can increase the ODN affinity towards its target. Moreover, the fact that cationic lipids have modified the ODN intracellular distribution raises the question about the role of lipids in this nuclear transport. Thus, we have studied also the intracellular localization of fluorescein-labeled oligonucleotides associated with rhodamine-labeled phosphatidylethanolamine/DOTAP liposomes. Fluorescent confocal microscopy of cells treated with fluorescent complexes show the F-ODN separates from the lipid after internalization and enters the nucleus leaving the fluorescent lipid in cytoplasmic structures (25). Thus, the physical separation of lipids and ODN in the cells strongly suggest that lipids do not carry ODN to the nucleus and have no influence on their hybridization ability.

Finally, cationic liposomes have increased the quantity of delivered ODN both in the cytoplasm and in the nucleus. The importance of the ODN nuclear uptake on their efficiency is still unknown since ODN can also hybridize to their target in the cytoplasm. Nevertheless, these studies suggest that nuclear localization of ODN correlates with an enhanced inhibitory activity. Moreover, for triple helix formation at least nuclear accumulation would be desirable.

UPTAKE PATHWAY FOLLOW BY ODN/CATIONIC LIPID COMPLEXES

It is now accepted that cationic lipids deliver plasmid DNA into the cell predominately via an endocytotic pathway (26-29) rather than after fusion with the plasma membrane (30). However, the delivery of oligonucleotides by cationic lipids have been suggested to be due to the fusion of cationic lipids with plasma membrane (8). Since, the mechanism of oligonucleotides delivery mediated by cationic lipids was controversial we have used several inhibitors of endocytosis to better characterize the cellular uptake process.

CV-1 cells (kidney fibroblast from Monkey) were incubated with fluorescently-labeled phosphorothioate oligonucleotides complexed to DOTAP in the presence of endocytosis inhibitors. The delivery was affected by incubation at 4°C, cytochalasin B which blocks the polymerization of microfilaments of actin that are known to be implicated in the endocytic process of uncoated vesicles, N-ethylmaleimide which inhibits the NSF protein activity required in the fusion of endosome membrane and azide/deoxyglucose which interferes with the cellular energy process (10). These inhibitor results show that complexes are endocytosed and suggest that internalization is mainly achieved by uncoated vesicles. Nocodazole (microtubule depolymerizing-agent) had no effect on delivery (8, 10) which suggests release of ODN from the complex takes place in the early stages of endocytosis, probably at the level of the pits or early endosomes since microtubules are known to be

involved in the later phase of endocytosis. This is strongly supported by a recent study showing that an early event in the endocytic pathway plays a key role in the fusion of cationic liposomes with endosomes (29). The liberation of the ODN does not require acidification since lysosomotropic agents (chloroquine, NH_4Cl, monensin and bafilomycin A) have no effect (8, 10).

These results are consistent with previous studies which suggest that cationic lipids deliver plasmid DNA by an endocytotic process (26-29) rather than a direct cytoplasmic delivery after fusion with cell membranes (30). However, we cannot exclude the possibility that some complexes can destabilize and/or merge directly with the plasma membrane, but it seems that this process is a less frequent event than delivery via the endocytotic route. Our results, taken together with the results from the groups cited above, point out the importance of an endocytic capability of the target cell in determining the delivery efficiency of oligonucleotides mediated by cationic agents.

MECHANISM OF ODN RELEASE FROM CATIONIC LIPIDS INTO CELLS

It seems evident that ODN and polynucleotides (DNA) have to dissociate from complexes in order to function. Several observations support this idea. Plasmid DNA must dissociate from the cationic liposome (28) and localize in the nucleus in order to be expressed (31). Moreover, the physical separation of the ODN and cationic liposomes in cells (25) raises the question about how they dissociate. Therefore we examined which types of molecules found in cells bring about the release of ODN from cationic lipids.

Oligonucleotide displacement from the complex was studied by fluorescent resonance energy transfer (FRET). Anionic liposome compositions (e.g. phosphatidylserine, phosphatidylglycerol, phosphatidylinositol and phosphatidic acid) that mimic the cytoplasmic

facing monolayer of the cell membrane released oligonucleotides from the complex at about a 1:1 (-/+) charge ratio (25). The displacement of ODN from complexes is dependent on the ratio of negative charges present on liposomes to positive charges present in complexes. Release of ODN from DOTAP was rapid (1-2 minutes) and can occur within the time scale of an endocytotic event (25). With ODN/DOGS the release was 2-3 times slower. The dissociation was independent of ionic strength and pH. Neutral liposomes could not displace the ODN from the cationic liposome. Physical separation of the F-ODN from monovalent (DOTAP) and multivalent (DOGS) cationic lipids was confirmed by PAGE gel shift assay (25). In the absence of a releasing agent, the oligonucleotide remained complexed to the cationic liposome and did not enter the gel but when the anionic liposomes were mixed with the complex, the oligonucleotide migrated into the gel. Fluid but not solid phase anionic liposomes are required for release which highlights the importance of lipid diffusion as a significant factor in augmenting release of ODN from the cationic lipsome. However the physical state of the cationic lipids does not effect the release. Water soluble molecules with a high negative linear charge density, dextran sulfate or heparin, also release oligonucleotides. However, ATP, spermidine, spermine, tRNA, DNA, polyglutamic acid, polylysine, bovine serum albumin or histone did not release oligonucleotides, even at 100 fold charge excess (-/+) (25).

Based upon these data, we have proposed the scheme illustrated in figure 1 that emphasizes the importance of cellular anionic lipids to explain how oligonucleotides and other nucleic acids are released from the complex into the cytoplasm of the cell (25). First the cell surface-associated complex is internalized by endocytosis (step 1). The complex initiates a destabilization of the endosomal membrane that results in a flip-flop of anionic lipids (step 2) that are predominately located on the cytoplasmic face of the membrane. The anionic lipids laterally diffuse into the complex and form a charged neutralized ion-pair with the cationic lipid (step 3). This leads to displacement of the oligonucleotide from the cationic lipid and its release into the cytoplasm. (step 4, Fig. 1).

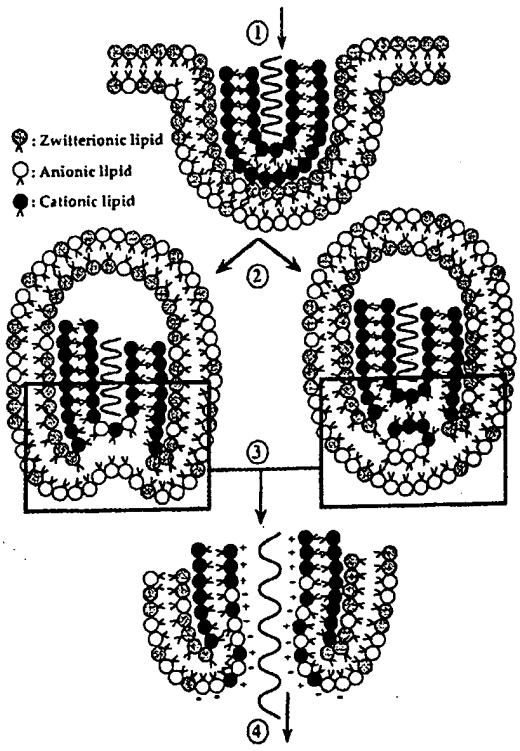

FIG. 1 Schematic representation of the ODN/cationic lipid complex uptake pathway and of the ODN endosomal release mechanism.

This model accounts for a variety of biological, biochemical and biophysical data. This anionic lipid driven uncoating of the complex is consistent with the lipid asymmetry of the plasma and endosomal membranes (32) as well as cell biological data that shows nucleic acid accessibility to the translation and transcription machinery. RNA delivered as a complex is accessible to the ribosome for translation (33), a T7 promoter on the delivered plasmid is accessible to cytoplasmic T7 polymerase (34, 35) and oligonucleotides and plasmid DNA are functional upon delivery (8, 10, 24, 30). Moreover, when plasmid DNA/cationic lipid complexes were directly injected into nucleus, thus bypassing the endocytosis steps, little reporter gene expression was

observed, suggesting that in this instance, where interactions with anionic lipid containing membranes was bypassed, DNA did not dissociate from the complex (28). The model is also consistent with electron microscopy observations of complexes in cells that show electron dense structures appearing in disrupted endosomes close to the plasma membrane (27, 28) as well the fluorescence microscopy observations on oligonucleotide delivery (8, 10, 25, 30).

The model is also based upon the biophysical properties of membrane fusion since conditions that promote close apposition of the lipid bilayers that precedes fusion lead to lipid mixing (36). Moreover, anionic lipids and not zwitterionic lipids dominate the lipid mixing process in an asymmetric fusion system (36). The importance of anionic lipid lateral diffusion in the release is supported by the requirement for a fluid anionic bilayer to release oligonucleotide from the complex (25). Perturbation of the membrane during fusion or disruption by peptides results in lipid flip-flop (32, 37) and this phenomenon would supply the anionic lipids from the cytoplasmic monolayer required to neutralize the cationic lipids in the complex. Cationic liposomes have been shown to fuse with endocytotic vesicles (29). The fusion process once started would be autocatalytic since the appearance of additional anionic lipids at the site of interaction would augment the adhesion of the cationic complex to the endosomal membrane.

The release mechanism would be particularly efficient for releasing oligonucleotides since only a small number of electrostatic interactions would have to be disrupted to release a single oligonucleotide (circa 15) where release of a 2.5 kB plasmid DNA would require circa 5,000 interactions to be disrupted to fully dissociate the plasmid DNA from the complex. This fact may explain why oligonucleotide delivery via cationic liposomes appears more effective than plasmid DNA delivery since there may be an insufficient number of anionic lipids in the cytoplasmic monolayer of a smaller endosome to disrupt the interactions between the plasmid and the cationic lipid. A back of the envelope estimation can be made of the number of anionic phospholipids in the cytoplasmic

monolayer of an endosome. Assume the complex is internalized into a 150 nm spherical endosome. This has a monolayer surface area of 1.76 X 10^4 nm^2. If we further assume that 70% of the area is occupied by phospholipids, 25% of these phospholipids are anionic and that each lipid has a surface area of 0.7 nm^2 then the cytoplasmic monolayer would contain about 4.4 X 10^3 anionic phospholipids. There is certainly enough anionic lipids in an endosome to release a sizeable number of oligonucleotides from each complex. However it must be emphasized that the release mechanism does not require that the complex be endocytosed, it proposes that anionic lipids are the biomolecules responsible for the actual dissociation of the nucleic acid from the cationic lipid.

Our proposal that endocytosis is the route for ODN delivery by cationic liposomes is based upon a variety of studies showing that endocytosis is the predominant route of internalization for most cell types studied (10, 27, 28, 29). This raises the question of why endocytosis appears to be required for destabilization and/or fusion? First, it has been clearly demonstrated that the major route of nucleic acids/cationic lipid complexes delivery is by endocytosis (10, 27, 28). Moreover, cationic liposomes have been shown to fuse with membranes only after endocytosis (29). A possible explanation is that internalization of the complexes into a compartment with a high radius of curvature may promote close contact between the two surfaces and provide a physical trigger for membrane destabilization as suggested by the efficiency of small anionic vesicles to displace the ODN in comparison to large vesicles (25). Alternatively compartmentalization may be the key; release of ODN from cationic lipids in the endosome could generate a mechanical or osmotic stress that ruptures the endosomal bilayer and releases the ODN into the cytoplasm. Release of the oligonucleotide from complexes on the surface might not generate the necessary stress on the membrane needed to rupture it. Finally, since it was suggested that endocytosis of complexes is mainly achieved by uncoated vesicles (10, 27), the absence of clathrin and the accessory proteins during the release process might make the uncoated vesicles more prone to rupture.

In summary, the biophysical release experiments described (25, 38), support a model for how anionic lipids mediate oligonucleotides release from cationic liposome complexes in cells (figure 1). This model should provide a useful starting point for the rationale improvement of this important nucleic acid delivery system.

CONCLUSIONS AND PERSPECTIVES

Cationic liposomes might be a useful *in vivo* ODN delivery vehicle since in all *in vitro* studies cationic liposomes have improved the potency of oligonucleotides (5). The understanding of ODN cellular delivery mechanisms mediated by cationic lipids provide new insights to further improve the process of nucleic acid delivery. Indeed, since the ODN induced aggregation and fusion of cationic liposomes (11), it is thus difficult to control the size of the complexes. In this context, efforts have to be made on order to obtain small and homogeneous complex preparations. In the same way, the uptake pathway follow by the complexes (endocytosis) point out the importance of an endocytic capability of the target cell in determining the delivery efficiency of oligonucleotides mediated by cationic agents.

Recently, cellular mechanisms for gene delivery mediated by cationic lipids have identified a number of steps at which lipid-mediated transfection was inefficient (28). From these results, it is clear that the behavior of plasmid DNA and ODN are very different. Indeed, the movement of plasmid DNA from cytoplasm to the nucleus was limiting to successful gene transfer (28) whereas ODN were localized into the nucleus after delivery by cationic lipids (8, 10, 25). Thus, this particular steps in the delivery process does not appear to be a limiting factor for ODN delivery. Similarly, the mechanism of ODN release from cationic lipids into cells (25) does not seem to be a limitation for the ODN delivery. However, even if the same mechanism has been demonstrated for DNA (38), this step could represent a barrier to gene delivery due to the high molecular weight of double stranded DNA (28).

The most critical point in the use of cationic liposomes is the interaction with blood components since serum inhibit their delivery efficiency (10, 30, 39). To date, the nature of interactions and the mechanism of serum inhibition are still unknown. We have recently shown that serum components and especially the BSA prevent the ODN delivery mediated by DOTAP at multiple steps of the cellular uptake including interactions with cell membranes (due to the charge neutralization), internalization (due to the size) and ODN intracellular release (due to steric hindrance). (40). However, some blood components can also destabilize the complexes. Indeed, heparin and oleic acid were able to displace the oligonucleotides from the cationic lipids (25, 40). The efficacy of heparin and oleic acid at releasing the oligonucleotide from the complex raises the question of whether these compounds or other fatty acids and glycosaminoglycans found in extracellular regions of the body might interfere with ODN delivery *in vivo* by bringing about release of nucleic acids before the complex can reach the target cell.

The *in vivo* delivery potential of cationic lipids as nucleic acid carriers still needs to be established and the benefit for oligonucleotide delivery*in vivo* remains unclear. Indeed, in two recent studies, the oligonucleotide activity *in vivo* did not require the presence of cationic liposomes or any other delivery system (41, 42). Conversely, in another report, the inhibitory activity of antisense oligonucleotides on tumor growth was significantly increased when complexed with cationic lipids and injected intraperitoneally (43). To explain this activity, it has been suggested that ascites proteins interfere less than serum proteins with the ability of cationic lipids to deliver oligonucleotides. In this context, further studies on the understanding of the interactions between the nucleic acid/cationic lipids complexes and biological fluids would allow improvements of polynucleotide cationic carriers. Similarly, better identification of blood components interacting with liposomes and of cells recognizing the liposome-bound opsonins will aid in improving the formulation of nucleic acid/cationic lipid complexes and the process of nucleic acid delivery.

ACKNOWLEDGMENTS

This work was partially supported by NIH GM30163, NIH DK46052 and P50 HL42368 (F.C.S.), Glaxo Inc. and Association pour la Recherche Contre le Cancer (O.Z.). We are grateful for the gift of oligonucleotides from Gerry Zon.

REFERENCES

1. Uhlmann, E. and Peyman, A. 1990. Antisense oligonucleotides: a new therapeutic principle. Chem. Rev. 90:544-584.

2. Crooke, S. T. and Lebleu, B. Antisense research and applications, CRC Press, Boca Raton, Florida.

3. Stein, C. A. and Cheng, Y.-C. 1993. Antisense oligonucleotides as therapeutic agents-is the bullet really magical? Science. 261:1004-1012.

4. Wagner, R. W., Mateucci, M. D., Lewis, J. G., Gutierrez, A. J., Moulds, C. and Froehler, B. C. 1993. Antisense gene inhibition by oligonucleotides containing C-5 propyne pyrimidines. Science. 260:1510-1513.

5. Zelphati, O. and Szoka Jr., F. C. 1996. Liposomes as a carrier for intracellular delivery of antisense oligonucleotides: a real or magic bullet? J. Controlled Release. In press.

6. Zelphati, O., Imbach, J.-L., Signoret, N., Zon, G., Rayner, B. and Leserman, L. 1994. Antisense oligonucleotides in solution or encapsulated in immunoliposomes inhibit replication of HIV-1 by several different mechanisms. Nucleic Acids Res. 22:4307-4314.

7. Chiang, M.-Y., Chan, H., Zounes, M. A., Freier, S. M., Lima, W. F. and Bennett, C. F. 1991. Antisense oligonucleotides inhibit intercellular adhesion molecule 1 expression by two distinct mechanisms. J. Biol. Chem. 266:18162-18171.

8. Bennett, C. F., Chiang, M.-Y., Chan, H., Shomaker, J. E. and Mirabelli, C. K. 1992. Cationic lipids enhance cellular uptake and activity of phosphorothioate antisense oligonucleotides. Mol. Pharmacol. 41:1023-1033.

9. Lappalainen, K., Urtti, A., Jääskeläinen, I., Syrjänen, K. and Syrjänen, S. 1994. Cationic liposomes mediated delivery of antisense oligonucleotides targeted to HPV 16 E7 mRNA in CaSki cells. Antiviral Res. 23:119-130.

10. Zelphati, O. and Szoka Jr., F. C. 1996. Intracellular distribution and mechanism of delivery of oligonucleotides mediated by cationic lipids. Pharm. Res. In press.

11. Jääskeläinen, I., Mönkkönen, J. and Urtti, A. 1994. Oligonucleotide-cationic liposome interactions. A physicochemical study. Biochim. Biophys. Acta. 1195:115-123.

12. Capaccioli, S., Di Pasquale, G., Mini, E., Mazzei, T. and Quattrone, A. 1993. Cationic lipids improve antisense oligonucleotide uptake and prevent degradation in cultured cells and in human serum. Biochem. Biophys. Res. Comm. 197:818-825.

13. Lappalainen, K., Urtti, A., Söderling, E., Jääskeläinen, I., Syrjänen, K. and Syrjänen, S. 1994. Cationic liposomes improve stability and intracellular delivery of antisense oligonucleotides into CaSki cells. Biochim. Biophys. Acta. 1196:201-208.

14. Itoh, H., Mukoyama, M., Pratt, R. E. and Dzau, V. J. 1992. Specific blockade of basic fibroblast growth factor gene expression in endothelial cells by antisense oligonucleotide. Biochem. Biophys. Res. Comm. 188:1205-1213.

15. Loke, S. L., Stein, C. A., Zhang, X. H., Mori, K., Nakanishi, M., Subasinghe, C., Cohen, J. S. and Neckers, L. M. 1989. Characterization of oligonucleotide transport into living cells. Proc. Natl. Acad. Sci. USA. 86:3474-3478.

16. Chin, D. J., Green, G. A., Zon, G., Szoka Jr., F. C. and Straubinger, R. M. 1990. Rapid nuclear accumulation of injected oligodeoxyribonucleotides. New Biol. 2:1091-1100.

17. Geselowitz, D. A. and Neckers, L. M. 1992. Analysis of oligonucleotide binding, internalization, and intracellular trafficking utilizing a novel radiolabeled crosslinker. Antisense Res. Dev. 2:17-25.

18. Noonberg, S. B., Garovoy, M. R. and Hunt, C. A. 1993. Characteristics of oligonucleotide uptake in human keratinocyte cultures. J. Invest. Derm. 101:727-731.

19. Zamecnik, P., Aghajanian, J., Zamecnik, M., Goodchild, J. and Witman, G. 1994. Electron migrographic studies of transport of oligodeoxynucleotides across eukaryotic cell membranes. Proc. Natl. Acad. Sci. USA. 91:3156-3160.

20. Leonetti, J. P., Mechti, N., Degols, G., Gagnor, C. and Lebleu, B. 1991. Intracellular distribution of microinjected antisense oligonucleotides. Proc. Natl. Acad. Sci. USA. 88:2702-2706.

21. Fisher, T. L., Terhorst, T., Cao, X. and Wagner, R. W. 1993. Intracellular disposition and metabolism of fluorescently-labeled unmodified and modified oligonucleotides microinjected into mammalian cells. Nucleic Acids Res. 21:3857-3865.

22. Sixou, S., Szoka Jr., F. C., Green, G. A., Giusti, B., Zon, G. and Chin, D. J. 1994. Intracellular oligonucleotide hybridization detected by fluorescence resonance energy transfer (FRET). Nucleic Acids Res. 22:662-668.

23. Clarenc, J.-P., Lebleu, B. and Leonetti, J.-P. 1993. Characterization of the nuclear binding sites of oligodeoxyribonucleotides and their analogs. J. Biol. Chem. 268:5600-5604.

24. Gao, X. and Huang, L. 1995. Cationic liposome-mediated gene transfer. Gene Ther. 2:710-722.

25. Zelphati, O. and Szoka Jr., F. C. 1996. Mechanism of oligonucleotide release from cationic liposomes. Proc. Natl. Acad. Sci. USA. In press.

26. Legendre, J.-Y. and Szoka Jr., F. C. 1992. Delivery of plasmid DNA into mammalian cell lines using pH-sensitive liposomes: comparison with cationic liposomes. Pharm. Res. 9:1235-1242.

27. Zhou, X. and Huang, L. 1994. DNA transfection mediated by cationic liposomes containing lipopolylysine: characterization and mechanism of action. Biochim. Biophys. Acta. 1189:195-203.

28. Zabner, J., Fasbender, A. J., Moninger, T., Poellinger, K. A. and Welsh, M. J. 1995. Cellular and molecular barriers to gene transfer by a cationic lipid. J. Biol. Chem. 270:18997-19007.

29. Wrobel, I. and Collins, D. 1995. Fusion of cationic liposomes with mammalian cells occurs after endocytosis. Biochim. Biophys. Acta. 1235:296-304.

30. Felgner, P. L., Gadek, T. R., Holm, M., Roman, R., Chan, H. W., Wenz, M., Northrop, J. P., Ringold, G. M. and Danielsen, M. 1987. Lipofection: a highly efficient, lipid-mediated DNA-transfection procedure. Proc. Natl. Acad. Sci. USA. 84:7413-7417.

31. Capecchi, M. R. 1980. High efficiency transformation by direct microinjection of DNA into cultured mammalian cells. Cell. 22:479-488.

32. Devaux, P. F. 1992. Protein involvement in transmembrane lipid asymmetry. Annu. Rev. Biophys. Biomol. Struct. 21:417-439.

33. Malone, R. W., Felgner, P. L. and Verma, I. M. 1989. Cationic liposome-mediated RNA transfection. Proc. Natl. Acad. Sci. USA. 86:6077-6081.

34. Rose, J. K., Buonocore, L. and Whitt, M. A. 1991. A new cationic liposome reagent mediating nearly quantitative transfection of animal cells. Biotechniques. 10:520-5.

35. Gao, X. and Huang, L. 1993. Cytoplasmic expression of a reporter gene by co-delivery of T7 RNA polymerase and T7 promoter sequence with cationic liposomes. Nucl. Acids Res. 21:2867-2872.

36. Düzgünes, N., Goldstein, J. A., Friend, D. S. and Felgner, P. L. 1989. Fusion of liposomes containing a novel cationic lipid, N-[2,3-(dioleyloxy)propyl]-N,N,N-trimethylammonium: induction by multivalent anions and asymmetric fusion with acidic phospholipid vesicles. Biochemistry. 28:9179-9184.

37. Fattal, E., Nir, S., Parente, R. A. and Szoka, J., F. C. 1994. Pore-forming peptides induce rapid phospholipid flip-flop in membranes. Biochemistry. 33:6721-6731.

38. Xu, Y. and Szoka Jr., F. C. 1996. On the mechanism of DNA release from cationic liposome/DNA complexes used in cell transfection. Biochemistry. 35:5616-5623.

39. Senior, J. H., Trimble, K. R. and Maskiewicz, R. 1991. Interaction of positively-charged liposomes with blood: implications for their application in vivo. Biochim. Biophys. Acta. 1070:173-179.

40. Zelphati, O. and Szoka Jr., F. C. 1996. Interactions of nucleic acid/cationic lipid complexes with blood components. Submitted.

41. Dean, N. and McKay, R. 1994. Inhibition of protein kinase C-α expression in mice after systemic administration of phosphorothioate antisense oligodeoxynucleotides. Proc. Natl. Acad. Sci. USA. 91:11762-11766.

42. Stepkowski, S. M., Tu, Y., Condon, T. P. and Bennett, C. F. 1994. Blocking of heart allograft rejection by intercellular adhesion molecule-1 antisense oligonucleotides alone or in combination with other immunosuppressive modalities. J. Immunol. 153:5336-5346.

43. Perlaky, L., Saijo, Y., Busch, R. K., Bennett, C. F., Mirabelli, C. K., Crooke, S. T. and Busch, H. 1993. Growth inhibition of human tumor cell lines by antisense oligonucleotides designed to inhibit p120 expression. Anti-Cancer Drug Design. 8:3-14.

IN THE UNITED STATES PATENT AND TRADEMARK OFFICE

Appl. No.	: 10/086,477	Confirmation No.	: 3225
Applicant	: Semple *et al.*		
Filed	: 3/1/02	Attorney Docket No.:	33846/US/3
Art Unit	: 1632	Customer No.	: 32,940
Examiner	: Nguyen, D.		
Title	: COMPOSITIONS FOR STIMULATING CYTOKINE SECRETION AND INDUCING AN IMMUNE RESPONSE		

DECLARATION
Pursuant to § 1.132

I, Michael J. Hope, declare the following:

1. I have a Ph.D. in Biochemistry from the University of London, UK. I have done research in the field of lipids and liposomal delivery vehicles for thirty (30) years and published many papers in the field. My curriculum vitae is attached. I am familiar with the significant variations in the liposomal physical structure that can result from changes in composition and method of preparation. I have been employed by Inex Pharmaceuticals Corporation, the assignee of the above-referenced patent application, as a research scientist since 1994. I am personally familiar with the inventor of the Wheeler patent mentioned below, who was a colleague and co-researcher with me at Inex. I am also knowledgeable about the lipid compositions described by the Wheeler patent and the use thereof in forming lipid nucleic acid complexes as a delivery vehicle.

2. I am a co-inventor of the instant invention, and thus I have read the specification, made the lipid-encapsulated nucleic acid particles described therein, and am knowledgeable about their structure. I have also read the Office Action dated December 22, 2003 and I have read and understand each of U.S. Patent Nos.: 5,703,055 to Felgner, 6,207,646 to Krieg; 5,976,567 to Wheeler; and 6,143,716 to Meers, as well as the 1999 review article by McCluskie and the 1998 *J. Immunotherapy* article by Bei. Through my research experience and familiarity with the structure of liposomal compositions I am able to recognize the types of lipid/nucleic acid structures that would be formed by the methods

described in each of the aforementioned references in comparison to the improved lipid/nucleic acid structures taught in the instant application.

3. I understand from reviewing the Office Action that the Examiner considers the lipid/nucleic acid compositions prepared by the methods described in the cited art, particularly Felgner, Wheeler or Meers, to be the same as or equivalent to the presently-claimed compositions having nucleic acid polymers fully encapsulated in a cationic lipid particle. I believe that the Examiner's opinion is incorrect, for the reasons that follow.

4. First, the Meers reference is directed principally to peptide-lipid conjugates and their use in liposomes. Meers would appear to be of very little relevance to our application since it does not describe with any specificity the making of a lipid/nucleic acid composition, let alone the lipid-encapsulated nucleic acid compositions of our invention.

5. Second, the methods disclosed in Felgner and Wheeler produce lipid/nucleic acid *complexes* in contrast to the lipid-*encapsulated* nucleic acid *particles* of our invention. This is significant for a number of reasons, many of which are already outlined in the specification of this application. In our invention the nucleic acids are *fully encapsulated* within the lipid membrane, which protects them from nuclease degradation upon *in vivo* administration and thus makes systemic administration more effective and more practical. In my view the prior art lipid/nucleic acid complexes or "aggregates" (see page 13 of the specification) of Felgner and Wheeler are unsatisfactory for this purpose since they are not serum stable, and thus they will decompose rapidly upon administration and much of the nucleic acid payload will be degraded before it can have therapeutic effect.

6. The problem of *in vivo* serum stability has been a long-standing one in the field of liposomal delivery vehicles. As discussed in our patent specification, the lipid-encapsulated nucleic acid particles of our invention solve this long-standing problem in the art. For immune stimulation in particular, adequate circulation time of the nucleic acid delivery vehicle is critical in order to achieve the desired objective of a systemic immune response. The prior art lipid/DNA complexes are inadequate for this purpose, as evidenced by some of our more recent data presented below, and as reported by a number of researchers in more recent journal articles.

7. Additional structural advantages of our lipid-encapsulated nucleic acid particles include their smaller size, generally having a mean diameter of about 50-200 nm, and the ability to achieve more uniformity in sizing, both of which are important features for intravenous formulation and administration. The lipid/nucleic acid complexes proposed by Felgner *et al.* and Wheeler *et al.* are deficient in these respects as well. For example, for the DODAC:DOPE/oligonucleotide complexes detailed below, which were prepared based on the teachings of the cited art, the size of the resulting complexes was 240 + 80 nm in diameter as measured by quasi-elastic light scattering using a Nicomp Model 370 particle sizer. Moreover, these lipid complexes are not well defined in size but consist of a "complex" of vesicle aggregates that are unstable over time.

8. I recognize Felgner *et al.* suggest generally at column 24 that "[t]he science of forming liposomes is now well developed. . . . The aqueous portion is used in the present invention to contain the polynucleotide material to be delivered to the target cell." As a skilled artisan, however, I understand the actual disclosure in Felgner to relate to lipid/DNA *complexes* which are inadequate and inferior for systemic immune stimulation for the reasons mentioned above. I do not find any discussion in Felgner *et al.* that would teach one to fully encapsulate an immunostimulatory nucleic acid as contemplated by our invention, and there is clearly no recognition by Felgner *et al.* of the surprising and synergistic effects of lipid-encapsulated oligonucleotides in immune stimulation.

9. I further recognize that Krieg *et al.* generally refer to the possibility of "associating" their immunostimulatory nucleic acids with lipids. Importantly, however, there is no teaching, suggestion or scientific basis provided by Krieg *et al.* to select lipids as opposed to the sterols or target cell specific binding agents also proposed, nor is there any basis given to fully encapsulate the nucleic acid as opposed to the standard approach of lipid complexes since both are mentioned. [Compare col. 12 with col. 33] Moreover, as with Felgner *et al.* there is certainly no suggestion in Krieg *et al.* of the surprising immune stimulatory properties that result from fully encapsulating nucleic acids in cationic lipid particles, since it was never actually accomplished in either reference.

10. We have developed additional *in vivo* data in tumor models that further demonstrates the effectiveness of our lipid encapsulation approach in comparison with lipid/nucleic acid

complexes, utilizing a complex much like those of Felgner *et al.* The cationic vesicles complexes were prepared using DOPE and the cationic lipid DODAC by dissolving the two lipids in chloroform at a 1:1 mole ratio and removing the solvent under a stream of nitrogen gas. The lipid film was then placed under vacuum to remove residual chloroform for > 4 h, protected from light before being hydrated with distilled water at a concentration of 40 mM lipid, and subjected to 5 freeze-thaw cycles using liquid nitrogen and warm (~50°C) water. The resulting multilamellar vesicles were extruded 10 times through two stacked 100 nm pore-size filters using an Extruder (Northern Lipids, Vancouver). The oligonucleotide 6295PS was mixed with the DODAC:DOPE vesicles in distilled water at a 1:1 vol/vol ratio at a concentration of 0.5 mg/ml oligonucleotide and at a cationic lipid/oligonucleotide charge (+/-) ratio of 0.15. Briefly, the 6295PS oligonucleotide, solubilized in distilled water, was pre-heated for 3 min at 80°C to convert quadruplexes and any higher ordered structures to the monomer form. The oligonucleotide (1 mg/ml, 0.375 ml) was then mixed quickly with an equal volume of the DODAC:DOPE vesicles (diluted to 12.8 mM) and allowed to incubate at room temperature for 30 minutes. The vesicle/oligonucleotide complexes were made within 4-6 hours of injection.

11. The same 6295PS oligonucleotide was also encapsulated in various cationic lipid vesicles made using DSPC, POPC or the classic composition DSPC:CH:DODAP:PEG-Cer-C14 at 20:45:25:10 as described in the instant application.

12. The figures attached to this declaration show the dramatically improved effect of lipid encapsulation in comparison with lipid/nucleic acid complexes. Figure 1 shows an effect on the stimulation of tetramer / CD8+ lymphocyte proliferation by ovalbumin. MHC-tetramer analysis is designed to detect CD8+ve, cytotoxic T lymphocytes (CTLs) that possess the appropriate T cell receptor to recognize and lyse target cells bearing the target antigen in the context of a MHC Class I complex. The lipid/nucleic acid complexes showed at best only a marginal increase in such CTLs in comparison with the control sample of ovalbumin alone. In contrast, the encapsulated oligonucleotides were at least four- to ten-fold more active in stimulating proliferation of responsive CTLs.

13. Figure 2 shows that the lipid/nucleic complexes had no effect (less than even the control) on the CTL response to target cells in a standard chromium release assay. In contrast, each of the lipid-encapsulated nucleic acids demonstrated a significant stimulation in the CTL response.

14. Figures 3 and 4 show the dramatically improved efficacy of our lipid-encapsulated nucleic acid particles in an established tumor model. As shown in Figure 3, at either 19 or 30 days after treatment, lipid/nucleic acid complexes reduced tumor volume much less efficaciously than a fully-encapsulated form of the same oligonucleotide. Similarly, Figure 4 shows that the lipid-encapsulated nucleic acid particles were much more effective in rendering the test animals tumor-free than the lipid/nucleic acid complexes.

15. The profound differences in immunostimulatory activity and tumor efficacy shown by this data are further proof of the significant immune stimulatory properties resulting from our lipid encapsulation approach. As we stated and demonstrated in our application, these immune stimulatory properties are evident even where 1) the nucleic acid is not sequence-specific (*i.e.* other than an antisense or gene expression sequence) and/or 2) the nucleic acid itself is not immunostimulatory. The significant immunostimulatory benefits of our invention went unrecognized by the prior art researchers, since they either employed inferior lipid/nucleic acid complexes (*e.g.* Felgner *et al.* and Dow *et al.*) or they merely generalized about potential lipid delivery possibilities without actually accomplishing any of them (*e.g.* Krieg *et al.*).

16. The aforementioned statements are true or based upon facts believed by me to be true. This declaration is made under penalty of perjury and with knowledge that false or misleading statements may jeopardize the invalidity or unenforceability of any rights in a patent that may be granted on the above-referenced application.

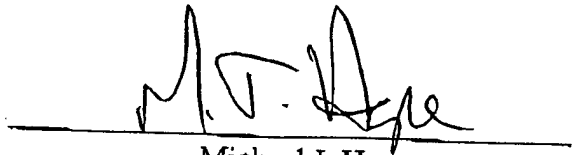

Michael J. Hope

June 23rd, 2004.

Date

1129172

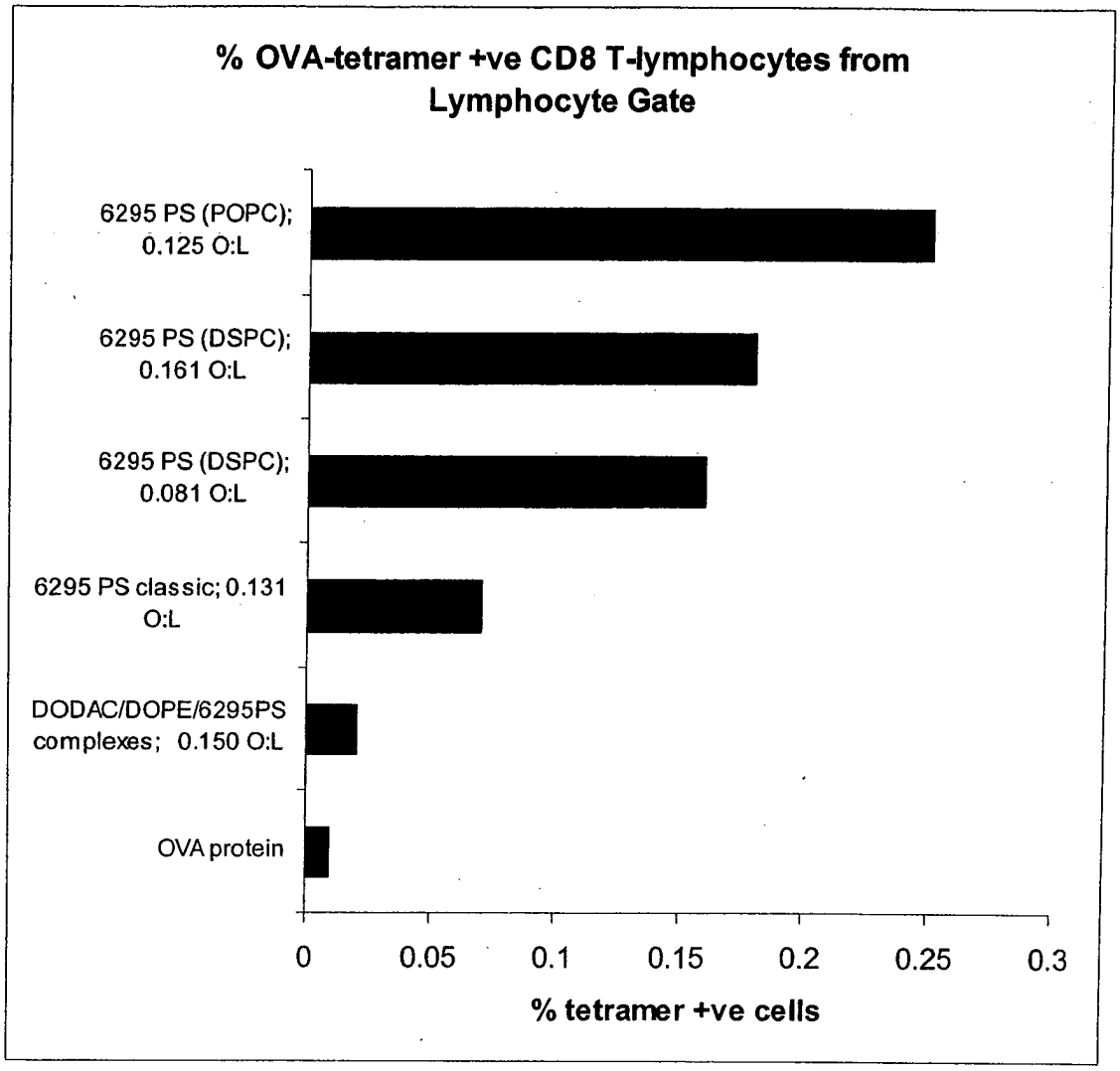
% OVA-tetramer +ve CD8 T-lymphocytes from Lymphocyte Gate
6295 PS (POPC); 0.125 O:L
6295 PS (DSPC); 0.161 O:L
6295 PS (DSPC); 0.081 O:L
6295 PS classic; 0.131 O:L
DODAC/DOPE/6295PS complexes; 0.150 O:L
OVA protein
0
0.05
0.1
0.15
0.2
0.25
0.3
% tetramer +ve cells

Figure 1

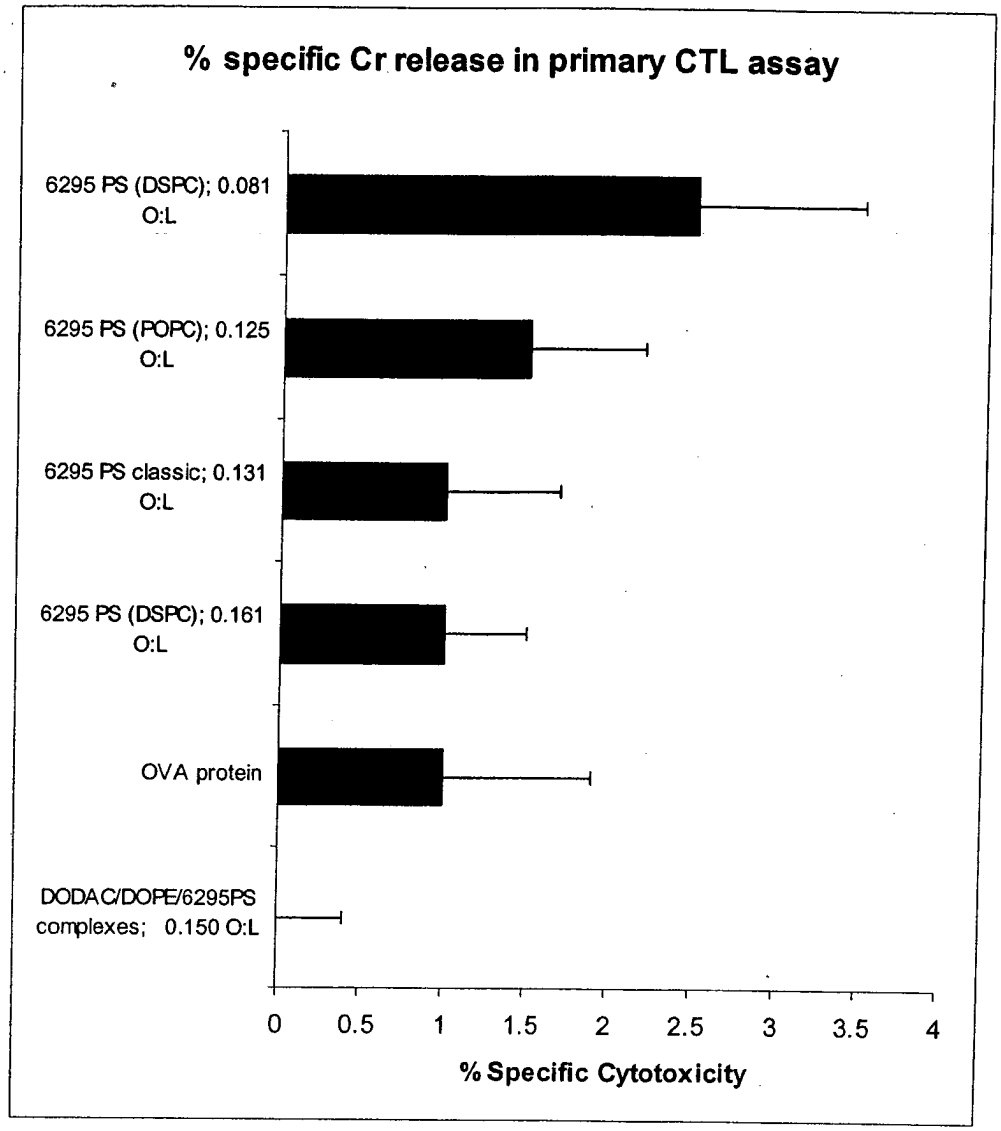
% specific Cr release in primary CTL assay
6295 PS (DSPC); 0.081 O:L
6295 PS (POPC); 0.125 O:L
6295 PS classic; 0.131 O:L
6295 PS (DSPC); 0.161 O:L
OVA protein
DODAC/DOPE/6295PS complexes; 0.150 O:L
0
0.5
1
1.5
2
2.5
3
3.5
4
% Specific Cytotoxicity

Figure 2

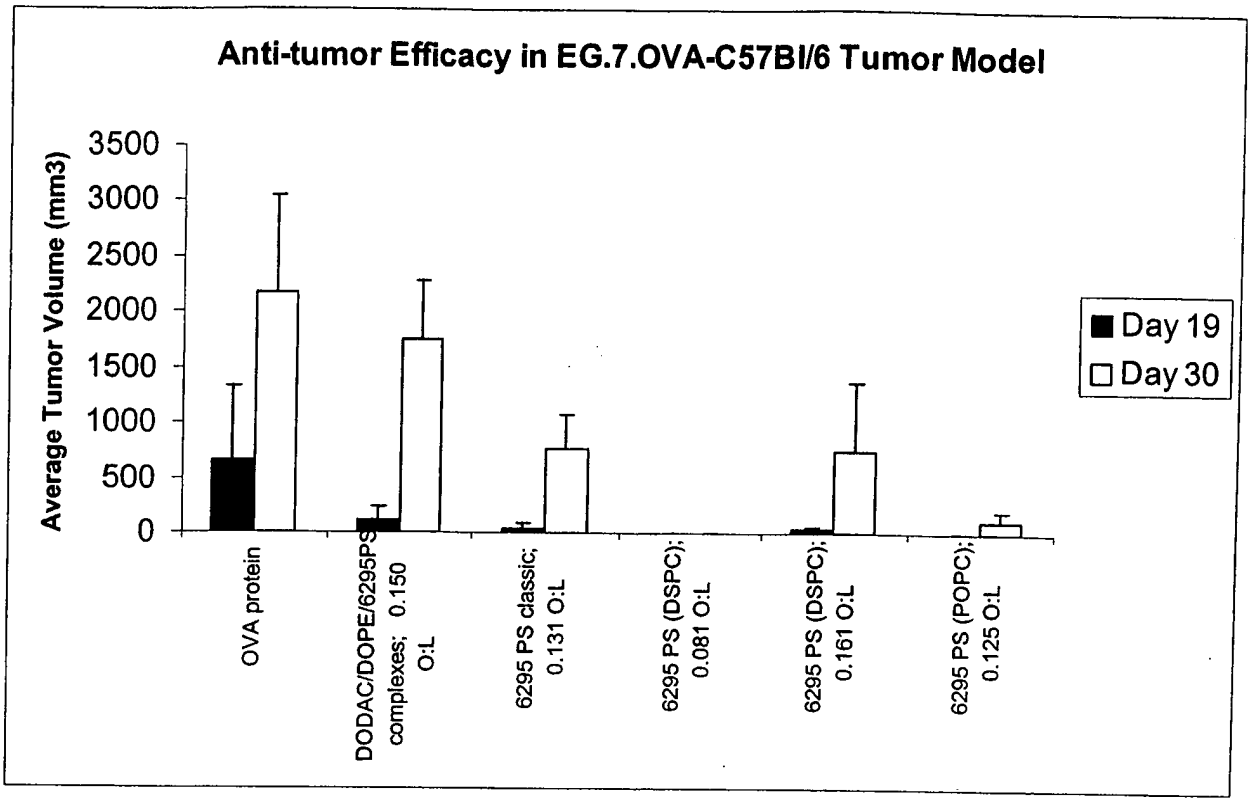
Anti-tumor Efficacy in EG.7.OVA-C57Bl/6 Tumor Model
Average Tumor Volume (mm3)
3500
3000
2500
2000
1500
1000
500
0
Day 19
Day 30
OVA protein
DODAC/DOPE/6295PS complexes; 0.150 O:L
6295 PS classic; 0.131 O:L
6295 PS (DSPC); 0.081 O:L
6295 PS (DSPC); 0.161 O:L
6295 PS (POPC); 0.125 O:L

Figure 3

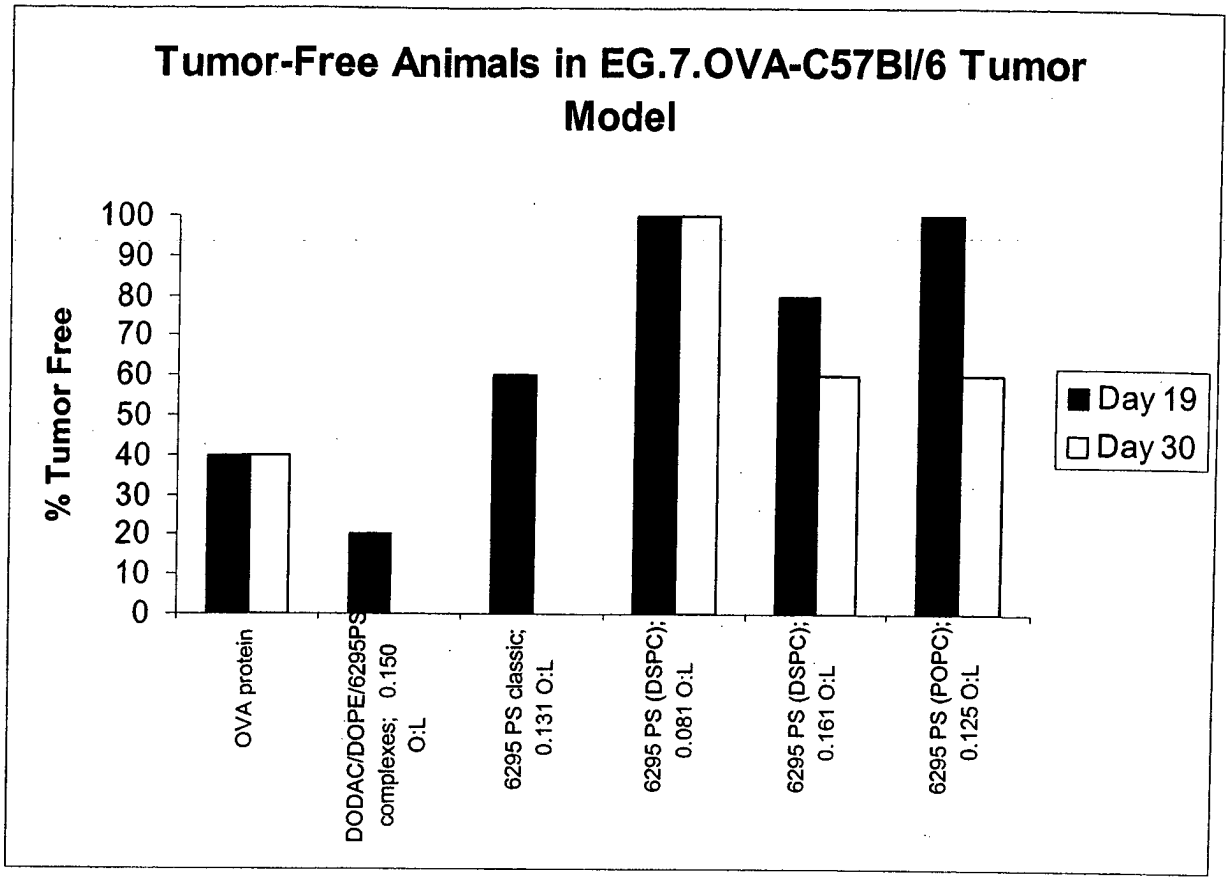
Tumor-Free Animals in EG.7.OVA-C57Bl/6 Tumor Model
% Tumor Free
100
90
80
70
60
50
40
30
20
10
0
OVA protein
DODAC/DOPE/6295PS complexes; 0.150 O:L
6295 PS classic; 0.131 O:L
6295 PS (DSPC); 0.081 O:L
6295 PS (DSPC); 0.161 O:L
6295 PS (POPC); 0.125 O:L
Day 19
Day 30

Figure 4